

THE ROLE OF PROTEASOME SPECIFIC CHAPERONES AND QUALITY CONTROL IN
ASSEMBLY OF THE PROTEASOME

by

PRASHANT SADANAND WANI

B.S., Moolji Jaitha College, 2005
M.S., North Maharashtra University, 2007

AN ABSTRACT OF A DISSERTATION

submitted in partial fulfillment of the requirements for the degree

DOCTOR OF PHILOSOPHY

Department of Biochemistry and Molecular Biophysics
Graduate Biochemistry Group

KANSAS STATE UNIVERSITY
Manhattan, Kansas

2015

Abstract

The proteasome is a large protease in the cell that contributes to the controlled degradation of proteins. This 2.5MDa 26S proteasome complex consists of a 19S regulatory particle (RP) that recognizes substrates and a 20S proteolytic core particle (CP) that hydrolyses substrates. To function optimally all 66 subunits of the proteasome complex need to assemble properly. Efficient and accurate assembly of the proteasome is achieved with the help of proteins that can monitor the quality of the proteasome during pre- and post-assembly processes. The work in this thesis described an investigation into two of such quality control mechanisms. Pba1-Pba2 dimer has been known to facilitate the CP assembly by interacting with the top of the α -ring of CP throughout CP maturation. After CP maturation, RP utilizes same surface to form a CP-RP complex. Our data showed that Pba1-Pba2 binds tightly to the immature CP and prevents RP association. Once matured CP has a reduced affinity for Pba1-Pba2 and shows a higher affinity towards RP, resulting the formation of 26S proteasome complex. Our results imply that during maturation, CP undergoes conformational changes that results in this switch in affinity. Mathematical models indicate that during assembly such an 'affinity switch' quality control mechanism is required to prevent immature CP-RP complex formations. These types of wrong dead end products prevent efficient proteasome complex formation.

Proteasomes formed with post-assembly defects are enriched with the proteasome associated protein Ecm29. Here Ecm29 is proposed to function as a quality control factor that inhibits such defective proteasomes to avoid aberrant protein degradation. This would require Ecm29 to preferably bind to mutant proteasomes. While we know Ecm29 interacts with RP as well as CP, we still don't understand well how it binds to proteasomes holoenzyme. Here, we identify that besides the Rpt5 subunit of RP, Ecm29 binds to alpha7. We showed that conserved acidic residues containing unstructured C-terminal region of the CP subunit alpha7 facilitates the Ecm29-Proteasome interactions. Further mapping revealed the importance of phosphorylation of serine residues at the alpha7 C-terminal tail for Ecm29 interaction. We anticipate that this study leads to identification of specificity of the Ecm29 for the defective proteasomes. Overall this will help us to understand the role of Ecm29 in regulation of defective proteasomes *in vivo*.

THE ROLE OF PROTEASOME SPECIFIC CHAPERONES AND QUALITY CONTROL IN
ASSEMBLY OF THE PROTEASOME

by

PRASHANT SADANAND WANI

B.S., Moolji Jaitha College, 2005
M.S., North Maharashtra University, 2007

A DISSERTATION

submitted in partial fulfillment of the requirements for the degree

DOCTOR OF PHILOSOPHY

Department of Biochemistry and Molecular Biophysics
Graduate Biochemistry Group

KANSAS STATE UNIVERSITY
Manhattan, Kansas

2015

Approved by:

Major Professor
Dr. Jeroen Roelofs

Copyright

PRASHANT SADANAND WANI

2015

Abstract

The proteasome is a large protease in the cell that contributes to the controlled degradation of proteins. This 2.5MDa 26S proteasome complex consists of a 19S regulatory particle (RP) that recognizes substrates and a 20S proteolytic core particle (CP) that hydrolyses substrates. To function optimally all 66 subunits of the proteasome complex need to assemble properly. Efficient and accurate assembly of the proteasome is achieved with the help of proteins that can monitor the quality of the proteasome during pre- and post-assembly processes. The work in this thesis described an investigation into two of such quality control mechanisms. Pba1-Pba2 dimer has been known to facilitate the CP assembly by interacting with the top of the α -ring of CP throughout CP maturation. After CP maturation, RP utilizes same surface to form a CP-RP complex. Our data showed that Pba1-Pba2 binds tightly to the immature CP and prevents RP association. Once matured CP has a reduced affinity for Pba1-Pba2 and shows a higher affinity towards RP, resulting the formation of 26S proteasome complex. Our results imply that during maturation, CP undergoes conformational changes that results in this switch in affinity. Mathematical models indicate that during assembly such an 'affinity switch' quality control mechanism is required to prevent immature CP-RP complex formations. These types of wrong dead end products prevent efficient proteasome complex formation.

Proteasomes formed with post-assembly defects are enriched with the proteasome associated protein Ecm29. Here Ecm29 is proposed to function as a quality control factor that inhibits such defective proteasomes to avoid aberrant protein degradation. This would require Ecm29 to preferably bind to mutant proteasomes. While we know Ecm29 interacts with RP as well as CP, we still don't understand well how it binds to proteasomes holoenzyme. Here, we identify that besides the Rpt5 subunit of RP, Ecm29 binds to alpha7. We showed that conserved acidic residues containing unstructured C-terminal region of the CP subunit alpha7 facilitates the Ecm29-Proteasome interactions. Further mapping revealed the importance of phosphorylation of serine residues at the alpha7 C-terminal tail for Ecm29 interaction. We anticipate that this study leads to identification of specificity of the Ecm29 for the defective proteasomes. Overall this will help us to understand the role of Ecm29 in regulation of defective proteasomes *in vivo*.

Table of Contents

List of Figures	ix
List of Tables	xi
Acknowledgements	xii
Dedication	xiii
Chapter 1 - Introduction	1
Chapter 2 - Maturation of the proteasome core particle induces and affinity switch that controls regulatory particle association.	16
Abstract	17
Introduction	18
Experimental Procedures	20
Yeast techniques and reagents	20
Antibodies	21
Proteasome purification	24
Reconstitution assay	24
Expression and purification of Pba1 and Pba2 complex	25
Salt dependent binding	25
Binding affinity measurements	26
Cyclohexamide chase	26
2D gel analysis	26
Mass spectrometry	27
MS Data analysis	27
MALDI-TOF Analyses	28
Numerical simulation	28
Results	30
The Pba1 and Pba2 complex prevents RP binding	30
RP readily displaces Pba1 and Pba2 from mature CP	32
A switch in affinity upon CP maturation	36
The Pba2 tail contributes to the affinity switch	37
Pba1 and Pba2 contribute to $\alpha 5$ and $\alpha 6$ incorporation	38

Preventing premature RP binding improves assembly efficiency	41
Discussion.....	44
Author contributions	44
References - Chapter2.....	45
Chapter 3 - Phosphorylation of the C-terminal region of proteasome subunit $\alpha 7$ is required for binding of the proteasome quality control factor Ecm29	49
Abstract.....	50
Introduction.....	51
Experimental procedures	54
Yeast techniques, plasmids and reagents	54
Antibodies used for immunoblots:.....	55
Proteasome purification	55
Yeast phenotypes	58
Fluorescent phospho- and coomassie blue staining	58
Apyrase assay.....	58
Results.....	59
C-terminal tail of $\alpha 7$ subunit is important for Ecm29 binding to the proteasome.	60
Effect of $\alpha 7$ C-terminal tail truncation in vivo.....	63
$\alpha 7$ phosphorylation is required for Ecm29 interaction to CP.	69
Discussion.....	73
Contributions	79
Acknowledgements.....	79
Funding	79
References – Chapter3	80
Chapter 4 - Discussion and future prospective	85
Pre-assembly quality control during CP assembly	87
Blm10 and its affinity with immature and mature CP.	88
Crystal structure of immature CP.....	88
Fate of immature CP-RP complex	89
CP formed in the absence of Pba1-Pba2 complex.	89
Post-assembly Quality control	91

Possible interaction sites on Ecm29	91
Specificity of Ecm29 for mutant proteasomes	93
Post-translation modification of the proteasome subunits and regulation of proteasome activity in disease conditions.	93
References – Discussion and future prospective	95
Appendix A - Supplementary Information for Chapter 2.....	98
Appendix B - Supplementary information for chapter 3	104

List of Figures

Figure 1.1 Proteasome and its subunits arrangements.	2
Figure 1.2 Stages in core particle (CP) assembly	8
Figure 2.1 Pba1-Pba2 prevents RP association with immature CP.	31
Figure 2.2 Pba1 and Pba2 are stable.	33
Figure 2.3 CP undergoes affinity switch upon maturation.	34
Figure 2.4 . Pba1-Pba2 are required for efficient incorporation of $\alpha 5$ and $\alpha 6$	39
Figure 2.5 Pba1-Pba2 prevents assembly deadlock.	42
Figure 3.1 $\alpha 7$ as the putative binding site for Ecm29.	59
Figure 3.2 unstructured C-terminal tail of the $\alpha 7$ is involved in the Ecm29 interaction to the proteasome.	62
Figure 3.3 $\alpha 7$ C-terminal truncation mimics as Ecm29 Δ	64
Figure 3.4 Effect of $\alpha 7$ C-terminal truncation on Ecm29 expression level and its association to the proteasome.	66
Figure 3.5 Exchange of Ecm29 promoter to eliminate differential transcription of Ecm29.	68
Figure 3.6 Phosphomutations at the C-terminal tail of the $\alpha 7$ and Ecm29 expression level.	70
Figure 3.7 Binding of Ecm29 to proteasomes depends on the phosphorylation of the C-terminal tail of $\alpha 7$	71
Figure 3.8 $\alpha 7$ in immature CP is already present in phosphorylated form.	74
Figure 3.9 RP-CP stabilization is not affected with the $\alpha 7$ C-terminal truncation.	76
Figure 4.1 CP subunits comparison between CP from wt and from Pba1 Δ	90
Figure 4.2 Predicted structure from amino acid sequence of yeast Ecm29 using Phyre ² program.	92
Figure 4.3 Model of quality control mechanism during pre-assembly and post-assembly of the proteasome.	94
Figure A.1 Supporting data related to Figure 2.1 Pba1-Pba2 prevents RP association with immature CP	98
Figure A.2 Supporting data related to Figure 2.2 CP undergoes affinity switch upon maturation.	99
Figure A.3 Supporting data related to Figure 3 Pba1-Pba2 prevents assembly deadlock.	101

Figure A.4 Supporting data related to Figure 4 Pba1-Pba2 are required for efficient incorporation of $\alpha 5$ and $\alpha 6$	102
Figure B.1 Supporting data related to figure 3.4 Effect of $\alpha 7$ C-terminal truncation on Ecm29 expression level and its association to the proteasome.	104
Figure B.2 Supporting data related to figure 3.7 Phosphorylation at the C-terminal tail of the $\alpha 7$ is necessary for the Ecm29 interaction to the proteasome.	105

List of Tables

Table 1.1 Diseases and the proteasome activity (modified from ¹⁵).....	4
Table 1.2 Chaperones for the proteasome assembly.....	5
Table 2.1 Yeast strains used for results in chapter-2	22
Table 2.2 Mass spectrometry analyses of band 1 and band 2 in Figure 2.4	40
Table 3.1 Yeast strains used for results in chapter-3.	56
Table 4.1 Mass spectrometry analysis of immature CP purified from Ump1-TAP tagged strain.	103

Acknowledgements

I would like to express my sincere gratitude to my advisor Dr. Jeroen Roelofs for the continuous support throughout of my Ph.D. study and research, for his motivation, enthusiasm, and immense knowledge. His guidance helped me through my research and writing of this thesis. I could not have imagined having a better advisor and mentor for my Ph.D. study. Thank you Jeroen for giving me an opportunity to work on diverse and exciting projects!

My sincere thanks also goes to my thesis committee members Dr. Mike Kanost, Dr. Stella Lee, and Dr. Michal Zolkeiwski, and former committee member Dr. Alexander Beeser for their encouragement, insightful comments, and feedback during my progress in graduate school.

I thank my fellow lab mates in Roelofs lab: Alex Ondracek, Xavier Capalla, Ranjit Singh, Alina and all undergraduate and graduate students for the stimulating discussions during lab meetings, constant support and for all the fun we have had in the last five years. My special thanks go to the friends, faculty and staff members in Department of Biochemistry and Molecular Biophysics and Division of Biology. I cannot thank enough to my roommate Siddharth, friends Ashima, Rohit, Sunil, Vinay, and Janu for being there as a family away from home.

In particular, I am grateful to have these people in my life ...my previous mentors Dr. Maheshwari, and Dr. Bhalsingh, for enlightening me the first glance of research and great friend and brother Dr. Avinash Veer who always believed in me and my potential to do research.

Last but not the least; I would like to thank my family: my parents Pushpalata and Sadanand Wani for trusting my decision to pursue career in research. Thank you to my beautiful and loving wife Ashwini who has a big contribution in supporting me, correcting me and improving me whenever I needed the most. Finally I must acknowledge my in-laws Surekha and Shantkumar Bagwe for being there as a source constant encouragement and support.

Dedication

This work is dedicated to my parents Pushpalata and Sadanand Wani, my in-laws Shantkumar and Surekha Bagwe and to my loving wife Ashwini.

Chapter 1 - Introduction

Large multisubunit complexes and challenges in their biogenesis.

Almost all cellular processes in the cell occur through protein-protein interactions. Most often these processes are either regulated through multi-protein cascades or through multi protein complexes. In multi-protein cascade pathways (e.g. blood coagulation), one step in the cascade is handled by the single protein at a time and then channeled to the next protein in the cascade via activation or via posttranslational modifications. Some of the crucial multistep processes in the cells however are accomplished by the protein complexes made of many subunits those either of one type (homomer) or different types (heteromer) of polypeptides (e.g. Spliceosome, Ribosome, Proteasome etc.). Here, each subunit of the complex can either have distinct role or perform ancillary function in order to complete the cumulative task by particular multisubunit complex. Proper assembly of these multisubunit complexes is essential to maintain their optimal biological functions. Therefore steps in the assembly processes of most of these large multisubunit complexes are evolutionary conserved. This shows the preserved importance of multisubunit assembly in order to conserve the crucial signaling pathways that facilitates the regulation for cell survival¹.

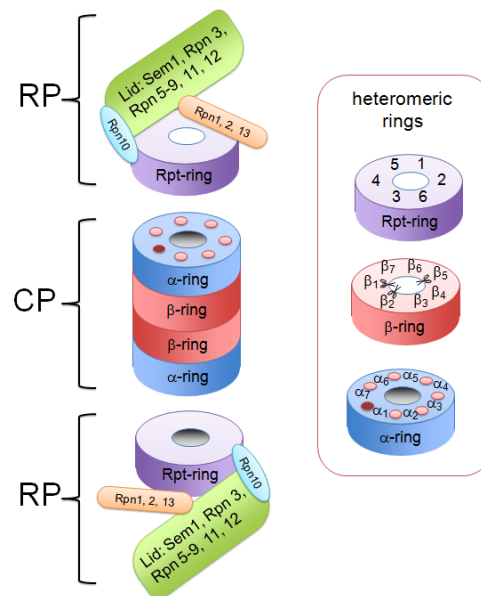
Multisubunit complex assembly is a complicated process where many subunits have to come together in a precise order. Here specific surface areas of the different subunits will have to interact with each other to form the functional complex. Cell takes the help of auxiliary proteins called chaperones that assist in the efficient formation of the multisubunit complexes. Many assembly chaperones have been identified over the last few years are specific for the specific protein complex assembly². Unlike the well-known traditional chaperones, the assembly chaperones do not process nascent protein folding into tertiary structures and are not promiscuous in their substrate choice. Additionally, assembly chaperones contain a variety of protein-protein interacting domains. Hence, these chaperones are associated with the precursor subunits and subcomplexes during assembly process to guide them for interaction with other subcomplexes. For example, Ribosome assembly in yeast involves more than 200 assembly factors and approximately 79 small nuclear RNAs to assist in the ribosome assembly process³. Similarly spliceosome requires seven 'sm' proteins to assist in the processing and arrangement of

snRNPs to form spliceosome⁴. Likewise, proteasome a protein degradation complex also takes help of ten chaperones to assemble into functional complex^{5,6}. Most often chaperones are not part of the final assembled product, hence they are timely released during assembly process. In addition, recently it has been shown that many of these chaperones are involved in avoiding nonspecific premature assembly formations and perform a type of a quality control function^{7,8}. Despite being identified for their importance in the assembly, the detailed mechanisms of function of many of these chaperones is still under investigation and certainly lack the clear understanding.

Proteasome: protein-degrading large multisubunit complex.

The work in this thesis is specifically focused on the assembly of the large protein degrading protease complex, proteasome. The typical 26S proteasome in yeast is a ~ 2500 kDa complex that is made up of two 19S regulatory particles (RP) and 20S core particle (CP). RP recognizes ubiquitinated protein substrates, deubiquitinate and unfold them into polypeptide form. Once unfolded, substrate is then translocated to the core particle. CP is a cylindrical-shaped structure that hydrolyzes the protein substrates into short peptides (Fig 1.1).

Figure 1.1 Proteasome and its subunits arrangements.



Arrangement of subunits in the typical 26S proteasome complex. Regulatory particle (RP) consists of base that is formed by six Rpt and two Rpn subunits and lid that is formed by 11 Rpn

subunits. Core particle (CP) consists of four rings. Out of these, outer two are α -rings and central two are β -rings each made up of seven subunits. Three of the seven β subunits namely $\beta 1$, $\beta 2$ and $\beta 5$ has proteolytic activity. β -rings are sandwiched between two α -rings that made up of seven α subunits in each rings⁹.

The RP has in total 19 subunits that are distributed over two subcomplexes, the base and the lid. The base contains six are AAA-ATPase subunits called Rpts (Rpt1 to Rpt6) and two largest non-ATPase subunits (Rpn1 and Rpn2). The other ten non-ATPase subunits (Rpn3, Rpn5 to Rpn13) are part of the lid subcomplex. Further, CP is made of four stacked rings with an arrangements of $\alpha_{1-7}\beta_{1-7}\beta_{1-7}\alpha_{1-7}$. There are two outer α -rings in the CP, each made up of seven α subunits ($\alpha 1$ to $\alpha 7$). Middle two β -rings are also made up of seven subunits ($\beta 1$ to $\beta 7$) each. RP through its base subunits is directly associated with the α -ring on both sides of the CP. Overall the proteasome complex is assembled by putting in total 66 subunits together¹⁰.

Protein substrate that needs to be degraded through proteasome are first tagged with the small 76 amino acid protein, ubiquitin. Ubiquitin tag on the substrate is added through Ub-activating (E1), Ub-conjugating (E2), and Ub-ligating (E3) enzyme cascade of UPS pathway. Although it is now well known that ubiquitin is not the sole warrant for degradation and ubiquitin-independent proteasomal degradation has also been observed for many substrates¹¹⁻¹⁴. Substrates that get ubiquitin tag are then recognized by the Rpn10 and Rpn13 subunits from RP. Prior to degradation the ubiquitin is recycled as it is removed through deubiquitinated by Rpn11 subunit. Ubiquitin molecules are then recycled for tagging onto the new protein substrate. The deubiquitinated substrate is then unfolded by the Rpt subunits though an ATP dependent process and translocated into the core particle through the α -ring that has the narrow substrate entry gate formed with the N-terminal ends of the α subunits. Once translocated substrate reaches to the β -ring, here three β subunits namely $\beta 1$, $\beta 2$ and $\beta 5$ those having post-acidic, tryptic, and chymotryptic activity respectively hydrolyzes protein into small peptides and peptides are then released from the proteasome. Overall the optimal protein hydrolysis by the proteasome demands proper functioning of all the components of the proteasome complex. One way to achieve this by assuring the efficient and precise formation of the proteasome holoenzyme complex.

Proteasome activity and diseases

Improper assembly of the complex can compromise the activity of the proteasome. This generally leads to either accumulation of aberrant or unwanted proteins or untimely degradation of essential proteins from the cell resulting into disturbed protein homeostasis. Many disease conditions have been reported where proteasome activity is either reduced or enhanced compared to its normal activity^{15,16}. The table 1.1 below summarizes some of these diseases.

Table 1.1 Diseases and the proteasome activity (modified from¹⁵)

Disease	proteasomes activity	Proteasome population affected
Cardiac dysfunction - transient ischemia - pressure overload	decreased activity decreased activity	26S proteasomes 26S proteasomes
Neurodegenerative - Alzheimer's - Parkinson's - amyotrophic lateral sclerosis - Huntington's	decreased activity decreased activity decreased activity decreased activity	20S/26S proteasomes 20S/26S proteasomes 20S/26S proteasomes 20S/26S proteasomes,
Cancer - multiple myeloma - renal carcinoma	increased activity, depressed expression	20S/26S proteasomes, immunoproteasomes
Cachexia - sepsis - metabolic acidosis	increased activity increased activity	20S/26S proteasomes 20S/26S proteasomes

Due to its direct or indirect involvement in many diseases including cancers and neurodegenerative diseases; proteasome in recent years has become a favorable target for the drug discovery. Over the last decade several molecules have been screened that can act as a proteasome inhibitors. Currently, FDA approved boronate derived molecule Bortezomib (brand name: Velcade) and epoxyketone derived proteasome inhibitor molecule carfilzomib (Kyprolis) are used for the treatment of cancer patients¹⁷. In recent studies, ixazomib (MLN9708) has been demonstrated as an effective reversible oral proteasome inhibitor that has now reached into Phase III trials¹⁸.

Since several key proteins in crucial signaling pathways in the cells are regulated through proteasome; inhibiting proteasome has shown to have severe side effects and hence combinational therapies are required in the treatments¹⁹. Moreover studies reporting increased

resistance to these proteasome inhibitors in cancer patients are not uncommon²⁰⁻²³. This demands the development of alternate strategies to regulate the proteasome activity in disease conditions rather than its inhibition. One way the proteasome activity can be modulated is by regulating the proteasome formation in the cell. Hence, improving our knowledge on the proteasome assembly will certainly help in identifying new specific targets that can be altered to control the proteasome activity specific to the diseases conditions.

Proteasome assembly and assembly chaperones.

Over the last couple of decades tremendous efforts there have been focused on elucidate the understanding of proteasome assembly. Biochemical and genetic analysis of proteasome assembly lead to rapid advancement in identification and characterization of proteins called chaperones that are specific for proteasome assembly. Ten different chaperones have been identified that contribute towards efficient proteasome formation but their timely role in the assembly pathway is not yet clearly understood⁹. In addition, new proteins are being identified that can function as proteasome chaperones indicating the complexity in regulation of proteasome assembly²⁴. Most importantly these assembly chaperones are evolutionary conserved from lower to higher eukaryotes as with proteasome subunits suggesting they have functional significance in the cell. Hence, detailed understanding of these chaperones functions is necessary as it directly affects the proteasome complex formation and might ultimately have impact on the functionality of the proteasome.

Table 1.2 Chaperones for the proteasome assembly

Proteasome Subcomplex	Chaperones (Human orthologue)
Regulatory Particle (RP)	Hsm3 (S5b) Nas2 (p27/Bridge-1) Nas6 (Gankyrin) Rpn14 (PAAF1) Adc17
Core Particle (CP)	Pba1 (PAC1 or PSMG1) Pba2 (PAC2 or PSMG2) Pba3 (PAC3 or PSMG3) Pba4 (PAC4 or PSMG4) Ump1 (POMP)

Proteasome assembly chaperones can be divided into two groups - RP assembly chaperones and CP assembly chaperones; due to their specificity for the assembly of particular subcomplexes. Table 1.2 above listed chaperones identified till now for the proteasome assembly with their human orthologue shown in bracket.

RP assembly and Chaperones

How cells precisely assemble an asymmetrical heterogeneous structure of 19S regulatory particle was a long standing question until last decade. The RP assembly is a complicated task since RP subunits contain varied domain structures that makes them structurally different²⁵. Hence, the spontaneous assembly of all the subunits together to form base and lid can be ruled out and certainly needs help from the chaperone.

Although assembly chaperones specific for the lid assembly has yet to be identified, different assembly modules have been presented for its assembly. Biochemical and mass spectrometric approaches have been used to identify lid intermediates formed when one or more Rpn subunits are mutated from yeasts. The current model for lid formation includes interaction between subcomplexes containing Rpn5, 6, 8, 9, and 11 as one module and Rpn3, Rpn7, and Sem1 as another^{26, 27}. The Rpn12 incorporation seems to join the assembly in the last stage and complete the lid assembly²⁸. The improper interaction between the subunits of these modules or formation of wrong lid subcomplex intermediate or no incorporation of Rpn12 can hinder the lid formation²⁸. This strongly indicates this process must be associated with the chaperones that help in promoting the precise lid formation and elimination of misassembled lid components through some quality control process²⁹.

In comparison to the lid assembly, formation of base that contains six AAA ATPases has been well studied and five assembly chaperones have been identified those are evolutionary conserved from yeast to human (Table 1.2). In yeast Hsm3 (human orthologue: S5b), Nas2 (p27), Nas6 (Gankyrin), Rpn14 (PAAF1) and recently reported Adc17 are known to function as base assembly chaperones. Although, RP chaperones require C-domain of the Rpt subunits for their interaction; the analysis of at least former four chaperones showed great variation among each other in terms of their structures^{6,9,24}. This suggests that base assembly is highly coordinated by maintaining specificity between Rpt subunit and particular RP chaperone that it binds to.

Specifically, Hsm3 interacts with the C-domain of Rpt1, Nas2 binds to Rpt5 C-domain, Nas6 that of Rpt3, and Rpt6 C-domain interacts with Rpn14. Similar to lid assembly, base assembly intermediates have also been observed in biochemical and structural studies of these chaperones. These intermediates are formed by one or more Rpt subunits and are associated with RP chaperones. Deletion of these chaperones affects the efficiency of the proteasome formation highlighting its importance⁶.

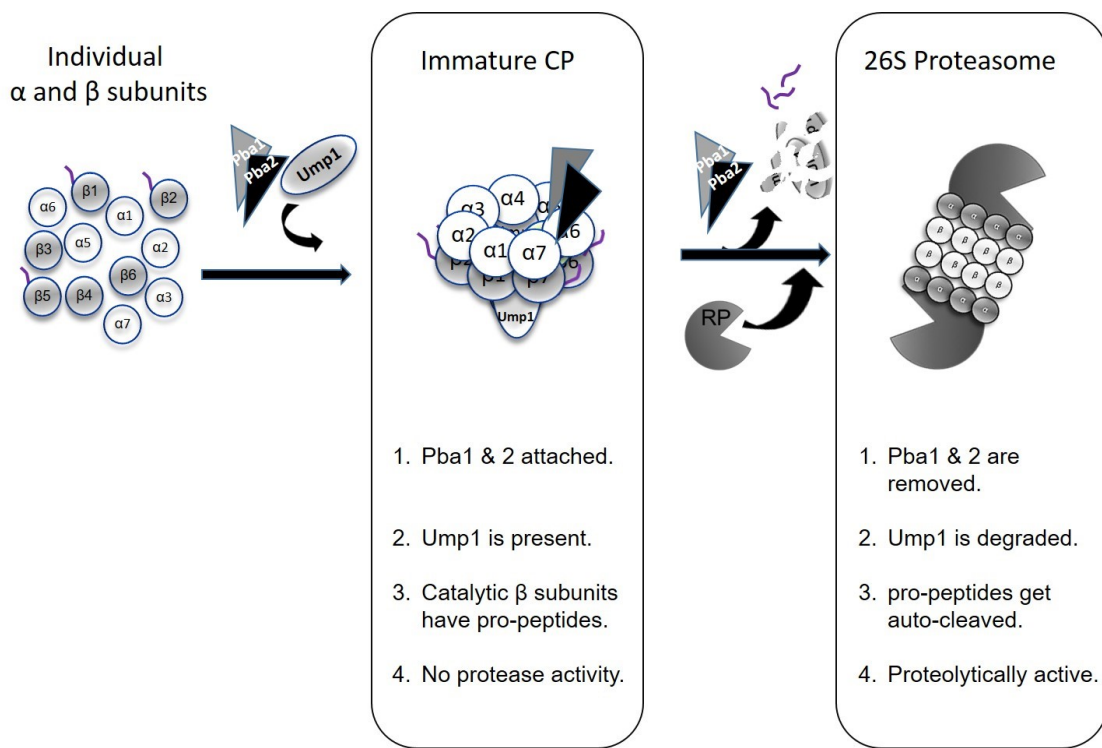
RP assembly can happen by two possible means. First, base subunits can form a specific heterodimers (Rpt1-Rpt2, Rpt3-Rpt6, and Rpt4-Rpt5) along with their chaperones. These dimers are then assembled onto the CP by docking their C-terminal tail into pockets on α -ring surface. Since chaperones are bound with assembly intermediates at the C-domain, there will be a steric interference for the RP to dock onto CP and hence this seems very unlikely. Second most accepted RP assembly pathway proposes removal of all the chaperones after formation of complete ATPase hexameric ring and then docking the ATPase ring onto α -ring surface of the CP. However the timely removal of the RP chaperones during ATPase ring formation is still not well understood. Once Base-CP are formed then lid is assembled using it as a platform³⁰.

CP assembly and Chaperones

Core particle made up of four rings each containing seven subunits is assembled with the help of five chaperones (Pba1, Pba2, Pba3, Pba4 and Ump1). Pba chaperones work in pairs and form heterodimers as Pba1-Pba2 and Pba3-Pba4. Core particle assembly starts with formation of α -ring where Pba1-Pba2 and Pba3-Pba4 nucleates the assembly process (Fig 1.2). Pba1-Pba2 are present on the outer side of the α -ring and hence proposed to prevent the α -ring dimerization. Pba3-4 are attached to other side of the α -ring where β -ring assembles, and hence Pba3-Pba4 has to be displaced from the α -ring before β 4 subunit is incorporated to avoid steric clash³¹. Three β subunits (β 1, β 2, β 5) those having catalytic sites are incorporated in inactive forms containing pro-peptide. Ump1 is a mostly unstructured protein that promotes the formation of precursor complexes of CP. Assembly intermediate containing heptameric α -ring together with partial β -ring (β 1 to β 6 subunits) and three chaperones (Pba1-Pba2 and Ump1) formed during core particle assembly is called 15S or immature core particle. During CP maturation process, two such immature core particles come together, β 7 subunit is incorporated, and proteolytic subunits are activated by pro-peptide auto-cleavage and forms the four ringed mature core particle. Ump1

that is trapped inside CP after CP maturation, becomes its first substrate and gets degraded. During CP assembly, Pba1 and Pba2 are the last chaperones released from the mature CP complex. Other than β subunit arrangement, Ump1 is also required for their pro-peptide cleavage since deletion of Ump1 causes CP formation that is not completely matured³². Since chaperones guide the assembly and help in stabilization of the assembly intermediated, deletion of these chaperones have impact on the complex formations and hence they carry out the important quality control function during the assembly process.

Figure 1.2 Stages in core particle (CP) assembly



Proteasome assembly: $\alpha 1$ to $\alpha 7$ subunits comes together with the help of Pba1-Pba2 and Pba3-Pba4 and forms the heptameric ring. Ump1 assist in assembly of the β -ring which has $\beta 1$ to $\beta 6$ subunits, Pba3-Pba4 is released during β -ring formation. Immature core particle formed has Pba1-Pba2 dimer on the α -ring, catalytic β subunits have pro-peptides and hence it does not have proteolytic activity. Two immature core particle joins together to form mature core particle where ump1 is degrade, Pba1-Pba2 are released, catalytic subunits becomes active and RP associated with the mature CP to form complete 26S proteasome.

Proteasome associate proteins:

Besides the proteasome subunits and assembly chaperones, additional proteins have been identified that associated with the proteasome. The interaction of most of the proteasome associated proteins is salt labile. Hence, to study these proteins the proteasome purification needs to be done under low salt conditions. These proteins are different from the assembly chaperones because they do not promote the assembly process. Instead, they interact with the assembled proteasome or proteasome subcomplexes and can modulate the proteasomal activity. These proteins perform variety of functions and hence they are part of the ubiquitin proteasome system³³.

Work in this thesis is focused on one of the proteasome associated protein called Ecm29. This 210 kDa elongated curved protein contains total 29 HEAT repeat domains and conserved in human (KIAA0368)^{34,35}. Previous work on Ecm29 has shown that it binds to the assembled proteasomes³⁶. Absence of ATP during proteasome purification from *ecm29Δ* strains results into dissociation of proteasome as CP and RP. Ecm29 has observed to be enriched on the proteasome in the absence of nucleotide and function to stabilize the complex^{37,38}. Mutations in proteasome subunits or mutations in the proteasome chaperones that result into defective proteasome complex formations also have higher level of Ecm29^{39,40}. Here, Ecm29 functions as a quality control factor that binds to such defective proteasomes and inhibits their ATPase activity. This mechanism of proteasome activity inhibition is crucial in order to avoid the aberrant protein degradation through mutant proteasomes.

Quality control in proteasome assembly

The variety of assembly intermediate modules formed during proteasome assembly are part of the quality control process that makes sure proper interactions between subunits as well as between intermediate subcomplexes are maintained and miss-assembly is prevented. Chaperones play an important role in the assembly process by their interactions with these modules and avoid the premature interactions. If such interactions happen as a result of mutations in proteasome subunits, mutations in assembly chaperones, or under stress conditions then proteasome assembly can go wrong and can form the misassembled proteasome. These proteasomes can be regulated by the Ecm29. Overall there is a pre-assembly as well post-assembly quality control mechanism is involved. The work reported in this thesis describes the

detailed investigation on two of such quality control mechanisms. We identified the new role of Pba1-Pba2 chaperones in a pre-assembly quality control during CP assembly. We also expanded our knowledge about post-assembly quality control mechanism by understanding interactions of Ecm29 with the assembled proteasome.

Pre-assembly quality control mechanism

Studies with RP chaperones Hsm3 and Nas2 have shown that in addition to help in Rpt ring formation it also prevent interaction of base intermediates with CP. C-terminal tail of the Rpt subunits dock into the pocket formed between two α subunits⁴¹. Interaction of RP chaperones to the same site on Rpt subunits during base assembly restrict docking of the RP assembly intermediates onto the CP and hence prevent formation of immature complex formations⁶. While the role of the RP chaperones in regulating the RP-CP association has been established; mechanistic understanding still awaits detailed biochemical experimentations.

Analysis of the CP chaperones have mainly focused for the role in the CP assembly. Two CP chaperones Pba1 and Pba2 have been identified in 2005 and several functions have been proposed⁴². Besides nucleating the formation of the α -ring, Pba1-Pba2 have been proposed to prevent α -ring dimerization. Furthermore, these chaperones might function to ensure “quality control” during the CP assembly³¹. However, the biochemical evidence supporting these functions is missing. Pba1-Pba2 are bound to the face of the CP cylinder and are released at the last stage in the CP assembly. We hypothesized Pba1-Pba2 also can regulate the association of CP with the RP during CP assembly process. Chapter-2 in this thesis describes our biochemical analysis of Pba1-Pba2 interactions with CP during CP maturation. By purifying CP assembly intermediate 15S immature CP in the presence and absence of Pba1-Pba2 we showed that Pba1-Pba2 interaction with the immature CP is necessary to prevent early association of RP with immature CP. Pba1-Pba2 in this case shows strong affinity for immature CP and loses its affinity for CP after CP maturation. RP on the other hand shows weak affinity for the immature CP and strong affinity for the mature CP. Conversely, RP shows weak affinity to immature CP and strong affinity for mature CP easily displacing Pba1-Pba2 from mature CP. Additionally we identified that the strong affinity interaction of Pba1-Pba2 with immature CP is contributed through the C-terminal tail Hb-Y-X motif of Pba2. These results implied that CP undergoes a conformational change during its maturation that results into the affinity switch. Further our

mathematical modeling studies suggest that this type quality control mechanism of affinity switch during CP assembly is necessary in order to prevent formation of wrong subcomplex assembly intermediates that cannot proceed into the efficient proteasome formation.

Post-assembly quality control mechanism

Assistance of assembly chaperones and regulation through pre-assembly quality control mechanism aid the proper and efficient proteasome formation. However defective proteasome formation still occurs in the cell either during physiological stress conditions or due to the mutations in either chaperones or proteasome subunits itself. Cell has evolved a mechanism to recognize such mutant proteasomes after proteasome assembly.

Chapter-3 in the thesis describes the post-assembly quality control mechanism in the proteasome that involves Ecm29. How Ecm29 recognizes mutant proteasome specifically over the normal proteasome is still unclear. To understand how Ecm29 recognizes mutant proteasomes, we first need to identify the Ecm29 interaction sites onto the RP as well CP of the proteasome. Previous data from our lab showed that Ecm29 interacts with the RP through its Rpt5 subunits. Our current biochemical studies reported in chapter 3 led us to the identification of Ecm29 interaction site on CP. We showed that Ecm29 binds to the $\alpha 7$ subunit of core particle. We further map the interaction sites on $\alpha 7$ and demonstrated that structurally unresolved C-terminal tail of the CP is important for Ecm29 interaction with the proteasome. The $\alpha 7$ C-terminal tail has conserved consecutive acidic residues and three serine phosphorylation sites. Proteasome purified from $\alpha 7$ phosphomutants of these serine residues confirms that Ecm29 binding to proteasome required $\alpha 7$ phosphorylation at C-terminal tail. Further, the $\alpha 7$ C-terminal tail is important *in vivo* as it rescues the phenotype observed from mutant proteasomes.

Overall elucidating the pre-assembly and post-assembly quality control mechanisms of proteasome formation improve our knowledge in regulation of proteasome in the cell *in vivo*. In a broader aspect, identification of key regulatory steps will help in the future for drug discovery that can modulate the proteasome activity by controlling dynamics of proteasome formation in disease conditions rather than its complete inhibition.

References -Introduction

1. Marsh, J.A., Hernandez, H., Hall, Z., Ahnert, S.E., Perica, T., Robinson, C.V., Teichmann, S.A. (2013) Protein complexes are under evolutionary selection to assemble via ordered pathways. *Cell*. **153**, 461-470.
2. Ellis, R.J. (2013) Assembly chaperones: A perspective. *Philos Trans R Soc Lond B Biol Sci*. **368**, 20110398.
3. Woolford, J.L., Jr, Baserga, S.J. (2013) Ribosome biogenesis in the yeast *saccharomyces cerevisiae*. *Genetics*. **195**, 643-681.
4. Chari, A., Golas, M.M., Klingenhager, M., Neuenkirchen, N., Sander, B., Englbrecht, C., Sickmann, A., Stark, H., Fischer, U. (2008) An assembly chaperone collaborates with the SMN complex to generate spliceosomal SnRNPs. *Cell*. **135**, 497-509.
5. Kusmierczyk, A.R., Hochstrasser, M. (2008) Some assembly required: Dedicated chaperones in eukaryotic proteasome biogenesis. *Biol Chem*. **389**, 1143-1151.
6. Roelofs, J. (2009) Chaperone-mediated pathway of proteasome regulatory particle assembly. *Nature*. **459**, 861-865.
7. Karbstein, K. (2013) Quality control mechanisms during ribosome maturation. *Trends Cell Biol*. **23**, 242-250.
8. Matsuo, Y. (2014) Quality control of pre-ribosome coupled with ribosome biogenesis. *Seikagaku*. **86**, 793-797.
9. Bedford, L., Paine, S., Sheppard, P.W., Mayer, R.J., Roelofs, J. (2010) Assembly, structure, and function of the 26S proteasome. *Trends Cell Biol*. **20**, 391-401.
10. Adams, J. (2003) The proteasome: Structure, function, and role in the cell. *Cancer Treat Rev*. **29 Suppl 1**, 3-9.
11. Eralles, J., Coffino, P. (2014) Ubiquitin-independent proteasomal degradation. *Biochim Biophys Acta*. **1843**, 216-221.
12. Fortmann, K.T., Lewis, R.D., Ngo, K.A., Fagerlund, R., Hoffmann, A. (2015) A regulated, ubiquitin-independent degron in IkappaBalpha. *J Mol Biol*. **427**, 2748-2756.
13. Ben-Nissan, G., Sharon, M. (2014) Regulating the 20S proteasome ubiquitin-independent degradation pathway. *Biomolecules*. **4**, 862-884.
14. Lee, D.H., Sherman, M.Y., Goldberg, A.L. (1996) Involvement of the molecular chaperone Ydj1 in the ubiquitin-dependent degradation of short-lived and abnormal proteins in *saccharomyces cerevisiae*. *Molecular and Cellular Biology*. **16**, 4773-81.

15. Dahlmann, B. (2007) Role of proteasomes in disease. *BMC Biochem.* **8 Suppl 1**, S3.
16. Schmidt, M., Finley, D. (2014) Regulation of proteasome activity in health and disease. *Biochim Biophys Acta.* **1843**, 13-25.
17. Moreau, P., Richardson, P.G., Cavo, M., Orłowski, R.Z., San Miguel, J.F., Palumbo, A., Harousseau, J.L. (2012) Proteasome inhibitors in multiple myeloma: 10 years later. *Blood.* **120**, 947-959.
18. Gupta, N., Zhao, Y., Hui, A.M., Esseltine, D.L., Venkatakrishnan, K. (2015) Switching from body surface area-based to fixed dosing for the investigational proteasome inhibitor ixazomib: A population pharmacokinetic analysis. *Br J Clin Pharmacol.* **79**, 789-800.
19. Chen, D., Frezza, M., Schmitt, S., Kanwar, J., Dou, Q.P. (2011) Bortezomib as the first proteasome inhibitor anticancer drug: Current status and future perspectives. *Curr Cancer Drug Targets.* **11**, 239-253.
20. Duvefelt, C.F., Lub, S., Agarwal, P., Arngarden, L., Hammarberg, A., Maes, K., Van Valckenborgh, E., Vanderkerken, K., Jernberg Wiklund, H. (2015) Increased resistance to proteasome inhibitors in multiple myeloma mediated by cIAP2 : Implications for a combinatorial treatment. *Oncotarget.*
21. Niewerth, D., Jansen, G., Assaraf, Y.G., Zweegman, S., Kaspers, G.J., Cloos, J. (2015) Molecular basis of resistance to proteasome inhibitors in hematological malignancies. *Drug Resist Updat.* **18**, 18-35.
22. Kale, A.J., Moore, B.S. (2012) Molecular mechanisms of acquired proteasome inhibitor resistance. *J Med Chem.* **55**, 10317-10327.
23. Lu, S., Wang, J. (2013) The resistance mechanisms of proteasome inhibitor bortezomib. *Biomark Res.* **1**, 13-7771-1-13.
24. Hanssum, A., Zhong, Z., Rousseau, A., Krzyzosiak, A., Sigurdardottir, A., Bertolotti, A. (2014) An inducible chaperone adapts proteasome assembly to stress. *Mol Cell.* **55**, 566-577.
25. Park, S., Tian, G., Roelofs, J., Finley, D. (2010) Assembly manual for the proteasome regulatory particle: The first draft. *Biochem Soc Trans.* **38**, 6-13.
26. Fukunaga, K., Kudo, T., Toh-e, A., Tanaka, K., Saeki, Y. (2010) Dissection of the assembly pathway of the proteasome lid in *saccharomyces cerevisiae*. *Biochem Biophys Res Commun.* **396**, 1048-1053.
27. Estrin, E., Lopez-Blanco, J.R., Chacon, P., Martin, A. (2013) Formation of an intricate helical bundle dictates the assembly of the 26S proteasome lid. *Structure.* **21**, 1624-1635.

28. Tomko, R.J., Jr, Hochstrasser, M. (2011) Incorporation of the Rpn12 subunit couples completion of proteasome regulatory particle lid assembly to lid-base joining. *Mol Cell*. **44**, 907-917.
29. Peters, L.Z., Karmon, O., David-Kadoch, G., Hazan, R., Yu, T., Glickman, M.H., Ben-Aroya, S. (2015) The protein quality control machinery regulates its misassembled proteasome subunits. *PLoS Genet*. **11**, e1005178.
30. Yu, Z., Livnat-Levanon, N., Kleifeld, O., Mansour, W., Nakasone, M.A., Castaneda, C.A., Dixon, E.K., Fushman, D., Reis, N., Pick, E., Glickman, M.H. (2015) Base-CP proteasome can serve as a platform for stepwise lid formation. *Biosci Rep*. **35**, 10.1042/BSR20140173.
31. Ramos, P.C., Dohmen, R.J. (2008) PACemakers of proteasome core particle assembly. *Structure*. **16**, 1296-1304.
32. Ramos, P.C., Hockendorff, J., Johnson, E.S., Varshavsky, A., Dohmen, R.J. (1998) Ump1p is required for proper maturation of the 20S proteasome and becomes its substrate upon completion of the assembly. *Cell*. **92**, 489-499.
33. Schmidt, M., Hanna, J., Elsasser, S., Finley, D. (2005) Proteasome-associated proteins: Regulation of a proteolytic machine. *Biol Chem*. **386**, 725-737.
34. Gorbea, C., Geoffrey, M.G., Teter, K., Randall, K.H., Rechsteiner, M. (2004) Characterization of mammalian Ecm29, a 26 S proteasome-associated protein that localizes to the nucleus and membrane vesicles. *The Journal of Biological Chemistry*; **279**, 54849-54861.
35. Andrey, V.K., Gorbea, C., Joaqu n Ortega, Rechsteiner, M., Alasdair, C.S. (2004) New HEAT-like repeat motifs in proteins regulating proteasome structure and function. *J Struct Biol*. **146**, 425-430.
36. Kleijnen, M.F. (2007) Stability of the proteasome can be regulated allosterically through engagement of its proteolytic active sites. *Nat Struct Mol Biol*. **14**, 1180-1188.
37. Hendil, K.B., Hartmann-Petersen, R., Tanaka, K. (2002) 26 S proteasomes function as stable entities. *J Mol Biol*. **315**, 627-636.
38. Leggett, D.S. (2002) Multiple associated proteins regulate proteasome structure and function. *Mol Cell*. **10**, 495-507.
39. Park, S., Kim, W., Tian, G., Steven, P.G., Finley, D. (2011) Structural defects in the regulatory particle-core particle interface of the proteasome induce a novel proteasome stress response. *The Journal of Biological Chemistry*; **286**, 36652-36666.

40. Stella Yu-Chien Lee, Ia, A.D., Roelofs, J. (2011) Loss of Rpt5 protein interactions with the core particle and Nas2 protein causes the formation of faulty proteasomes that are inhibited by Ecm29 protein. *The Journal of Biological Chemistry*; **286**, 36641-36651.
41. Smith, D.M. (2007) Docking of the proteasomal ATPases' carboxyl termini in the 20S proteasome's alpha ring opens the gate for substrate entry. *Mol Cell*. **27**, 731-744.
42. Hirano, Y. (2005) A heterodimeric complex that promotes the assembly of mammalian 20S proteasomes. *Nature*. **437**, 1381-1385.

Chapter 2 - Maturation of the proteasome core particle induces and affinity switch that controls regulatory particle association.

Prashant S. Wani¹, Michael A. Rowland³, Alex Ondracek², Eric J. Deeds^{3,4#} and Jeroen Roelofs^{1,2#}

*1- Graduate Biochemistry Group, Department of Biochemistry and Molecular Biophysics,
Kansas State University, Manhattan, Kansas 66506 USA*

*2- Molecular, Cellular, and Developmental Biology Program, Division of Biology, Kansas State
University, Manhattan, Kansas 66506 USA*

3- Center for Bioinformatics, University of Kansas, Lawrence, KS 66047 USA

4- Department of Molecular Biosciences, University of Kansas, Lawrence, KS 66047 USA

Published in the Nature Communication journal, volume 6, Article number: 6384,
doi:10.1038/ncomms7384, 16 March 2015.

Abstract

Proteasome assembly is a complex process, requiring 66 subunits distributed over several subcomplexes to associate in a coordinated fashion. Ten proteasome-specific chaperones have been identified that assist in this process. For two of these, the Pba1-Pba2 dimer, it is well established that they only bind immature core particles (CPs) *in vivo*. In contrast, the regulatory particle (RP) utilizes the same binding surface but only interacts with the mature CP *in vivo*. It is unclear how these binding events are regulated. Here, we show that Pba1-Pba2 binds tightly to the immature CP, preventing RP binding. Changes in the CP that occur on maturation significantly reduce its affinity for Pba1-Pba2, enabling the RP to displace the chaperone. Mathematical modelling indicates that this ‘affinity switch’ mechanism has likely evolved to improve assembly efficiency by preventing the accumulation of stable, non-productive intermediates. Our work thus provides mechanistic insights into a crucial step in proteasome biogenesis.

Introduction

The selective and timely degradation of polypeptide chains in the cell is important for overall protein homeostasis as well as an integral part of many cellular processes. Many proteins destined for degradation undergo a modification where ubiquitin is covalently attached to lysine residues. The ubiquitin-tag targets substrates to the proteasome, where they are deubiquitinated, unfolded, and hydrolyzed into short peptide fragments. The proteasome itself is a complex molecular machine, containing 66 subunits that must assemble into a 2.5 MDa complex. The subunits are broadly organized into a regulatory particle (RP or 19S, also called PA700 in mammals) that is responsible for substrate recognition, deubiquitination, and unfolding, and a proteolytically active core particle (CP or 20S)¹. The CP is formed by four stacked rings, each consisting of seven unique α -subunits or seven unique β -subunits, in an $\alpha_{1-7} \beta_{1-7} \beta_{1-7} \alpha_{1-7}$ arrangement. During CP maturation, the β 1 (Pre3), β 2 (Pup1), and β 5 (Pre2) subunits become proteolytically active through an autocatalytic process that removes propeptides present within these subunits. This occurs when two half CPs, often referred to as 15S or immature CP, dimerize. In yeast, five assembly chaperones, Ump1, Pba1 (also called Poc1), Add66 (also called Pba2 or Poc2), Irc25 (also called Pba3, POC3, or DMP2), and Poc4 (also called Pba4 or Dmp1) have been found to bind the CP prior to its maturation (reviewed in ²). Here, we will refer to these factors as Ump1 and Pba1 to Pba4. Each of these has a human ortholog, known as POMP, and PSMG1 to PSMG4 (also called PAC1 to PAC4). Pba3 and Pba4 form a dimer that binds to α 5 (Pup2) and promotes proper α -ring assembly³⁻⁵. The Pba3-Pba4 dimer must dissociate before the β 4 (Pre1) subunit can join the complex due to extensive steric clashes with this subunit⁴. The chaperone Ump1 associates with immature CP after the α -ring forms. Upon dimerization of half CPs, Ump1 is retained inside the CP and is degraded as part of the maturation process⁶. Pba1 and Pba2 form a dimer that, like Ump1, is present on the half CP, but binds on the outside of the CP cylinder base^{7,8}. Although Pba1-Pba2 has been shown to prevent α -ring dimerization in mammals⁹, its cellular functions remain poorly characterized.

While the CP can be found in the cell by itself (a.k.a. the free CP), in most cases it acts in consortium with a set of associated factors^{10,11}. In yeast the RP, Blm10, and Pba1-Pba2 can all bind to the ends of the CP cylinder, although the later has only been shown to bind mature CP *in vitro*^{8,12-14}. Blm10 (PSME4/PA200 in humans) has been proposed to function in CP

maturation^{15,16}, CP localization¹⁷, and activation of protein degradation¹⁸⁻²⁰. In recent years it has become clear that these interaction partners all utilize a similar mechanism where C-terminal tails dock into pockets located at the interface between CP α -subunits, often facilitated by a conserved C-terminal HbYX-motif^{8,12,19,21-24}. The C-terminal tail of Pba1 docks into the α 5- α 6 (Pup2-Pre5) pocket and the Pba2 tail in the α 6- α 7 (Pre5-Pre10) pocket⁸. Interestingly, the α 5- α 6 pocket is also utilized by Blm10 and the RP subunits Rpt1 and Rpt5, while the α 6- α 7 pocket can associate with Rpt4 and Rpt5^{12-14,24}. This suggests that the RP, Blm10, and Pba1-Pba2 compete with one another for CP binding.

Since the full α -ring forms early in assembly, one would expect *a priori* that any CP binding partner would interact with both mature and immature CPs. While Blm10 can indeed associate with both forms of the CP, the RP is only found associated with mature particles, and Pba1-Pba2 only binds immature CP *in vivo*^{9,16,25-27}. These observations imply that the binding of these factors to the CP is tightly regulated. The RP chaperones Nas2, Nas6, Hsm3, and Rpn14 (known in humans as PSMD9/p27, PSMD10/gankyrin, PSMD5/S5b, and PAAF1/Rpn14 respectively) are one example of this regulation: they all have the capacity to interfere with the association of immature RP subcomplexes and the CP²⁸⁻³⁴. Despite intense research over the last decade, however, surprisingly little is known about the mechanisms that control the interaction between the CP and its binding partners.

In this work, we demonstrate that the Pba1-Pba2 dimer associates tightly with immature CP and prevents them from associating with the RP. Upon CP maturation, however, the affinity of Pba1-Pba2 for the CP changes dramatically, presumably due to a subtle conformational change in the α -ring that impacts the Pba1-Pba2 binding surface. Consistent with this we observed that the Pba2 tail, which plays a negligible role in mature CP binding, contributes substantially to immature CP binding. Mathematical models of proteasome assembly demonstrated that this “affinity switch” is crucial for achieving high yields of functional molecules. Finally, our results reveal that Pba1-Pba2 is also required for efficient incorporation of α 5 and α 6 into the immature CP.

Experimental Procedures

Yeast techniques and reagents

Yeast strains used are summarized in Table 2.1. Genomic manipulation of yeast was done using a PCR based approach^{50,51}. Upon transformation of yeast, successful integration was confirmed by positive PCR for integration and negative PCR for wildtype. Pba1 knockout primer pRL 252 (5'-AAG ATA TCA TCG CAC TAC AGT AAA ATT TTC ATT TAT AGC GCG GAT CCC CGG GTT AAT TAA-3') and pRL253 (5'-CTC TTT CAC TCG CCA TTA CTG ACA TTC TGT GAT CGC CAT CAT CGA TGA ATT CGA GCT CGT-3') and Pba2 knockout primers pRL254 (5'-ACT TCA GGA AAG AAT AGC ACA AAA CCC AAA GGA ACA TAC GCG GAT CCC CGG GTT AAT TAA-3') and pRL255 (5'-TAT ATG CAC TTG TAT AGA AAA CAG ATA TAC TTC TCG GTT CAT CGA TGA ATT CGA GCT CGT-3') were used together with templates pAG25 (natMX4) and pAG32 (hphMX4)⁵¹ in a PCR to prepare DNA for yeast transformation. To create a strain deleted for Blm10, smash and grab prepared genomic DNA from a strain where the Blm10 ORF was replaced with ClonNAT selection cassette²⁷ was used as template for PCR with the following primers: pf2Blm10 (5'-CTG TCA TCA GGG CTT G-3') and pr2Blm10 (5'-GTT GAT CAT TCT CAG TGG-3'). To produce C-terminal truncation of Pba1 that deleted the codons coding for the last three amino acids of Pba1, *pba1-ΔCT3*, primers pRL210 (5'-TGG AGG TGT GAT AGC GCG GCA ATT GGT GCA CAA TCA GGC TGA GGC GCG CCA CTT CT-3') and pRL253 (5'-CTC TTT CAC TCG CCA TTA CTG ACA TTC TGT GAT CGC CAT CAT CGA TGA ATT CGA GCT CGT-3') were used with pFA6a-3HA-kanMX6 as template⁵⁰. To create *pba2-ΔCT3* primers pRL211 (5'-GCA TAC GGA ATG GCG GAT GCA AGA GAT AAA TTT GTA GAT TGA GGC GCG CCA CTT-3') and pRL255 (5'-TAT ATG CAC TTG TAT AGA AAA CAG ATA TAC TTC TCG GTT CAT CGA TGA ATT CGA GCT CGT-3') were used with pFA6a-3HA-TRP1 as template⁵⁰. Integrations were confirmed by PCR and sequencing. To create a strain with C-terminal YFP tag fused to β2 we used a knock-in DNA fragment synthesized from pDH6 as template (a generous gift of the Yeast Resource Center) in a PCR with primers pRL73 (5'-AAT ATT TGT GAC ATA CAA GAA GAA CAA GTC GAT ATA ACG GCT GGT CGA CGG ATC CCC GGG -3') and pRL74 (5'-TGA TTT ACT ATA CTA AAA TAT ACT TAA GTT CTA TGT TTT ACT ATC GAT GAA TTC GAG CTC G -3'). Gibson cloning kit (NEB) was used to create a CEN plasmid that

expresses His-Myc Pba2 utilizing the promoter and terminator of *PBA2*. pRS416 was digested with BamHI and mixed with two PCR products that were generated using yeast gDNA as template together with the following primer pairs: pRL274 (5'-TGC AGC CCG GGG GAG TCC TCG ATT TGA CTG GAA AC-3') with pRL275 (5'-CAG ATC TTC CTC GCT AAT CAG CTT CTG CTC CAT CGT ATG TTC CTT TGG GTT TTG TGC-3') and pRL276 (5'-GAG GAA GAT CTG CAC CAC CAT CAC CAT CAC CAT GGA AGC AGC TGC CTG GTG TTG CC-3') with pRL277 (5'-CGC TCT AGA ACT AGT GAA ATT CAA AGA GAT GTT ACA GAC-3') using the manufacturers protocol. The resulting plasmid is pCEN-His-Myc-Pba2 (pJR643).

Antibodies

A polyclonal antibody that recognizes the Pba1-Pba2 complex was generated using a standard immunization protocol (Rockland Immunochemicals, Inc.) with a dimer of Pba1 and His-tagged Pba2 purified from E.coli as the antigen (see Appendix Figure A.1). Ecm29 and Rpn5 were detected using polyclonal antibodies kindly provided by Dr. Dan Finley (Harvard Medical School, Boston, MA). Monoclonal antibodies for $\alpha 7$ and Rpt5 were kindly provided by Dr. William Tansey (Vanderbilt-Ingram Cancer Center, Nashville, TN). Polyclonal anti-pup1 ($\beta 2$) antibody was a generous gift from Dr. R. Jürgen Dohmen (University of Cologne, Cologne, Germany). Antibodies recognizing Rpt1 and Blm10 were purchased from ENZO life sciences and THETM HIS-tag antibody was obtained from GenScript. Peroxidase-conjugated secondary antibodies were purchased from Jackson Immunoresearch Laboratories and for Fig. 2.2F Rabbit TrueBlot® IgG HRP from Rockland Immunochemicals was used. Anti-Myc antibody (9E10) was derived from an atcc hybridoma cell line (#CRL1729). The monoclonal anti-pgk-1 antibody was purchased from life technologies (#459250). All antibodies were used in 1:000 dilutions in TBST, except those against pgk-1 (1:10,000), Pba1-Pba2 (1:500), Myc (1:5), and Rpt5 (1:5,000). Uncropped images from the most important immunoblots are provided as Supplementary Figure 5 in [online version](#) of the journal article.

Table 2.1 Yeast strains used for results in chapter-2

Strain	*	Genotype	Figure	Ref.
sUB61	A	MAT α lys2-801 leu2-3, 2-112 ura3-52 his3- Δ 200 trp1-1	A.2A-B	(2)
sDL135	A	MAT α pre1::PRE1-TEVProA(HIS3)	2.1A-D, 2.3A-B, 2.3E, 2.4C, A.1A, A.2A, A.2C-D, A.4B.	(3)
sDL133	A	MAT α rpn11::RPN11-TEVPro(HIS3)	2.3B.	(4)
SY36	A	MAT α rpt1::HIS3, ProA-TEV-RPT1 in pEL36 (TRP)	A.2C-D.	(3)
Ump1Tap	B	MAT A ump1::UMP1- CBP-TEV-ZZ-(His3MX6)	2.1C-D, 2.3C, 2.4A, 2.4C, A.1C, A.2C-D, A.4.	(5)
sJR789	A	MAT A pba1::NAT pre1::PRE1-TEVProA(HIS3)	A.1A.	(a)
sJR790	A	MAT A pba2::HYG pre1::PRE1-TEVProA(HIS3)	A.1A.	(a)
sJR601	A	MAT α pba1::HYG pba2::NAT	2.2B	(a)
sJR605	A	MAT A pba1::HYG pba2::NAT pre1::PRE1-TEVProA(HIS3)	2.1A-B, A.1A.	(a)
sJR791	A	MAT A blm10::NAT rpn11::RPN11-TEVProA(HIS3)	A.1A.	(a)
sJR792	B	MAT A pba1::NAT ump1::UMP1- CBP-TEV-ZZ-(His3MX6)	2.1C, 2.4C, A.1C.	(a)
sJR793	B	MAT A pba1::HYG blm10::NAT ump1::UMP1- CBP-TEV-ZZ-(His3MX6)	2.1C-D, 2.3D, A.1C.	(a)
sJR794	B	MAT A blm10::NAT ump1::UMP1- CBP-TEV-ZZ-(His3MX6)	A.1C.	(a)
sJR795	B	MAT A pba1::PBA1 Δ CT3 (KAN) ump1::UMP1- CBP-TEV-ZZ-(His3MX6)	2.3F.	(a)

sJR782	B	MAT A pba2::PBA2 Δ CT3 (KAN) ump1::UMP1- CBP-TEV-ZZ-(His3MX6)	2.3F.	(a)
sJR809	B	MAT A pba1::PBA1 Δ CT3 (KAN) pba2::PBA2 Δ CT3 ump1::UMP1- CBP-TEV-ZZ- (His3MX6)	2.3F.	(a)
sJR797	A	MAT α pup1::PUP1-YFP (KAN) pre1::PRE1- TEVProA(HIS3)	2.3B, A.2B.	(a)
sJR852	A	MAT A pba2::NAT	2.2B	(a)
sJR853	A	MAT A pba2::NAT HIS-MYC-PBA2(URA)	2.2C	(a)
sJR857	A	MAT α pba1::HYG	2.2B	(a)

*All "A" strains have background genotype (lys2-801 leu2-3, 2-112 ura3-52 his3- Δ 200 trp1-1)

All "B" strains have BY4741 background genotype (MAT A his3 Δ 0 leu2 Δ 0 met15 Δ 0 ura3 Δ 0).

(a) This Study

Proteasome purification

The purification of proteasomes and proteasome subcomplexes from yeast were in essence performed as described previously^{29-31,38}. Specific yeast strains were grown overnight in 2 to 3 liters of YPD media (final A600 ~ 10.0). Cells were collected and washed with H₂O. Pellets were resuspended in 1.5 pellet volume of lysis buffer (50 mM Tris [pH8.0], 5 mM MgCl₂, 1 mM EDTA, 1 mM ATP) and lyzed by French press (1200 Psi.). Lysates were cleared by centrifugation (10,000g for 30mins) and supernatant was filtered through cheesecloth prior to incubation with IgG beads (MP Biomedical; 0.75 ml resin bed volume per 25 gram of cell pellet). After 1 hour of incubation (rotating at 4 °C), IgG beads were collected in an Econo Column (Bio-Rad) and washed with 50 bed volumes of ice-cold wash buffer (50 mM Tris [pH 7.5], 5 mM MgCl₂, 100 mM NaCl, 1 mM EDTA, 1 mM ATP). Next, material was washed with 15 bed volumes of cleavage buffer (50 mM Tris [pH 7.5], 5 mM MgCl₂, 1 mM DTT, 1 mM ATP). Bead-bound proteasome complex was either directly analyzed by loading on the SDS-PAGE after boiling with equal amount of 2X SDS PAGE sample buffer or eluted by incubation with His-Tev protease (Invitrogen). Protease was removed by incubation with talon resin prior to concentrating the proteasome complexes using 100-kDa concentrator (PALL Life Sciences). Proteasome purifications were used directly or stored at -80 °C in the presence of 5% glycerol.

Reconstitution assay

Proteasome core particles and regulatory particles³⁸ were purified as described previously³⁸ using strain sJR797 and SY36 respectively. 12.5 nM of CP and 62.5 nM of purified Pba1-Pba2 dimer protein were reconstituted in reconstitution buffer (50 mM Tris-HCl [pH 7.5], 5 mM MgCl₂, 1 mM ATP, 50 mM NaCl, 10% glycerol) (Appendix Figure A.2) and incubated for 30 minutes at 30 °C. Next, increasing amounts of RP were added to different tubes (0 nM, 1.25 nM, 2.5 nM, 6.25 nM, 12.5 nM, 25 nM in reconstitution buffer), and the volume was adjusted to 20 μ l for all samples. Samples were incubated for 30 minutes at 30 °C. To analyze the reconstitution assay, 1/10 volume of native gel loading buffer (50 mM Tris-HCl [pH 7.4], 50% glycerol, 60 ng ml⁻¹ xylene cyanol) was added and samples were loaded onto native gel⁵². First, gels were analyzed by in gel protease activity using LLVY-AMC as substrate. Next, samples were transferred to pvdf membrane for immunoblotting as described previously³⁸.

Expression and purification of Pba1 and Pba2 complex

The ORF of *PBA1* was amplified from yeast gDNA by PCR using primers pRL145 (5'-CTG TTG GAT CCA TGC TTT TTA AAC AAT GGA ATG ACT TAC CAG-3') and pRL146 (5'-CGG GAA TTC TCA TAT ATA TAG GCC TGA TTG TG-3'). The PCR product was cloned into pNU247, a pGEX-6PK-1 derived plasmid, using the enzymes BamHI and EcoRI. The ORF of *PBA2* was amplified from yeast gDNA by PCR using primers pRL147 (5'-GGC AGA TCT TGA AAA CCT GTA TTT CCA GGG ACA GGA TCC GAT GAG CTG CCT GGT GTT G-3') and pRL148 (5'-CTC GAG CTC TCA ATT GTA TAA ATC TAC-3'). The PCR product was cloned into pRSF Duet-1 (EMD Millipore) using BglII and BamHI sites. The resulting plasmids were introduced together into Rosetta DE3 cells (stratagene) to enable co-purification of GST-tagged Pba1 and His-tagged Pba2. Transformed cells were inoculated in LB supplemented with kanamycin, ampicillin and chloramphenicol and incubated at 37 °C with shaking at 200 rpm. At an OD₆₀₀ of 0.6, IPTG was added to 0.1 mM final concentration and the culture was incubated overnight at 37 °C with shaking. Cells were harvested by centrifugation (6,000 g, 10 min., 4 °C), washed in sterile H₂O and resuspended in lysis buffer (20 mM Tris-HCl [pH 8.0], 100 mM NaCl and 0.1% Triton X-100) supplemented with protease inhibitor cocktail tablet (Roche). Lysis was performed at 900 psi using a French press system. Lysate was cleared by centrifugation (10,000 g, 30 min. at 4 °C). To the clear cell lysate glutathione agarose resin (GoldBio) (100 µl per 100 ml culture) was added and samples were incubated at 4 °C for 1 hour. The resin was washed four times with total 50 bed volumes of PBS buffer containing 0.1% triton X-100 and 0.02% Na-azide. To elute the Pba1-Pba2 dimer, resin was washed and resuspended in GST precision cleavage buffer (50 mM Tris-HCl [pH 6.8], 150 mM NaCl, 1 mM DTT, and 0.01% Triton X-100) and incubated overnight in the presence of GST-precision protease. Eluted material was further purified using an AKTA purifier with a HiLoad Superdex 200 column equilibrated with reconstitution buffer (50 mM Tris-HCl [pH 7.5], 5 mM MgCl₂, 50 mM NaCl, 1 mM ATP, and 1 mM DTT). Fractions containing Pba1-His-Pba2 protein were collected and concentrated using 10 KDa concentrator (PALL Life Sciences).

Salt dependent binding

To test for salt dependent binding as described in Figure 2.2, indicated strains were processed using our standard proteasome purification protocol, up until the IgG beads washing

step. Here, 20 bed volumes of a different wash buffer were used (50 mM Tris-HCl [pH 7.5], 5 mM MgCl₂, 1 mM EDTA, and 1 mM ATP, 0.1% triton X-100). Next, washed IgG beads were distributed equally amongst five eppendorf tubes. Beads were resuspended in 5 bed volumes of buffer (50 mM Tris-HCl [pH 7.5], 5 mM MgCl₂, 1 mM EDTA, and 1 mM ATP, 0.1% triton X-100) containing different concentrations of NaCl (0 mM, 100 mM, 250 mM, 500 mM, and 1000 mM NaCl) and incubated for 3 minutes at room temperature under rotation. Beads were pelleted by centrifugation (500 g, 1 minutes at 4 °C). This washing step was performed two additional times. Next, beads were washed twice with 5 bed volumes of low salt buffer (50 mM Tris-HCl [pH7.5], 5 mM MgCl₂, 1 mM DTT, 1 mM ATP, and 0.1% triton X-100). Finally, samples were resuspended in 2X SDS-PAGE sample buffer and loaded on 12% SDS-PAGE.

Binding affinity measurements

Binding kinetics of the His-tagged Pba1-Pba2 to purified mature CP were measured using bio-layer interferometry on a BLItz instrument (ForteBio). The Pba1-Pba2 complex was immobilized on a Ni-NTA biosensor using a 4.5 μM solution. Different concentrations of CP (from 0.0 μM to 1.8 μM) in reconstitution buffer (50mM Tris [pH 7.5], 5mM MgCl₂, 50mM NaCl, 1mM ATP, 10% Glycerol) were used as analyte. Advanced kinetic experiment setup was used and kinetic parameters (k_{on} and k_{off}) and affinity (K_D) were calculated from a global fit (1:1) of the BLItz instrument data using the BLItz software.

Cyclohexamide chase

Specific yeast strains were grown overnight in 5 ml of YPD or minimal selection media. The next day, cells were diluted to OD₆₀₀ 0.3 in fresh medium and allowed to grow up to logarithmic growth (OD₆₀₀ 1.0). Cells were then treated with cyclohexamide (100μg ml⁻¹) for the indicated number of minutes and cells equivalent to 1 ml of OD₆₀₀ 2.0 of cells were collected at each time point. Equal amounts of protein extract from each time point were then loaded on 11% SDS-PAGE and a western blot was performed.

2D gel analysis

Ump1-containing immature CP complexes were purified from sJR792 and sJR793 using the proteasome purification protocol described above. 25 μg of each purified complex was vacuum dried and rehydrated in 140 μl of 2D rehydration buffer (8 M Urea, 2% CHAPS, 20 mM

DTT, 0.002% Bromophenol Blue, 0.5% ZOOM® carrier ampholytes pH 3-10 (Life technology)). Isoelectric focusing was done using ZOOM® IPG Strips - pH 3-10NL (non-linear) according to the manufacturer's protocol. Next, IEF strips were incubated in 1X SDS PAGE sample buffer for 10 minutes. Strips were inserted into 12% percent SDS PAGE to run for the 2nd dimension. After electrophoresis, gels were either stained with coomassie brilliant blue or used to transfer samples to pvdf for subsequent analysis by immunoblotting.

Mass spectrometry

MS-grade solvents were purchased from Burdick & Jackson or Baker, sequencing grade trypsin from Promega and other solutions were the highest grade available from Sigma-Aldrich. For digestions, samples were denatured by SDS-PAGE (gel bands or spots), reduced with TCEP, alkylated with IAA, and digested overnight with 4 $\mu\text{g ml}^{-1}$ trypsin, using Tris-HCl (pH 8.5) to buffer all solutions. For LC-MS/MS analyses, samples were analyzed on a hybrid LTQ-Orbitrap mass spectrometer (Thermo Fisher Scientific) coupled to a New Objectives PV-550 nanoelectrospray ion source and an Eksigent NanoULC chromatography system. Peptides were analyzed by trapping on a 5 cm pre-column using a vented column configuration, followed by analytical separation on a New Objective 75 μm ID fused silica column with an integral fused silica emitter, packed in house with 40 cm of 3- μm Magic C18 AQ beads. Peptides were eluted using a 5-40% ACN/0.1% formic acid gradient performed over 100-200 min at a flow rate of 250 nL min^{-1} .

During elution, samples were analyzed using Top Six methodology, consisting of one full-range FT-MS scan (nominal resolution of 60,000 FWHM, 300 to 2000 m/z) and six data-dependent MS/MS scans performed in the linear ion trap. MS/MS settings used a trigger threshold of 8,000 counts, monoisotopic precursor selection (MIPS), and rejection of parent ions that had unassigned charge states, were previously identified as contaminants on blank gradient runs, or that had been previously selected for MS/MS (dynamic exclusion at 150% of the observed chromatographic peak width).

MS Data analysis

Centroided ion masses were extracted using the extract_msn.exe utility from Bioworks 3.3.1 and were used for database searching with Mascot v2.2.04 (Matrix Science). The search

parameters used were: 6.0 PPM parent ion mass tolerance, 0.6 Da fragment ion tolerance, allow up to 1 missed cleavage; variable modifications, carbamidomethyl (C), oxidation (M), propionamide (C), and pyro-glu (N-term Q). Database searching was conducted using the *Saccharomyces cerevisiae* plus filter, resulting 134809 entries. Peptide and protein identifications were validated using Scaffold v2.2.00 (Proteome Software) and the PeptideProphet algorithm⁵³. Searches were performed using thresholds of 1% peptide false discoveries and 1% protein false discoveries with at least two peptides identified. Proteins that contained similar peptides and could not be differentiated based on MS/MS analysis alone were grouped to satisfy the principles of parsimony.

MALDI-TOF Analyses

Protein spots and gel blanks from 2-D gels were excised and digested with trypsin (8 $\mu\text{g ml}^{-1}$). For MALDI-TOF analyses, peptide extracts were mixed with alpha-cyano-4-hydroxycinnamic acid and analyzed on a Voyager DE-PRO instrument operated in reflectron mode. Individual TOF spectra were routinely externally calibrated with a known peptide mix (100 ppm accuracy). Supplemental strategies included desalting and concentration of peptide extracts on miniature C-18 affinity columns (OMIX tips from Agilent), and internal recalibration of MALDI-TOF spectra using trypsin autolysis products (20 ppm accuracy). MALDI-TOF ion peaks were extracted using Data Explorer 4.0. Spectra were deisotoped at a peak detection threshold of 5% BP intensity, and a peak list from the m/z range 500 to 3000 was built using the five most intense peaks from each 100- m/z interval. Alternatively, weaker spectra were analyzed using manually optimized peak detection windows that visually tracked the baseline noise threshold. Peptide mass fingerprint searches were conducted using MASCOT (v2.2). Protein identifications were accepted if their MASCOT probability based MOWSE scores (PBM) were statistically significant, and if the PBM of the top-ranked candidate was markedly superior to that of the next-ranked candidate. Experimental peptide masses were assessed for systematic divergence from hypothetical calculated peptide masses, wherein random mass deviations were used to reject candidate identifications.

Numerical simulation

Our model of proteasome assembly was represented as a system of Ordinary Differential Equations (ODEs). We numerically integrated these ODEs using the CVODE library in the

SUNDIALS package⁵⁴. A description of the model itself, along with the full set ODEs, can be found in the Supplementary Note 1 and Supplementary Note 2 respectively of the online [supplementary file](#) of journal article. The concentrations of the different proteins in this model were estimated from experimental measurements in yeast⁵⁵, and the interaction parameters (association rates, dissociation rates, affinities, etc.) were taken from bio-layer interferometry measurements (Appendix Figure A.2A).

Results

The Pba1 and Pba2 complex prevents RP binding

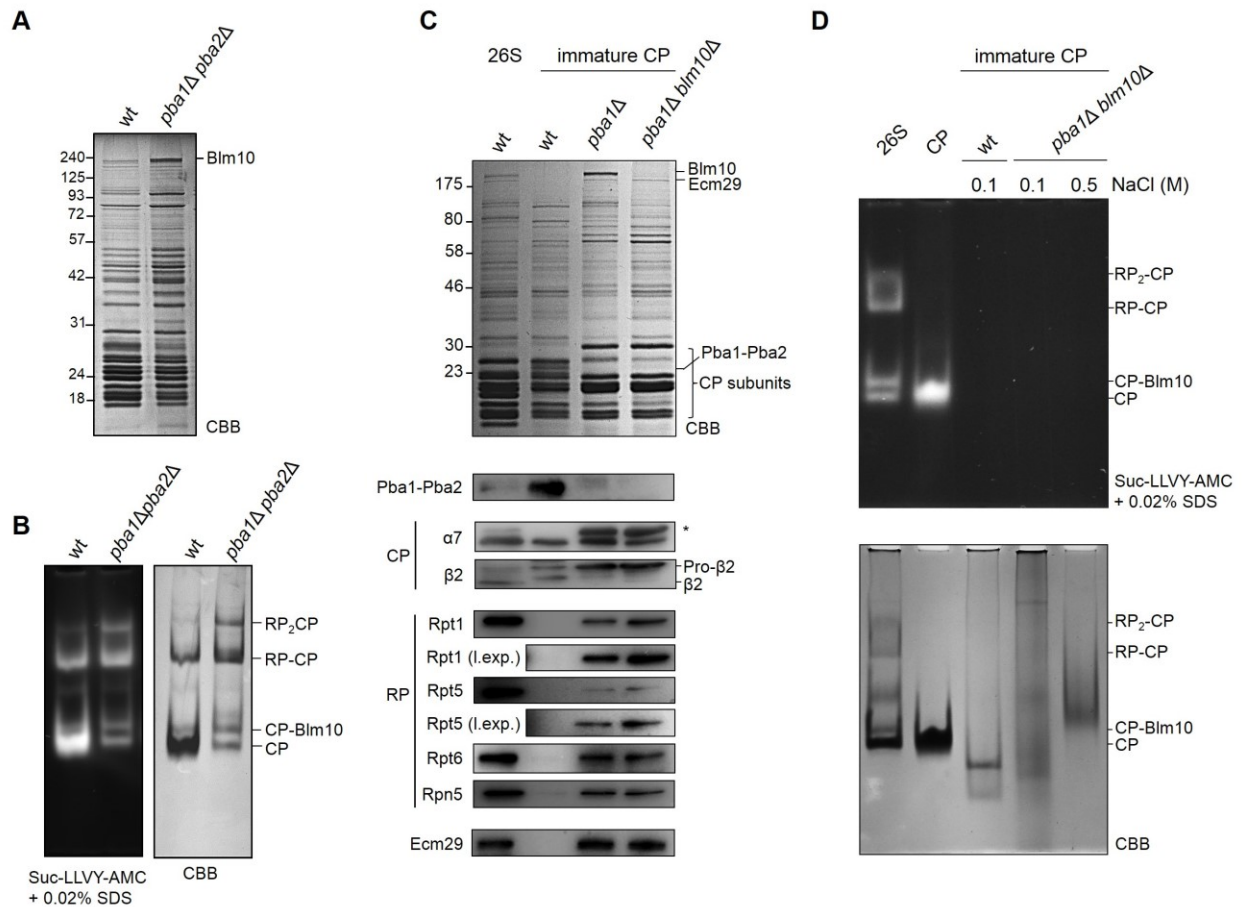
As mentioned above, Pba1-Pba2 and Blm10 likely compete with each other for binding to the CP α -ring. Consistent with this idea, upon purification of proteasomes from *pba1* Δ , *pba2* Δ or *pba1* Δ *pba2* Δ yeast strains we observed increased levels of Blm10 (Fig. 2.1A, 2.1B, and Appendix Figure A.1). However, *in vivo* Pba1-Pba2 is normally only found on the immature CP, and it has been postulated that one function of Pba1-Pba2 could be to prevent RP from binding to immature CP^{8,9,35,36}. To test this hypothesis, we first affinity-purified immature CP using TAP-tagged Ump1 (Fig. 2.1C and 2.1D). Mass spectrometry analyses confirmed that these purifications contained all seven α subunits in addition to β 1 to β 5, Pba1, Pba2 and Ump1 (Appendix Table A.1). β 6 (Pre7) and β 7 (Pre4) were undetectable, as has been observed before³⁷. The presence of Pba1-Pba2 was also confirmed by immunoblotting (Fig. 2.1C and Appendix Figure A.1). Propeptides for β 1, β 2, and β 5 were detected by immunoblotting or mass spectrometry (Fig. 2.1C and Appendix Table A.1). Taken together, these data indicate we purified a form of CP that has not matured yet.

RP was not detected above background levels in purifications of immature CP when assessed using several RP specific antibodies (Fig. 2.1C). To understand how the presence of Pba1-Pba2 might impact interactions of RP with the immature CP, we deleted *PBA1*. The deletion of *PBA1* resulted in the absence of both Pba1 and Pba2 from immature CP, and the appearance of the RP (Fig. 2.1C). Thus, upon deletion of Pba1, the surface of the α -ring becomes available for interaction with RP. Particularly striking was the presence of Ecm29 in this deletion background; Ecm29 is a proteasome-associated protein that only associates with RP-CP species and not free RP or free CP^{38,39}. It has been found recruited to mutant proteasome forms^{29,40}, potentially indicating specific recruitment on these samples where RP associates prematurely with CP.

Previously, it has been shown that Blm10 associates with both mature CP^{17,26,27,38} and immature CP^{15,16,26}. We consistently observed higher levels of Blm10 on immature CP purified from a *pba1* Δ strain compared to wildtype (Fig. 2.1C and Appendix Figure A.1). The deletion of *BLM10* together with *PBA1* caused a modest further increase of RP binding to immature CP,

consistent with the fact that the RP and Blm10 compete for CP binding. Interestingly, a deletion of *BLM10* in strains that contain functional Pba1-Pba2 did not cause the RP to associate with immature CP (Appendix Figure A.1), suggesting that it is mainly the Pba1-Pba2 dimer that blocks association of RP with immature CP.

Figure 2.1 Pba1-Pba2 prevents RP association with immature CP.



(A) Proteasomes were purified from indicated strains, resolved by SDS-PAGE, and stained with Coomassie Brilliant Blue (CBB). (B) Native gel analysis of samples from (A) stained in gel with the proteasome substrate suc-LLVY-AMC (left) or stained with CBB. (C) 26S proteasome or immature CP were affinity-purified using ProA-tagged β4 or TAP-tagged Ump1 respectively. Purified complexes were resolved on SDS-PAGE and stained with CBB (top) or immunoblotted for Pba1-Pba2, indicated proteasome subunits (CP indicates core and RP indicates regulatory

particle subunits), and Ecm29. The asterisk marks a non-specific band. (D) 26S proteasome and CP were purified using standard protocols. Immature CP was purified and washed with buffers containing the indicated NaCl concentrations. Samples were resolved on a native gel and stained with either suc-LLVY-AMC (top) or with CBB (bottom).

Analysis of immature CP on native gel shows a distinct band that migrates faster than CP and lacks hydrolytic activity (Fig. 2.1D). The deletion of *PBA1* resulted in a smear instead of a well-resolved species (Fig. 2.1D lower panel). This smearing is likely caused by different factors associated with the immature CP in the absence of Pba1-Pba2, since including a washing step with high salt resulted in a more distinct band on native gel (Fig. 2.1D lower panel). The band does not migrate similar to wildtype immature CP, which might be caused by the absence of Pba1-Pba2 or a different composition of the immature CP (Fig. 2.1C and below). Our results thus indicate that the Pba1-Pba2 dimer shields the immature CP from other factors that can interact with the α -ring surface.

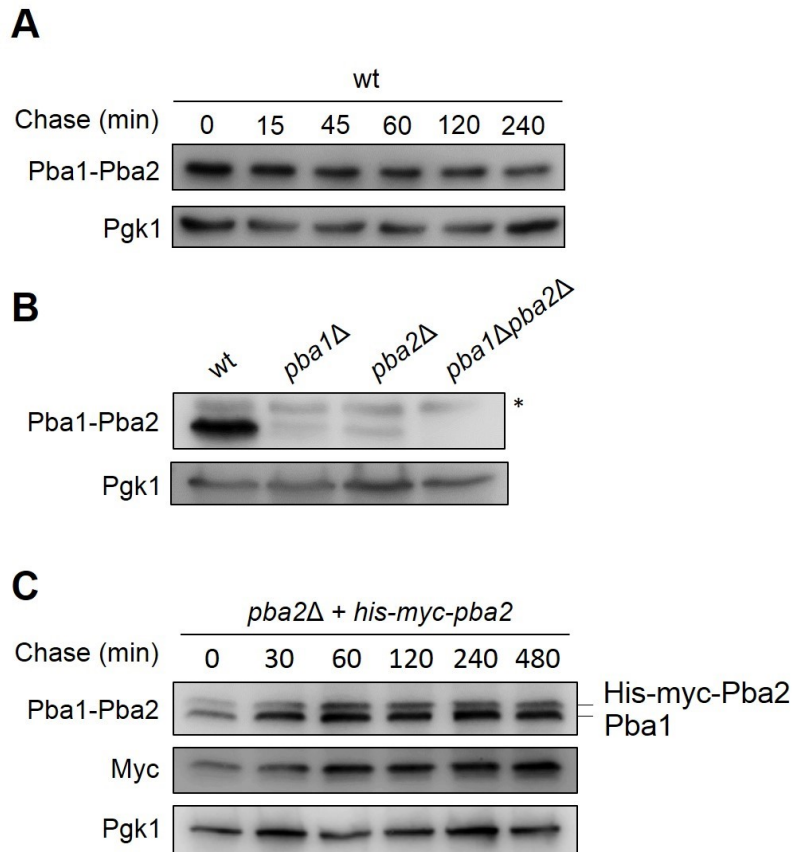
RP readily displaces Pba1 and Pba2 from mature CP

Crystal structures of Blm10 or Pba1-Pba2 bound to the CP and cryoEM structures of RP-CP complexes show that they bind with the CP exclusively through the α ring^{8,12-14}. Since both Ump1-bound immature CP (Appendix Table A.1) and mature CP have a complete α_{1-7} ring, it is unclear what drives the difference in binding behavior observed between mature CP and immature CP. An attractive mechanism that has been proposed posits that Pba1-Pba2 binds to immature CP, but upon maturation, Pba1-Pba2 is degraded, which enables the formation of RP-CP complexes. This model is supported by the observation that, upon overexpression of a flag-tagged version of the human orthologs PSMG1 (PAC1) or PSMG2 (PAC2), the flag-tagged protein is unstable in HeLa cells⁹. On the other hand, for the yeast orthologs no detectable degradation of Pba1-Pba2 by the mature CP has been observed *in vitro*^{7,8}.

To test the stability of Pba1-Pba2 *in vivo*, we conducted chase experiments using an antibody that recognizes endogenous Pba1-Pba2 (Fig. 2.2A). These data suggested that the Pba1-Pba2 dimer is stable. To address the possibility that one of the two subunits is unstable, we next determined steady state levels of Pba1 and Pba2 in the *pba2* Δ and *pba1* Δ strains respectively. Here, a subtle difference in migration between the two proteins can be observed, indicating the

antibody recognizes both endogenous Pba1 and endogenous Pba2 (Fig. 2.2B). The strongly reduced signal upon deletion of *PBA1* or *PBA2* might indicate that subunits incapable of forming dimers are subject to degradation in a process unrelated to CP maturation. This finding could potentially explain perceived differences between the yeast and mammalian systems⁹. Finally, we also reintroduced a His-Myc-tagged version of Pba2 in a *pba2Δ* background using a CEN plasmid and the endogenous promoter to prevent overexpression. Chase experiments with the later strain also showed both subunits are stable (Fig. 2.2C). In sum, our findings indicate that Pba1-Pba2 is not degraded as part of the CP maturation process in yeast.

Figure 2.2 Pba1 and Pba2 are stable.



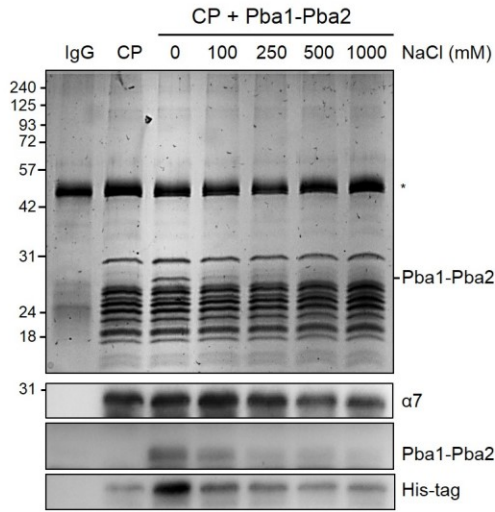
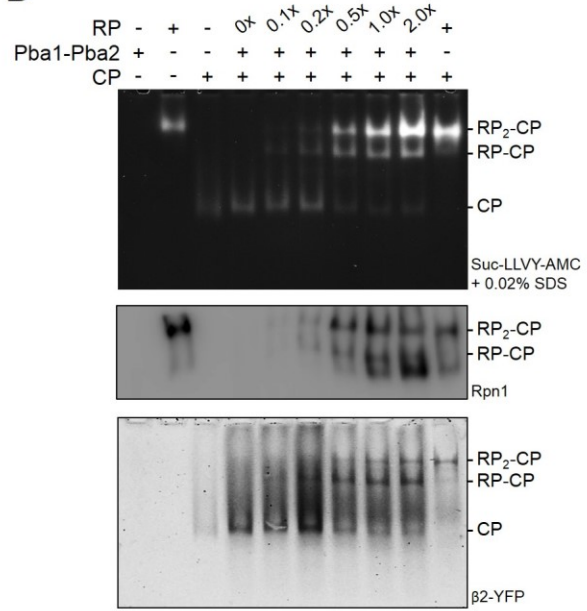
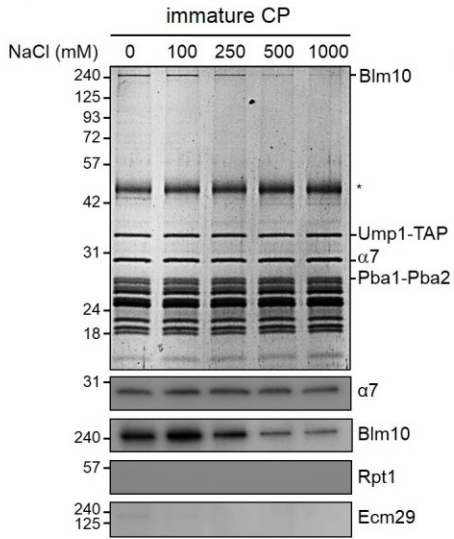
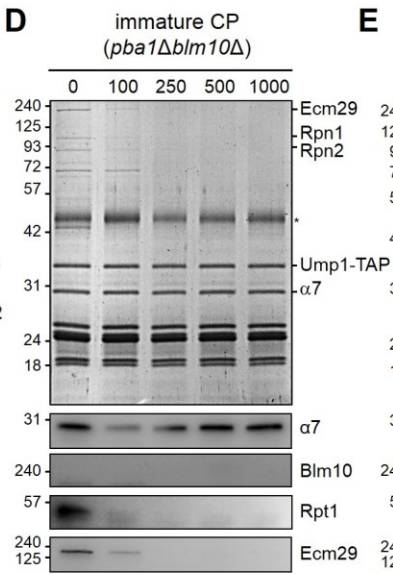
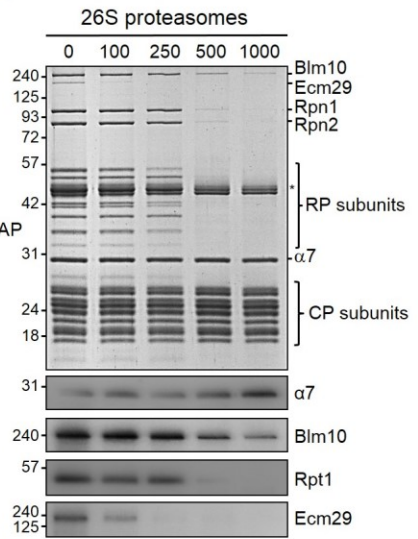
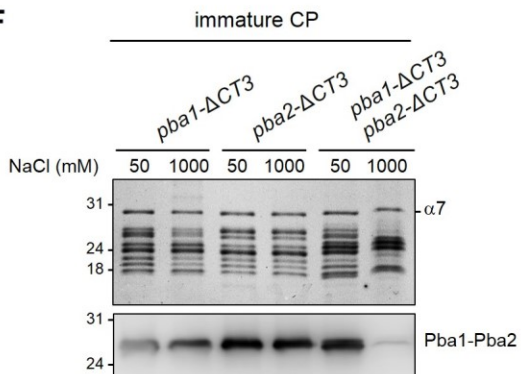
(A) Cyclohexamide chase of wildtype using antibodies that recognize endogenous Pba1-Pba2. 100 $\mu\text{g ml}^{-1}$ of cyclohexamide was added to logarithmically growing samples at $t=0$. Samples were collected at indicated times and lysed in SDS sample buffer. Immunoblots show levels of Pba1-Pba2 with Pgk1 as a loading control. Pba1-Pba2 has a long half-life inconsistent with the

previously proposed model that Pba1-Pba2 is degraded during the assembly process. (B) Steady state levels of Pba1-Pba2 in total lysate. (C) Cyclohexamide chase as in (A) but from a strain that expresses His-Myc-tagged Pba1 from a CEN plasmid under its own promoter.

Since CP does not degrade Pba1-Pba2, RP must be able to displace it directly or with the help of other factors. Previous work using surface plasmon resonance had shown that the interaction between mature CP and Pba1-Pba2 is salt-labile⁸. We also observe that this interaction can be disrupted with low salt concentrations when we reconstituted *E. coli* purified Pba1-Pba2 onto resin-bound CP purified from yeast (Fig. 2.3A). Using bio-layer interferometry, we measured a K_D of $\sim 1 \mu\text{M}$ for Pba1-Pba2 with mature CP in 50 mM NaCl (Appendix Figure A.2), which is similar to the 3 μM reported by Stadtmueller et al. under physiological salt concentrations⁸. Considering the reported nanomolar range affinities between the RP subunit containing complexes and CP^{21,30}, these findings suggest that the RP will likely displace Pba1-Pba2 from the mature CP.

To further test this we developed an *in vitro* reconstitution assay. First, we combined mature CP with increasing ratios of Pba1-Pba2 to determine the stoichiometry of binding on native gel. Pba1-Pba2 binds to the CP, but does not cause a mobility shift (Appendix Figure A.2). Since a fivefold excess of Pba1-Pba2 showed maximum CP binding, we challenged reconstitutions with that ratio of Pba1-Pba2 to CP with increasing amounts of RP (Fig. 2.3B). We found that the RP associates with the CP starting at low concentrations where Pba1-Pba2 is in 20 fold excess over RP. This indicates that the RP can readily replace Pba1-Pba2 bound to mature CP. These analyses are complicated by a small amount of active RP₂-CP that co-purifies with our RP preparations (³⁸ and Fig. 2.3B lane 2). However, looking at the singly-capped RP-CP or visualizing exclusively the reconstituted CP by utilizing YFP-tagged CP (Fig. 2.3B lowest panel), we know the RP is reconstituted onto Pba1-Pba2-CP complexes. These data suggest that Pba1-Pba2 bound to mature CP cannot prevent RP association. Hence, there is no need for Pba1-Pba2 degradation to produce RP-CP complexes.

Figure 2.3 CP undergoes affinity switch upon maturation.

A**B****C****D****E****F**

(A) Affinity-resin bound purified CP was reconstituted with heterologously expressed His-tagged Pba1-Pba2 dimer. Samples were washed with buffer containing the indicated NaCl concentrations. Next, samples were resolved on SDS-PAGE and stained with CBB or immunoblotted for the indicated proteins. (B) YFP-tagged CP was first reconstituted with 5 fold molar excess of Pba1-Pba2 and challenged with different amounts of purified RP (molar excess over CP indicated). Samples were resolved on a native gel to determine complex composition in samples: Top panel, proteolytic active complexes were visualized using in gel suc-LLVY-AMC hydrolytic activity assay. Middle panel, native gel was immunoblotted for the RP subunit Rpn1. Lower panel, native gel was analyzed for YFP signal. (C-F) Immature CP or 26S proteasome from wildtype or indicated strains were purified, split into different samples and washed with buffer containing the indicated NaCl concentrations. Samples were resolved on SDS-PAGE and stained with CBB or immunoblotted for indicated proteins. The asterisk indicates an IgG resin-derived band.

A switch in affinity upon CP maturation

We hypothesized that a specific mechanism must exist that ensures Pba1-Pba2 cannot be replaced by RP when bound to immature CP. This could involve regulatory proteins, like the RP chaperones that associate with RP complexes. However, those chaperones cannot fully prevent RP-immature CP association as we observed RP binding in *pba1* Δ cells (Fig. 2.1C). As an alternative mechanism, we envisioned a conformational change in the α ring upon maturation that changes the binding surface between the CP and associated proteins. In general, the CP has more structural plasticity than has been appreciated⁴¹. More specifically, during the final steps of CP maturation, β 7 is incorporated, immature CP dimerizes, autoproteolytic cleavage activates the three active sites (β 1, β 2 and β 5), and Ump1 is degraded². The β 7 subunit is in direct contact with the α -subunits that bind to Pba1-Pba2, α 6 and α 7⁸, providing a direct opportunity to induce a conformational change in the α ring. Alternatively, autoproteolytic activation might provide a trigger that induces a conformational change in CP, as modification of active sites has been shown to change properties of the α -ring^{38,42}.

To test for differences in binding behavior between mature and immature CP, we characterized the salt dependence of several different interactions. First, we used TAP-tagged

Ump1 to purify immature CP associated with endogenous Pba1-Pba2. Here, even washes with buffers containing 1M NaCl washed off very little of the Pba1-Pba2 complex from immature CP (Fig. 2.3C). This is in sharp contrast to the Pba1-Pba2 association with mature CP, which is highly salt labile (Fig. 2.3A and ⁸). Next, to test if the RP also shows a change in binding behavior, we purified immature CP from the *pba1Δ blm10Δ* strain and exposed it to washes with different salt concentrations. In these samples, the RP consistently washes off in buffers containing 100 mM NaCl (Fig. 2.3D), while 250 to 500 mM NaCl is required to disrupt the binding between RP and mature CP (Fig. 2.3E and ³⁹). These data suggest that the immature CP has a high affinity for Pba1-Pba2 and a low affinity for the RP. Upon maturation, the affinities are reversed and the RP has a much higher affinity for the mature CP than Pba1-Pba2. For RP binding to the immature CP we cannot exclude that the reduced binding is due to differences in immature CP composition upon *PBA1* deletion (see below). However, in reconstitution assays we were unable to expel Pba1-Pba2 from normal immature CP, even though the base subcomplex of the RP efficiently reconstituted on mature CP (Appendix Figure A.2C and A.2D) and can expel Pba1-Pba2 from mature CP (Fig. 2.3B). Interestingly, the binding of Blm10 to both mature and immature CP shows a disruption of the interaction at similar salt concentrations, suggesting that Blm10 is not sensitive to the affinity switch (compare Fig. 2.3C and 2.3E). This is consistent with the fact that Blm10 has been observed on mature as well as immature CP under physiological conditions^{17,26}. In all, these data reveal an affinity switch during CP maturation that at least in part can explain the exclusive binding of Pba1-Pba2 to immature CP and RP to mature CP.

The Pba2 tail contributes to the affinity switch

Pba1 and Pba2 both contain an HbYX-motif that is required for functionality^{7,8}, and a crystal structure of Pba1-Pba2 bound to the CP shows that both C-termini dock in a specific α -pocket⁸. Interestingly, in the interaction with the mature CP, the tail of Pba2 contributes only minimally to binding, since its deletion reduces the affinity with only 2-3 fold⁸. In comparison, deleting the tail of Pba1, reduced the affinity > 100 fold. The differential contribution to the affinity can be rationalized through analysis of the structure itself. Pba2 binds in an unusual manner to the CP, lacking several hydrogen bonds commonly observed for HbYX-motif binding in the α pockets (e.g. for the HbYX of Pba1 or Blm10). For example, the hydroxyl group of the

tyrosine residue in the Pba2 HbYX-motif is far (4.2 Å) removed from the closest potential hydrogen bond partner^{8,12}. Despite the apparent minor role in binding to the CP, the HbYX-motif of Pba2 is physiologically relevant, since mutant strains with a truncated tail show phenotypes similar to mutants lacking the Pba1 HbYX-motif^{7,8}. Only after deletion of both HbYX-motifs, however, do strains show phenotypes that mimic *pba1*Δ strains^{7,8}. Hence, the HbYX-motif of Pba2 has an unidentified but important physiological function. We hypothesized that the HbYX-motif of Pba2 is more important for binding with the immature CP as compared to the mature CP, thereby contributing to the observed affinity switch. Such a difference might arise from small changes in the conformation of the α6-α7 pocket, or from the fact that changes in Pba1-α5-α6 interactions could limit the ability of Pba2 to interact fully with its pocket in the mature CP.

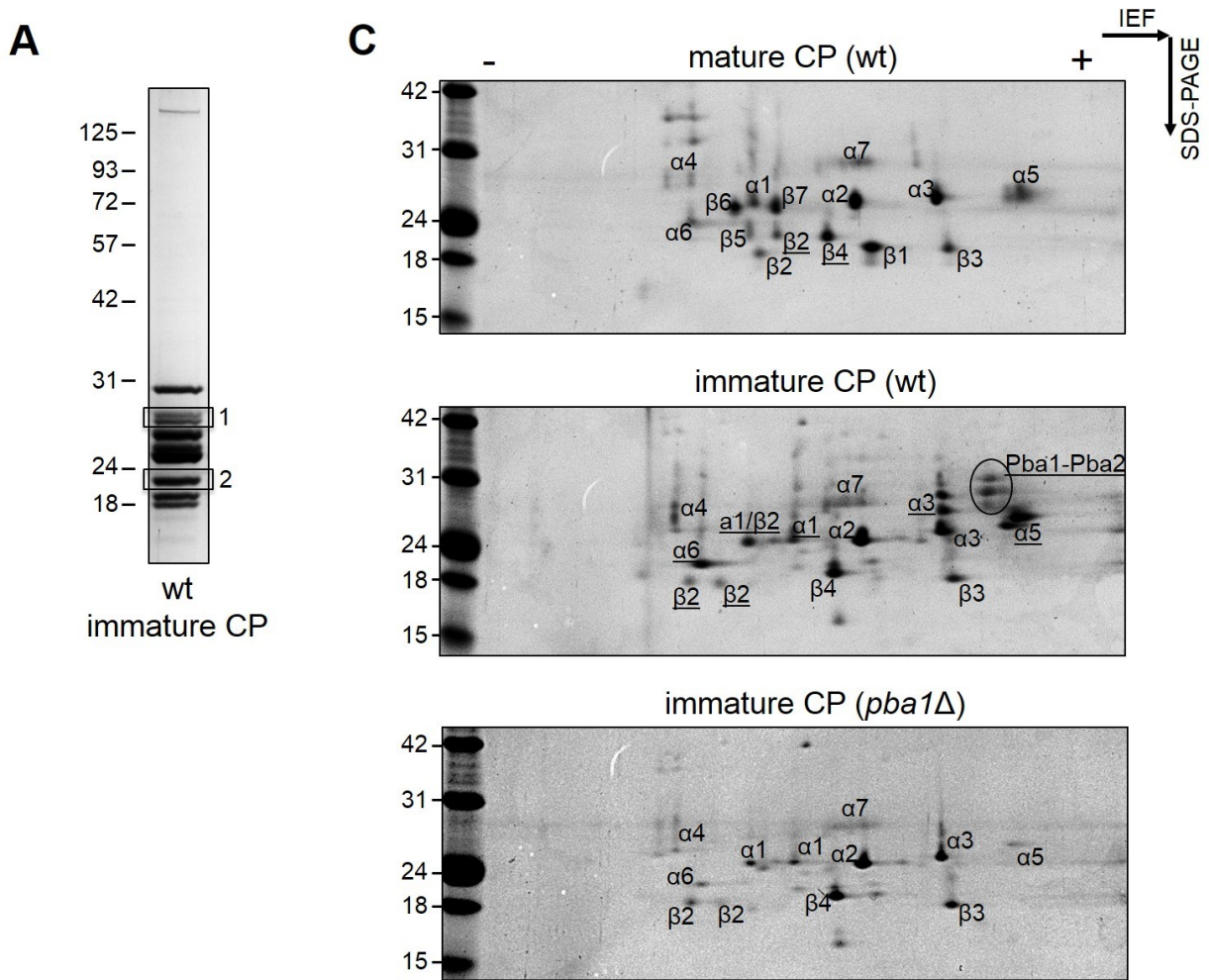
The model described above predicts that both the Pba2 and Pba1 HbYX-motif would have a role in binding to the immature CP. To test this, we deleted the HbYX-motif from Pba1 (*pba1*-ΔCT3), Pba2 (*pba2*-ΔCT3), or both together (*pba1*-ΔCT3 *pba2*-ΔCT3) in an Ump1-Tap tagged background. Next, we tested the salt lability of Pba1-Pba2 binding to immature CP. To our surprise, Pba1-Pba2 remained bound to immature CP in both the *pba1*-ΔCT3 and *pba2*-ΔCT3 background even after washes with 1 M NaCl (Fig. 2.3F). The binding of Pba1-Pba2 to the immature CP is thus very different compared to the mature CP, as the latter showed a highly salt dependent interaction that depends largely on the Pba1 tail (Fig. 2.3A and ⁸). Only after deletion of both the Pba1 and Pba2 HbYX-motif (*pba1*-ΔCT3 *pba2*-ΔCT3) did we observe loss of binding of the Pba1-Pba2 complex to immature CP with high salt washes (Fig. 2.3F). Thus, in contrast to binding to mature CP, both the Pba1 and Pba2 HbYX-motif contribute substantially to the affinity of Pba1-Pba2 for immature CP. This suggests that a major contributor to the molecular mechanism of the affinity switch derives from differences in how the Pba2 HbYX-motif docks into the α6-α7 pocket.

Pba1 and Pba2 contribute to α5 and α6 incorporation

On purification of immature CP from a *pba1*Δ strain we noticed a reduced level of a specific proteasome core particle subunit after SDS-PAGE analysis (compare Fig. 2.3C and 2.3D). Based on the running behavior, previous assignments by other labs^{26,43} and our own mass spectrometry analysis (Fig. 2.4A and 2.4B) we determined this was the subunit α6. This suggests that there is a reduced level of α6 present in immature proteasomes in the absence of Pba1.

Additional mass spectrometry analysis suggested that besides $\alpha 6$ there might also be reduced levels of $\alpha 5$. To test this, we ran 2D gels of mature CP from wildtype and immature CP from

Figure 2.4 . Pba1-Pba2 are required for efficient incorporation of $\alpha 5$ and $\alpha 6$



(A) Immature CP from wildtype strain was purified and resolved on SDS-PAGE. Two bands that were consistently absent or reduced in a *pba1* Δ background (See Fig. 2.1C, 2.3C, and 2.3D)

were excised and submitted to mass spectrometry analysis for identification (see Table 1). Band 1 was identified as Pba1 and Pba2, while $\alpha 6$ was the major component of Band 2, consistent with previous assignments^{15,26,43}. **(B)** Unique peptides from the mass spectrometry analyses in **(a)** that cover regions of the pro-peptides of $\beta 1$, $\beta 2$, and $\beta 5$ are underlined with the pro-peptide sequence in bold. **(C)** Purified mature or immature CP from indicated strains were resolved by two-dimensional gel electrophoresis using a non-linear ZOOM® IPG strip (pH 3–10) followed by SDS-PAGE. Gels were stained with CBB. Proteins spots were assigned based on immunoblotting (Appendix Figure A.3A), mass spectrometry analyses (underlined and Appendix Figure A.3B), and previous assignments^{26,43}.

Table 2.2 Mass spectrometry analyses of band 1 and band 2 in Figure 2.4

Band	Protein Name	Standard Name	Systematic Gene Name	# unique peptides	# total Spectra	% coverage
1	Pba1	Pba1	YLR199C	9	25	42
	Pba2	Add66	YKL206C	10	23	35
	$\alpha 5$	Pup2	YGR253C	7	10	28
	$\beta 5$	Pre2	YPR103W	6	8	21
	$\alpha 7$	Pre10	YOR362C	4	7	18
	$\alpha 4$	Pre6	YOL038W	5	6	23
	$\alpha 1$	Scl1	YGL011C	2	2	8
2	$\alpha 6$	Pre5	YMR314W	16	32	75
	Ump1	Ump1	YBR173C	7	20	47
	$\beta 1$	Pre3	YJL001W	9	15	39
	$\beta 5$	Pre2	YPR103W	2	2	9
	$\beta 2$	Pup1	YOR157C	2	2	8

wildtype and *pba1* Δ strains (Fig. 2.4C and Appendix Figure A.3). These gels confirmed the substantial reduction in levels of $\alpha 5$ and $\alpha 6$ from immature CP purified from *pba1* Δ strains. Pba1 thus likely has a role in efficient incorporation of $\alpha 5$ and $\alpha 6$, similar to Pba3-Pba4, which has a role in controlling $\alpha 3$ (Pre9) and $\alpha 4$ (Pre6) incorporation. However, $\alpha 5$ and $\alpha 6$ are essential

subunits of the proteasome, making a potential role for Pba1-Pba2 in formation of alternative proteasomes, as was proposed for Pba3-Pba4³, unlikely. Considering the thermodynamic stability of rings once they have formed⁴⁴⁻⁴⁶, the reduced level of these two subunits most likely indicates a slow incorporation of these subunits into the α ring in a *pba1* Δ strain. However, and alternative or additional role of Pba1-Pba2 might be the stabilization of $\alpha 5$ and $\alpha 6$ once they have been incorporated into the α ring, in particular as $\alpha 5$ and $\alpha 6$ appear to be absent in the high salt wash of the *pba1*- Δ CT3 *pba2*- Δ CT3 strain (Fig. 2.3F).

Preventing premature RP binding improves assembly efficiency

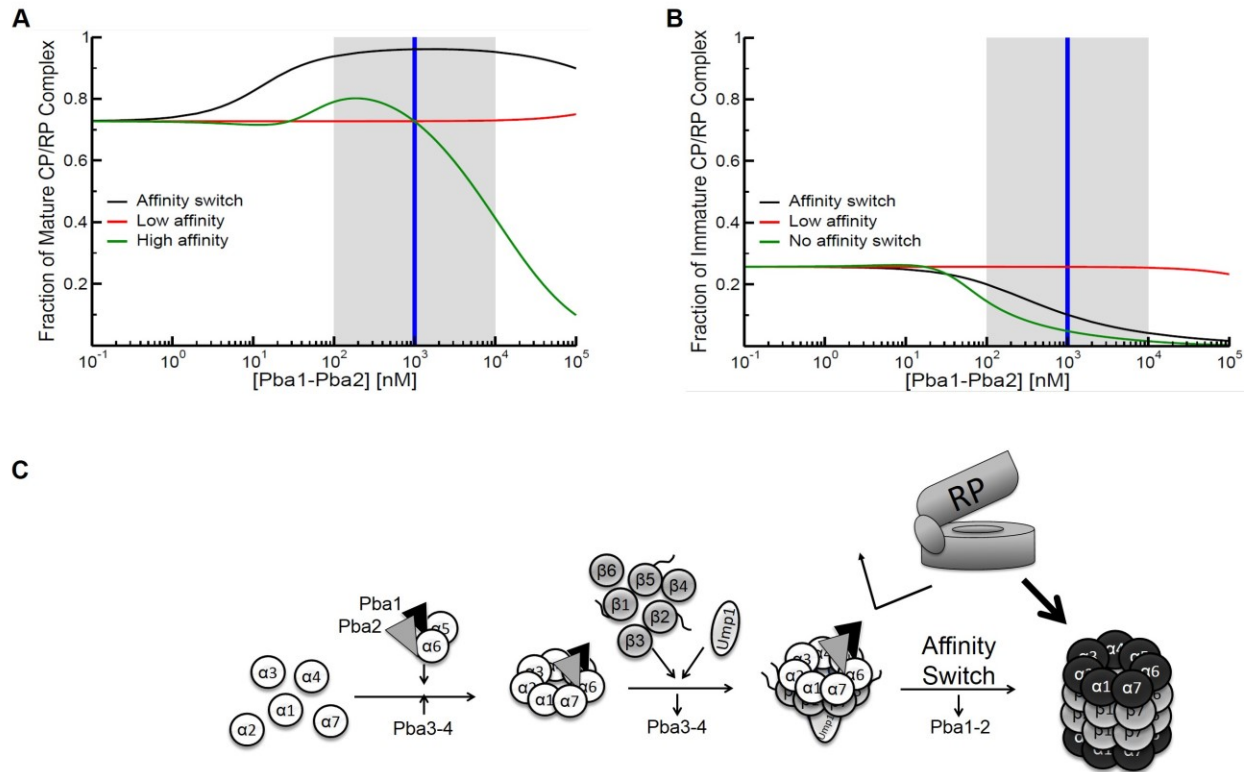
Our data provide experimental evidence and mechanistic insight into a role of Pba1-Pba2 in preventing binding of RP to immature CP. To better understand the importance of the observed affinity switch, we developed a mathematical model in which we manipulated the affinity of Pba1-Pba2 for the CP α ring.

In our model of proteasome assembly, the α -ring is nucleated by the formation of an $\alpha 5$ - $\alpha 6$ dimer and we kept the roles of the Pba3-Pba4 chaperone^{1,47,48} implicit. After α -dimers form, other α subunits can bind on either end of the complex, eventually leading to the formation of the α ring. We ignored subsequent steps in CP maturation (addition of the β subunits, half proteasome dimerization, etc.) in order to reduce the complexity of the model. To test the effect of the proposed affinity switch, we used various affinities for Pba1-Pba2 dimer bound to intermediates as well as the full α -ring. We only included fully-formed RPs in this model, assuming the RP chaperones would prevent association between immature RPs and CP subunits^{28-31,33,34}. Finally, since the Rpt ring of the RP makes many contacts with the α subunits of the CP^{13,49}, RP binding to α -ring structures was considered to be stable when the α -intermediate in question contained more than one subunit⁴⁴⁻⁴⁶.

We used this model to analyze how proteasome assembly efficiency (defined as the formation of fully active 26S RP-CP complexes) depends on the concentration of Pba1-Pba2 for three different scenarios. In the first, we implemented the affinity switch that was implied by our data (Fig. 2.5A and 2.5B, black lines). In the affinity switch model, the K_D of Pba1-Pba2 for the mature CP was taken to be 1 μ M (Appendix Figure A.2A), and the K_D of Pba1-Pba2 for immature CP was taken to be 3 orders of magnitude stronger (1 nM) to represent the lack of

dissociation of the chaperones from immature CP even in high salt (Fig. 2.3C). The other two scenarios lacked an affinity switch and the affinity of Pba1-Pba2 for mature and immature CP was either low (1 μ M, “low affinity”, Fig. 2.5A and 2.5B, red lines) or high (1 nM, “high affinity”, Fig. 2.5A and 2.5B, green lines).

Figure 2.5 Pba1-Pba2 prevents assembly deadlock.



(A) Mathematical models were designed to investigate the function of Pba1-Pba2 (see text for details). The graph explores three scenarios. In the first (black line), we incorporated an affinity switch in our model. The Y-axis shows fraction of assembled proteasomes, which reaches 1 within the likely physiological range of concentrations of Pba1-Pba2 in the presence of an affinity switch (gray area). The second scenario (green line) assumed a high affinity rather than an affinity switch, while the third considered a low affinity (red line). **(B)** This graph displays the fraction of complexes where the RP is associated with the CP prior to CP maturation, yielding unproductive, deadlocked complexes. **(C)** Proposed conceptual model for the role of Pba1-Pba2 in CP maturation (see text for details).

As can be seen in Figure 2.5A, the behavior of these three scenarios is quite different. The presence of an affinity switch results in very high assembly yield compared to the absence (i.e. very low concentrations) of Pba1-Pba2; going from 75% to almost 100%. The improved assembly results from a decrease in RP binding to immature CP intermediates (Fig. 2.5B). When the concentration of Pba1-Pba2 reaches unphysiologically high levels ($\sim 100 \mu\text{M}$), it overcomes the affinity switch and begins to interfere with 26S assembly by blocking RP association with mature CP (Fig. 2.5A). The 75% yield in the absence of Pba1 or Pba2 fits well with *in vivo* data, where the deletion of Pba1 or Pba2 does not cause a severe phenotype^{25,26}, but likely causes a reduction in assembly yield substantial enough to explain synergistic phenotypes with other proteasome mutants^{25,26}.

If we remove the affinity switch, however, the robust increase in assembly yields due to the presence of Pba1-Pba2 is no longer observed in the model. When affinities are uniformly low (Fig. 2.5A, red line), Pba1-Pba2 simply does not bind either immature or mature CP well enough at physiological concentrations to have an impact on assembly yields. When affinities are uniformly high, on the other hand, Pba1-Pba2 block RP binding to both the mature and immature CP, resulting in lower yields (Fig. 2.5B, green line).

While the results in Figure 2.5 suppose a particular concentration of both RP and CP subunits in the cell, independent variations in these concentrations do not influence the overall trends observed in the model (Appendix Figure A.4A). Similarly, changes to the size of the affinity switch also do not influence the general behavior of the model (Appendix Figure A.4B). Our model thus provides a robust explanation for the functional role of the Pba1-Pba2 affinity switch: by blocking premature RP-CP association, these chaperones prevent the stabilization of intermediates that would lead to CP assembly deadlock⁴⁴. The switch from a high-affinity to low-affinity binding conformation upon CP maturation ensures that the chaperone “gets off” the complex at the right time, allowing the RP to bind once the CP is fully formed.

Discussion

Figure 2.5C summarizes our current conceptual model of the role of Pba1-Pba2. CP assembly starts with the formation of the α_{1-7} ring. In the early steps of assembly, both the Pba1-Pba2 and the Pba3-Pba4 dimers have a role in efficient ring formation. Pba3-Pba4 has a role in ring nucleation and ensures incorporation of α_3 ³. The presence of Pba1-Pba2 ensures the efficient incorporation or stabilization of α_5 and α_6 . Next, the β -subunits assemble onto the α -ring; at this step in the process, Pba3-Pba4 must dissociate from the complex to avoid steric clashes with the β_4 subunit⁴. However, Pba1-Pba2 remains bound until late in the assembly process, shielding the external surface of the α -ring from RP and Blm10 and also preventing α -ring dimerization⁹.

After assembly of the β -ring several steps must occur, including dimerization of immature half proteasomes and autocatalytic activation^{1,48}. Our results show that maturation of the CP causes a change in the binding of Pba1-Pba2 to the CP. While the structural basis of the affinity switch has yet to be determined, our data suggest that conformational changes in the CP that accompany maturation impact the capacity of the HbYX-motif on Pba2 to interact with the α_6 - α_7 pocket. The affinity switch we have identified allows the chaperone to specifically protect the immature CP from interactions with regulatory factors, thereby preventing the formation of unproductive complexes that decrease the assembly yield of functional proteasomes. It is likely that other assembly chaperones (particularly those that bind to immature RPs, e.g. Nas6) utilize a similar mechanism, preventing association with larger assemblies prior to completion of subcomplex assembly. Small structural changes that accompany maturation likely reduce the affinity for these chaperones, allowing for the coordinated exchange of possible binding partners during the assembly process.

Author contributions

P.S.W., A.O. and J.R. performed the experiments and constructed the yeast strains. M.A.R. and E.J.D. generated the model and performed the calculations. Studies were conceived by P.S.W., E.J.D., and J.R. Manuscript was written by P.S.W., E.J.D. and J.R. with input from all authors.

References - Chapter2

1. Marques, A.J., Palanimurugan, R., Matias, A.C., Ramos, P.C., and Dohmen, R.J. (2009) Catalytic mechanism and assembly of the proteasome. *Chem.Rev.* **109**, 1509-1536
2. Ramos, P.C., and Dohmen, R.J. (2008) PACemakers of proteasome core particle assembly. *Structure.* **16**, 1296-1304
3. Kusmierczyk, A.R., Kunjappu, M.J., Funakoshi, M., and Hochstrasser, M. (2008) A multimeric assembly factor controls the formation of alternative 20S proteasomes. *Nat.Struct.Mol.Biol.* **15**, 237-244
4. Yashiroda, H. (2008) Crystal structure of a chaperone complex that contributes to the assembly of yeast 20S proteasomes. *Nat.Struct.Mol.Biol.* **15**, 228-236
5. Takagi, K. (2014) Pba3-Pba4 heterodimer acts as a molecular matchmaker in proteasome alpha-ring formation. *Biochem.Biophys.Res.Commun.* **450**, 1110-1114
6. Ramos, P.C., Hockendorff, J., Johnson, E.S., Varshavsky, A., and Dohmen, R.J. (1998) Ump1p is required for proper maturation of the 20S proteasome and becomes its substrate upon completion of the assembly. *Cell.* **92**, 489-499
7. Kusmierczyk, A.R., Kunjappu, M.J., Kim, R.Y., and Hochstrasser, M. (2011) A conserved 20S proteasome assembly factor requires a C-terminal HbYX motif for proteasomal precursor binding. *Nat.Struct.Mol.Biol.* **18**, 622-629
8. Stadtmueller, B.M. (2012) Structure of a proteasome Pba1-Pba2 complex: implications for proteasome assembly, activation, and biological function. *J.Biol.Chem.* **287**, 37371-37382
9. Hirano, Y. (2005) A heterodimeric complex that promotes the assembly of mammalian 20S proteasomes. *Nature.* **437**, 1381-1385
10. Schmidt, M., and Finley, D. (2014) Regulation of proteasome activity in health and disease. *Biochim.Biophys.Acta.* **1843**, 13-25
11. Kish-Trier, E., and Hill, C.P. (2013) Structural biology of the proteasome. *Annu.Rev.Biophys.* **42**, 29-49
12. Sadre-Bazzaz, K., Whitby, F.G., Robinson, H., Formosa, T., and Hill, C.P. (2010) Structure of a Blm10 complex reveals common mechanisms for proteasome binding and gate opening. *Mol.Cell.* **37**, 728-735
13. Lander, G.C. (2012) Complete subunit architecture of the proteasome regulatory particle. *Nature.* **482**, 186-191
14. Beck, F. (2012) Near-atomic resolution structural model of the yeast 26S proteasome. *Proc.Natl.Acad.Sci.USA.* **109**, 14870-14875

15. Marques, A.J., Glanemann, C., Ramos, P.C., and Dohmen, R.J. (2007) The C-terminal extension of the beta7 subunit and activator complexes stabilize nascent 20S proteasomes and promote their maturation. *J.Biol.Chem.* **282**, 34869-34876
16. Fehlker, M., Wendler, P., Lehmann, A., and Enenkel, C. (2003) Blm3 is part of nascent proteasomes and is involved in a late stage of nuclear proteasome assembly. *EMBO Rep.* **4**, 959-963
17. Weberruss, M.H. (2013) Blm10 facilitates nuclear import of proteasome core particles. *EMBO J.* **32**, 2697-2707
18. Tar, K. (2014) Proteasomes associated with the Blm10 activator protein antagonize mitochondrial fission through degradation of the fission protein Dnm1. *J.Biol.Chem.* **289**, 12145-12156
19. Dange, T. (2011) Blm10 protein promotes proteasomal substrate turnover by an active gating mechanism. *J.Biol.Chem.* **286**, 42830-42839
20. Qian, M.X. (2013) Acetylation-mediated proteasomal degradation of core histones during DNA repair and spermatogenesis. *Cell.* **153**, 1012-1024
21. Beckwith, R., Estrin, E., Worden, E.J., and Martin, A. (2013) Reconstitution of the 26S proteasome reveals functional asymmetries in its AAA+ unfoldase. *Nat.Struct.Mol.Biol.* **20**, 1164-1172
22. Gillette, T.G., Kumar, B., Thompson, D., Slaughter, C.A., and DeMartino, G.N. (2008) Differential roles of the COOH termini of AAA subunits of PA700 (19S regulator) in asymmetric assembly and activation of the 26S proteasome. *J.Biol.Chem.* **283**, 31813-31822
23. Smith, D.M. (2007) Docking of the proteasomal ATPases' carboxyl termini in the 20S proteasome's alpha ring opens the gate for substrate entry. *Mol.Cell.* **27**, 731-744
24. Tian, G. (2011) An asymmetric interface between the regulatory and core particles of the proteasome. *Nat.Struct.Mol.Biol.* **18**, 1259-1267
25. Le Tallec, B. (2007) 20S proteasome assembly is orchestrated by two distinct pairs of chaperones in yeast and in mammals. *Mol.Cell.* **27**, 660-674
26. Li, X., Kusmierczyk, A.R., Wong, P., Emili, A., and Hochstrasser, M. (2007) beta-Subunit appendages promote 20S proteasome assembly by overcoming an Ump1-dependent checkpoint. *EMBO J.* **26**, 2339-2349
27. Schmidt, M. (2005) The HEAT repeat protein Blm10 regulates the yeast proteasome by capping the core particle. *Nat.Struct.Mol.Biol.* **12**, 294-303
28. Barrault, M.B. (2012) Dual functions of the Hsm3 protein in chaperoning and scaffolding regulatory particle subunits during the proteasome assembly. *Proc.Natl.Acad.Sci.USA.* **109**, E1001-E1010

29. Lee, S.Y., De, I.M., and Roelofs, J. (2011) Loss of Rpt5 protein interactions with the core particle and Nas2 protein causes the formation of faulty proteasomes that are inhibited by Ecm29 protein. *J.Biol.Chem.* **286**, 36641-36651
30. Park, S. (2013) Reconfiguration of the proteasome during chaperone-mediated assembly. *Nature.* **497**, 512-516
31. Roelofs, J. (2009) Chaperone-mediated pathway of proteasome regulatory particle assembly. *Nature.* **459**, 861-865
32. Park, S. (2009) Hexameric assembly of the proteasomal ATPases is templated through their C termini. *Nature.* **459**, 866-870
33. Ehlinger, A. (2013) Conformational dynamics of the rpt6 ATPase in proteasome assembly and rpn14 binding. *Structure.* **21**, 753-765
34. Satoh, T. (2014) Structural basis for proteasome formation controlled by an assembly chaperone nas2. *Structure.* **22**, 731-743
35. Sahara, K., Kogleck, L., Yashiroda, H., and Murata, S. (2014) The mechanism for molecular assembly of the proteasome. *Adv.Biol.Regul.* **54**, 51-58
36. Kunjappu, M.J., and Hochstrasser, M. (2014) Assembly of the 20S proteasome. *Biochim.Biophys.Acta.* **1843**, 2-12
37. Lehmann, A., Janek, K., Braun, B., Kloetzel, P.M., and Enenkel, C. (2002) 20S proteasomes are imported as precursor complexes into the nucleus of yeast. *J.Mol.Biol.* **317**, 401-413
38. Kleijnen, M.F. (2007) Stability of the proteasome can be regulated allosterically through engagement of its proteolytic active sites. *Nat.Struct.Mol.Biol.* **14**, 1180-1188
39. Leggett, D.S. (2002) Multiple associated proteins regulate proteasome structure and function. *Mol.Cell.* **10**, 495-507
40. Mota, D.L. (2013) The proteasome-associated protein Ecm29 inhibits proteasomal ATPase activity and in vivo protein degradation by the proteasome. *J.Biol.Chem.* **288**, 29467-29481
41. Arciniega, M., Beck, P., Lange, O.F., Groll, M., and Huber, R. (2014) Differential global structural changes in the core particle of yeast and mouse proteasome induced by ligand binding. *Proc.Natl.Acad.Sci.USA.* **111**, 9479-9484
42. Osmulski, P.A., Hochstrasser, M., and Gaczynska, M. (2009) A tetrahedral transition state at the active sites of the 20S proteasome is coupled to opening of the alpha-ring channel. *Structure.* **17**, 1137-1147
43. Choudhuri, A.U., Tokumoto, T., Dohra, H., Ushimaru, T., and Yamada, S. (2008) Functional and biochemical characterization of the 20S proteasome in a yeast temperature-sensitive mutant, rpt6-1. *BMC Biochem.* **9**, 20

44. Deeds, E.J., Bachman, J.A., and Fontana, W. (2012) Optimizing ring assembly reveals the strength of weak interactions. *Proc.Natl.Acad.Sci.USA*. **109**, 2348-2353
45. Bray, D., and Lay, S. (1997) Computer-based analysis of the binding steps in protein complex formation. *Proc.Natl.Acad.Sci.USA*. **94**, 13493-13498
46. Saiz, L., and Vilar, J.M. (2006) Stochastic dynamics of macromolecular-assembly networks. *Mol.Syst.Biol.* **2**, 2006.0024, 1-11
47. Kusmierczyk, A.R., and Hochstrasser, M. (2008) Some assembly required: dedicated chaperones in eukaryotic proteasome biogenesis. *Biol.Chem.* **389**, 1143-1151
48. Murata, S., Yashiroda, H., and Tanaka, K. (2009) Molecular mechanisms of proteasome assembly. *Nat.Rev.Mol.Cell Biol.* **10**, 104-115
49. Lasker, K. (2012) Molecular architecture of the 26S proteasome holocomplex determined by an integrative approach. *Proc.Natl.Acad.Sci.USA*. **109**, 1380-1387
50. Longtine, M.S. (1998) Additional modules for versatile and economical PCR-based gene deletion and modification in *Saccharomyces cerevisiae*. *Yeast*. **14**, 953-961
51. Goldstein, A.L., and McCusker, J.H. (1999) Three new dominant drug resistance cassettes for gene disruption in *Saccharomyces cerevisiae*. *Yeast*. **15**, 1541-1553
52. Elsasser, S., Schmidt, M., and Finley, D. (2005) Characterization of the proteasome using native gel electrophoresis. *Methods Enzymol.* **398**, 353-363
53. Keller, A., Nesvizhskii, A.I., Kolker, E., and Aebersold, R. (2002) Empirical statistical model to estimate the accuracy of peptide identifications made by MS/MS and database search. *Anal.Chem.* **74**, 5383-5392
54. Hindmarsh, A.C. (2005) SUNDIALS: Suite of nonlinear and differential/algebraic equation solvers. *Acm Trans.Math Software*. **31**, 363-396
55. Ghaemmaghami, S. (2003) Global analysis of protein expression in yeast. *Nature*. **425**, 737-741

Chapter 3 - Phosphorylation of the C-terminal region of proteasome subunit $\alpha 7$ is required for binding of the proteasome quality control factor Ecm29

Prashant S. Wani¹, Xavier Capalla², Alex Ondracek², and Jeroen Roelofs^{1,2#}

*1. Graduate Biochemistry Group, Department of Biochemistry and Molecular Biophysics,
Kansas State University, 336 Ackert Hall, Manhattan, Kansas 66506, USA*

*2. Molecular, Cellular and Developmental Biology Program, Division of Biology, Kansas State
University, 338 Ackert Hall, Manhattan, Kansas 66506, USA*

Keyword: Ecm29, Proteasome, $\alpha 7$ phosphorylation,

Abstract

The proteasome degrades many short-lived proteins that are labeled with an ubiquitin chain. The identification of phosphorylation on the proteasome suggests that degradation of these substrates can also be regulated at the proteasome. In yeast and humans, the unstructured C-terminal region of $\alpha 7$ contains an acidic patch with serine residues that are phosphorylated. Although these were identified more than a decade ago, the molecular implications of $\alpha 7$ phosphorylation have remained unknown. Here, we showed that the yeast Ecm29, a protein involved in proteasome quality control, requires the phosphorylated tail of $\alpha 7$ for its association with proteasomes. This is the first example of proteasome phosphorylation dependent binding of a proteasome regulatory factor. Ecm29 is known to inhibit proteasomes and is often found enriched on mutant proteasomes. We showed that the ability of Ecm29 to bind to mutant proteasomes requires the $\alpha 7$ tail binding site, besides a previously characterized Rpt5 binding site. The need for these two binding sites, which are on different proteasome subcomplexes, explains the specificity of Ecm29 for proteasome holoenzymes. It was also a key prediction of our model that proposes Ecm29 can recognize a misalignment between those two subcomplexes.

Introduction

The ubiquitin proteasome system (UPS) is present in all eukaryotes and enables cells to degrade many proteins in a highly regulated fashion¹. Numerous enzymes are required to specifically label proteins that are destined for degradation with ubiquitin. Ubiquitin, a short polypeptide, is normally covalently attached to lysine residues present in the target protein. The ubiquitinated proteins become substrates for the proteasome, a 2.5 MDa protease complex. The proteasome holoenzyme consists of 33 unique polypeptides that are assembled into two main subcomplexes: the regulatory particle (RP) and the core particle (CP). The RP recognizes ubiquitinated substrates either through direct interaction with proteasome subunits that function as ubiquitin receptors, like Rpn10 or Rpn13, or through recognition of adaptors that bind ubiquitinated substrates and the proteasome, such as Rad23 or Dsk2. The RP removes the ubiquitin from substrates and unfolds them. The unfolding occurs at an AAA-ATPase ring formed by the six homologous proteasome subunits Rpt1 to Rpt6. The Rpt ring abuts the CP and is responsible for threading substrates into the CP where the proteolytic active sites are located. The CP is formed by four hetero-heptameric rings that are stacked upon one another, resulting in a hollow, cylinder-like structure. CP subunits are of two types, α and β arranged in stacked rings to form an $\alpha_{1-7}\beta_{1-7}\beta_{1-7}\alpha_{1-7}$ structure. β_1 , β_2 , and β_5 are the catalytic subunits that provide the protease activity required for protein degradation.

The proteasome is an abundant complex in the cell, therefore it is important for the cell to assemble all 66 subunits that comprise this RP₂-CP complex efficiently and correctly. To achieve this, proteasome assembly is tightly orchestrated in the cell with the help of ten dedicated assembly chaperones^{2,3}. Five of these chaperones, Hsm3, Nas2, Nas6, Rpn14, and Adc17, are dedicated to RP assembly. The other five chaperones, Pba1, Pba2, Pba3, Pba4, and Ump1, assist in CP assembly. Interestingly, these chaperones not only promote the formation of specific subcomplexes, but several also prevent the premature association of RP and CP. For example, the CP chaperones Pba1-Pba2 prevent the association of RP with immature CP^{4,5}. Similarly, the RP chaperones are capable of blocking mature CP from interacting with RP⁶⁻⁹. Thus, it appears that the final step in assembly, the association of CP with RP, is tightly controlled.

The chaperones, under normal conditions, only bind to proteasome subcomplexes and are not found on the holoenzyme or mature CP. Several other proteasome-associated components have been identified that have binding sites on either CP or RP¹⁰. However, these have also been found associated with 26S proteasomes or mature CP, suggesting they regulate proteasome activity or assist in proteasome function. Indeed, several assist in delivery of substrates to the proteasome, modify the ubiquitin chains on substrates, or change the hydrolytic activity of the core particle¹⁰. Ecm29 is a unique proteasome component as it is the only one known to bind to the RP (Rpt5) as well as the CP^{11, 12}. Nevertheless, it is normally only found on singly and doubly capped proteasomes, i.e. RP-CP complexes and RP₂-CP complexes^{11, 13}.

Ecm29 is a large protein (210 kDa) predicted to contain 29 HEAT repeats. Both CryoEM analyses and structure predictions of Ecm29 suggest that Ecm29 forms an elongated and curved protein similar to many other proteins with multiple HEAT repeats^{11, 14}. Several functions have been proposed for yeast Ecm29 and the human ortholog KIAA0368. For example, it has been suggested to remodel proteasomes under stress conditions^{15, 16}, as well as play a role in localizing proteasomes to membrane components¹⁷⁻¹⁹. Initially, it was thought to positively regulate proteasome function as it stabilizes the RP-CP interaction in the absence of nucleotide^{11, 13}. However, Ecm29 has been shown to inhibit proteasome activity *in vivo* and *in vitro*^{12, 20}.

The inhibition by Ecm29 involves two mechanisms: first, Ecm29 binding induces closure of the substrate entry channel^{15, 20}. This channel is found on the top and bottom of CP and is normally opened by RP. Second, Ecm29 reduces the ATPase activity of proteasomes. This ATPase activity is required to unfold substrates so that they can enter the CP¹². Interestingly, Ecm29 has been found enriched on a variety of proteasome mutants^{15, 20-22}. These and other data led to the proposed function of Ecm29 as a quality control factor that recognizes aberrant proteasomes^{12, 20-22}.

It remains poorly understood why Ecm29 is enriched on mutant proteasomes. Ecm29 could specifically recognize faulty proteasomes¹², it could be an unstable proteasome substrate that is stabilized resulting from reduced proteasome activity^{21, 22}, or it could be upregulated in strains with proteasome mutations¹⁵. To better understand how Ecm29 associates with the proteasome and regulates proteasome activity, it is crucial to understand where Ecm29 binds to

the proteasome complex. Using a crosslinking approach on purified proteasomes, followed by a purification of Ecm29 and mass spectrometry analyses to identify proteins, we previously identified the RP subunit Rpt5 as an interaction partner of Ecm29¹². However, no CP subunits were identified.

Here, we report the identification of an Ecm29 binding site on the core particle subunit $\alpha 7$. Truncation of the C-terminal tail of $\alpha 7$ substantially diminishes the Ecm29 interaction with the proteasome in both wild type and in mutant proteasomes. Phenotypic analyses confirm that this tail of $\alpha 7$ is important for Ecm29 binding to proteasomes *in vivo* as well. Interestingly, the tail of $\alpha 7$ has a conserved acidic region that contains three serine residues that are known to be phosphorylated. Mutation of these sites indicates that Ecm29 depends on $\alpha 7$ phosphorylation for its interaction with the CP. Thus, our data reveal an additional level of complexity to the binding of Ecm29 to proteasomes and identify a function for the phosphorylation sites in the tail of $\alpha 7$.

Experimental procedures

Yeast techniques, plasmids and reagents

Yeast strains used are summarized in table 1. Genomic manipulation of yeast was done using a PCR based approach^{56, 57}. Upon transformation of yeast, successful integration was confirmed by positive PCR for integration and negative PCR for wild type. To make $\alpha 7$ - $\Delta 40$, primer pRL207: 5'- TGC TAC AGG AAG CTA TCG ATT TTG CCC AAA AAG AAA TTA ACT GAG GCG CGC CAC TTC T-3' and pRL66: 5'-TCA ACT CTT TGG TTC TTC TTA ACG TAT TAT CAG AAT GTC ATC GAT GAA TTC GAG CTC G -3' were used. $\alpha 7$ - $\Delta 19$ that contains the acidic patch and phosphorylation sites, primers pRL 248: 5'-TGA CAG TGA TAA CGT CAT GTC CAG TGA TGA TGA AAAT GCT TGA GGC GCG CCA CTT CT -3' and pRL66, for $\alpha 7$ - $\Delta 19$ (S/A) that replaces three Serine to Alanine (S258A, S263A and S264A) from $\alpha 7$ tail pRL319: 5'- ATC GAT TTT GCC CAA AAA GAA ATT AAC GGC GAT GAT GAC GAG GAC GAA GAT GAC GCG GAT AAC GTC ATG GCG GCC GAT GAT GAA AAT GCT TGA GGC GCG CCA CTT CT -3' and pRL 66 were used. To make $\alpha 7$ - $\Delta 19$ (S/D) that represents the phospho mimic (S258D, S263D and S264D), pRL320: 5'- ATC GAT TTT GCC CAA AAA GAA ATT AAC GGC GAT GAT GAC GAG GAC GAAG ATG ACG ACG ATA ACG TCA TGG ATG ACG ATG ATG AAA ATG CTT GAG GCG CGC CAC TTC T -3' and pRL66 were used. All truncations and point mutations were confirmed by PCR followed by sequencing. To delete C-terminal last three amino acids from Rpt5 subunit, pRLS2-Rpt5: 5'- AAT ATG TAG ATA TGT GAA TGG CGG CTT GAT AAA TCA AAA TAT TAT TAT TTA TCG ATG AAT TCG AGC TCG -3' and pRLS3-Rpt5- $\Delta 3$: 5'- TCG TTG AGG GTA TAA GTG AAG TTC AAG CAA GAA AAT CGA AAT CGG TAT CCT AGG GCG CGC CAG ATC TGT T -3' were used. The templates used for the above PCR reactions indicated above were pFA61-3HA-kanMX6 (KAN) and pYM24 (HYGRO), primers were designed to eliminate the 3-HA tags.

Ecm29 promoter changes were done by using pRL194: 5'- TCT CCA CGA GCT GTT TTT CTT TCG CTT CGT CAG AAG AAA TGG A TC CGG AAT GGT GAT GGT GAT GGT GGT GCA TCG ATG AAT TCT CTG TCG -3' and pfEcm29 Ntag s1: 5'- CAA TAA TTA TAG AAA AGT TTC TAT TTC ACC ACG AAC AAC ATT CGT ACG CTG CAG GTC GAC

-3' with pYM-N15 to add GDP overexpression promoter. To add ADH weak expression promoter to Ecm29, pYM-N7 was used with pRL194 and pfEcm29-Ntag-s1. Integrations, truncations and mutations were confirmed by PCR and sequencing.

Antibodies used for immunoblots:

Ecm29 and Rpn8 were detected using polyclonal antibody (generous gift by Dan Finley, Harvard Medical School, Boston, MA). Anti- α 7 monoclonal antibody was purchased from Enzo Life Sciences and anti-Pgk1 monoclonal antibody was purchased from Invitrogen. Peroxidase-conjugated secondary antibodies were purchased from Jackson Immunoresearch Laboratories.

Proteasome purification

Specific yeast strains were grown overnight in 2 to 3 liter of YPD media (final $A_{600} \sim 10.0$). Cells were collected and washed with H_2O . Pellets were resuspended in 1.5 pellet volume of lysis buffer (50 mM Tris [pH8.0], 5 mM $MgCl_2$, 1 mM EDTA, and 1 mM ATP) and lysed using a French Press at 1200 Psi. Lysates were cleared by centrifugation (10,000 g; 30 minutes) and the supernatant was filtered through cheesecloth. Concentration of cell lysate was measured using NanoDrop 2000 Spectrophotometer using the Protein A_{280} program and cell lysate equivalent to 50 mg of protein was boiled with 1X SDS-PAGE sample buffer for 5 minutes at 96 °C. Next, samples were resolved on 11% SDS-PAGE. For proteasome purification cell lysate were filtered through cheesecloth prior to incubation with IgG beads (MP Biomedical; 0.75 ml resin bed volume per 25 gram of cell pellet). After 1 hour of incubation (rotating at 4 °C), IgG beads were collected in an Econo Column (Bio-Rad) and washed with 50 bed volumes of ice-cold wash buffer (50 mM Tris [pH 7.5], 5 mM $MgCl_2$, 50 mM NaCl, 1 mM EDTA, 1 mM ATP). Next, material was washed with 20 bed volumes of cleavage buffer (50 mM Tris [pH 7.5], 5 mM $MgCl_2$, 1 mM DTT, and 1 mM ATP). Bead-bound proteasome complex was eluted by incubation with His-Tev protease (Invitrogen). The protease was removed by incubation with talon resin (Goldbio) prior to concentrating the proteasome complexes using 100 kDa concentrator (PALL Life Sciences). Purified proteasome were resolved on SDS-PAGE or on native gel as described previously⁵⁶. To store samples, 5% final concentration glycerol was added and samples were stored at -80 °C.

For core particle purification proteasome bound IgG beads were incubated with 5 bed volumes of wash buffer containing 500 mM NaCl for 1hr at 4 °C under constant rotation. After

incubation, the beads were washed with 50 bed volumes of wash buffer with 500 mM NaCl. Elution and concentration of core particle complexes were as described above for proteasome complexes.

Table 3.1 Yeast strains used for results in chapter-3.

Strain	Genotype	Figure	Ref.
sUB61	MAT α lys2-801 leu2-3, 2-112 ura3-52 his3- Δ 200 trp1-1	3.3A-B, 3.4, 3.5A-D, B.1	⁵⁷
sDL135	MAT α pre1::PRE1-TEV-ProA (HIS3)	3.2B, 3.2D	¹¹ (a)
sDL133	MAT α rpn11::RPN11-TEV-ProA (HIS3)	3.2B-C, 3.6B, 3.7A, B.2B-C	⁵⁸
sMK141	MAT α ecm29::TRP	3.3A-B, 3.4, B.1	¹²
sJR 211	MAT α ecm29::TRP rpn11::RPN11-TEVProA (HIS3)	3.9	
sJR544	MAT α ecm29::TRP rpt5::RPT5 Δ 3 (HYG)	3.3A-B, 3.4, B.1	²⁰
sJR556	MAT A rpt5::RPT5 Δ 3 (HYG)	3.3A-B, 3.4, 3.5C-D, B.1	³²
sJR768	MAT α pre10::PRE10 Δ 40 (KAN)	3.3A-B, 3.4, 3.5A-B, B.1	(a, b)
sJR770	MAT α pre10::PRE10 Δ 40 (KAN) pre1::PRE1-TEVProA (HIS3)	3.2B, 3.2D	(b)
sJR 822	MAT α ecm29::TRP pre10::PRE10 Δ 40 (KAN) rpn11::RPN11-TEVProA (HIS3)	3.9	(b)
sJR805	MAT A pre10::PRE10 Δ 40 (KAN) rpt5::RPT5 Δ 3 (HYG)	3.3A-B, 3.4, B.1	(b)
sJR810	MAT α pre10::PRE10 Δ 40 (KAN) rpn11::RPN11-TEVPro (HIS3)	3.2B-C, 3.6B, 3.7A, B.2B-C	(b)
sJR839	MAT A ecm29:: pGDP-H7-ECM29 (NAT)	3.5A-B	(b)
sJR840	MAT A pre10::PRE10 Δ 40 (KAN) ecm29:: pGDP-H7-ECM29 (NAT)	3.5A-B	(b)
sJR816	MAT α ecm29:: pADH1-ECM29 (NAT)	3.5C-D	(b)
sJR820	MAT α ecm29:: pADH1-ECM29 (NAT) rpt5::RPT5 Δ 3 (HYG)	3.5C-D	(b)

sJR884	MAT α pre10::PRE10 Δ 19(KAN) rpn11::RPN11-TEVPro (HIS3)	3.6B, 3.7A, B.2B-C	(b)
sJR887	MAT α pre10::PRE10 Δ 19(S/A) (KAN) rpn11::RPN11-TEVPro (HIS3)	3.6B, 3.7A, B.2B-C	(b)
sJR887	MAT α pre10::PRE10 Δ 19(S/D) (KAN) rpn11::RPN11-TEVPro (HIS3)	B.2B-C	(b)
sJR912	MAT α pre10::PRE10 Δ 19 (KAN) rpt5::RPT5 Δ 3 (HYG) rpn11::RPN11-TEVPro (HIS3)	3.7B	(b)
sJR911	MAT α pre10::PRE10 Δ 19 (S/A) (KAN) rpt5::RPT5 Δ 3 (HYG) rpn11::RPN11-TEVPro (HIS3)	3.7B	(b)
Ump1-TAP	MAT A ump1::UMP1- CBP-TEV-ZZ-(His3MX6)	3.8	(*, #)
Ump1 Δ	MAT α ump1::UMP1 (KAN)	3.3A-B, 3.4, B.1	(*, #)
sJR856	MAT α Ump1 Δ (KAN) pre10::PRE10 Δ 40 (HIS3)	3.3A-B, 3.4, B.1	(*, #, b)

(a) *PRE1* encodes for the proteasome subunit β 4 and *PRE10* for α 7

(b) this study

* BY4741 background genotype (his3 Δ 0 leu2 Δ 0 met15 Δ 0 ura3 Δ 0).

Ref : Ghaemmaghami, S. (2003) Global analysis of protein expression in yeast. *Nature*.

425, 737-741

Yeast phenotypes

Indicated strains were incubated in 3 ml of YPD for overnight at 30 °C. Next day, cells equivalent to 1.0 at OD₆₀₀ were collected and washed with 100 µl sterile water. Cell pellet is then resuspended in 133 µl of sterile water and 4-fold serial dilutions were made in sterile water in 96 well plate. Diluted cells were then spotted on the indicated plates and incubated at indicated temperatures. Growth was monitored for 3 days on YPD plates and for 5-6 days on synthetic media plates.

Fluorescent phospho- and coomassie blue staining

10 µg Proteasome complex purified from the indicated samples were mixed with the 6X loading buffer and boiled for 5 minutes at 95 °C. Boiled samples were cooled to room temperature and resolved on 11% SDS-PAGE gel. To detect the phosphorylated proteins, gel was subjected to fluorescent photo staining by using Pro-Q® Diamond phosphoprotein gel stain according to the manufacturer's recommendations (Life Technologies) and scanned with a Typhoon-9410 imager from Amersham Biosciences (excitation at 532 nm and an emission filter of 560nm longpass). After destaining, the gel was treated with Coomassie Blue and imaged using a Gbox image system (SynGene) with GeneSnap software.

Apyrase assay

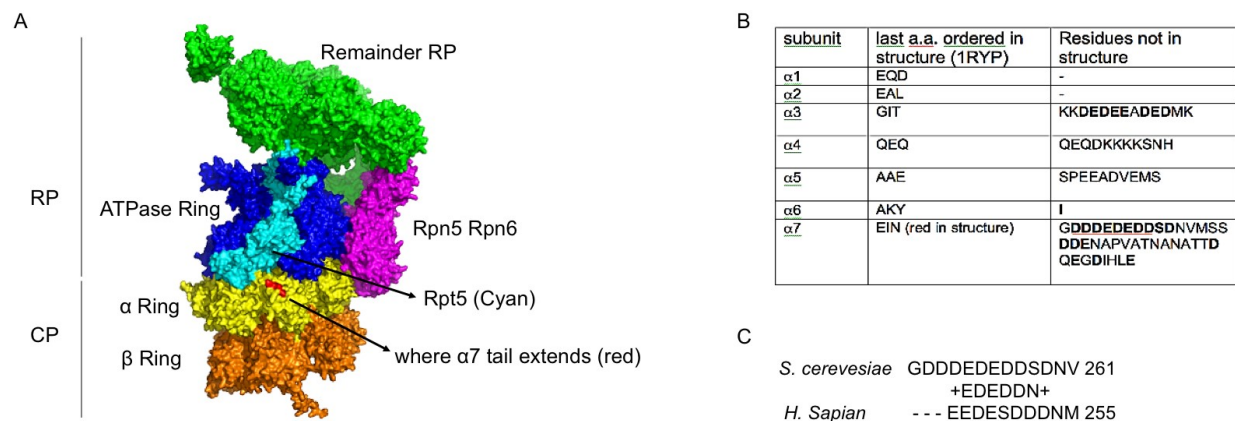
Equal amount of proteasome purified from the indicated strains were inhibited by 200 nM proteasome inhibitor Epoxomicin in final volume and incubating at 30°C for 30 minutes. Both inhibited and non-inhibited proteasome samples are then subjected to apyrase treatment by adding apyrase (Sigma) in 0.024 mU/µl as final concentration diluted in apyrase buffer (50 mM Tris pH 7.5, 5 mM MgCl₂, 0.25 mM ATP) and analyzed on nondenaturing gel. Dissociation of proteasome is monitored by in-gel activity assay using LLVY-AMC followed by immunoblotting with CP antibody α 7.

Results

$\alpha 7$ subunit of CP as putative binding partner for Ecm29

Ecm29 is predicted to bind CP as well as RP¹¹. We hypothesized that the CP binding surface of Ecm29 should be in close proximity to RP binding site, Rpt5¹². Nevertheless, Ecm29 is a large protein with a likely elongated and curved structure, thus the CP binding site does not necessarily have to be adjacent to Rpt5. Recent mapping of the RP-CP interaction and structural insights from several cryoEM structures of the proteasome provide a detailed understanding of the location of Rpt5 with respect to CP (Fig. 3.1A)²³⁻²⁶. The C-terminus of Rpt5 docks into a pocket formed at the interface of the CP subunits $\alpha 5$ and $\alpha 6$ ²³⁻²⁶ and has also been shown to be able to occupy the pocket between $\alpha 6$ and $\alpha 7$ ²³. The face of the CP cylinder provides the interaction surface with the RP. Here, the α -subunits have N-termini that extend and contributes to the formation of the CP gate²⁷. This area is unlikely to be available for Ecm29 binding, because it is covered by the RP in the 26S proteasomes²⁴⁻²⁶. Thus, Ecm29 is more likely to bind to the side facing surfaces of α -subunits.

Figure 3.1 $\alpha 7$ as the putative binding site for Ecm29.



(A) CryoEM-based model of the Proteasome²⁶ (PDB- 4B4T) showing regulatory particle (RP) and core particle (CP). Rpt5 is displayed in cyan and other Rpt subunits in blue. Lid subunits Rpn5 and Rpn6 that interact with the CP are shown in purple and the remainder of RP is shown

in green. All core particle α subunits are colored in yellow, with the last three ordered amino acids of $\alpha 7$ shown in red. β subunits are colored in orange. (B) Amino acid sequences from the α -ring subunits beyond crystal structure²⁸ and model presented²⁶. Second column shows the last three ordered amino acids for each α subunit. Third column shows C-terminal amino acids that were not resolved in the structure. Consecutive acidic residues in C-terminal of $\alpha 7$ residues that forms the acidic patch are underlined as red line. (C) Sequence alignment of acidic patch in the C-terminal tail of $\alpha 7$ from *S. cerevisiae* and *H. sapiens*.

Interestingly, four out of seven α -subunits of the α -ring ($\alpha 3$, $\alpha 4$, $\alpha 5$, and $\alpha 7$) have C-terminal amino acid sequences (≥ 10 residues) that are not resolved in the crystal structure of the CP and are likely to extend from the side face of the CP²⁸. From these $\alpha 7$ is particularly interesting because it contains the longest extension, 40 residues, and this region contains a patch of acidic residues (Fig. 3.1B). Human $\alpha 7$ has a similar C-terminal tail that extend beyond the crystal structure and harbors numerous acidic residues (Fig. 3.1C)²⁹. Thus, features of the $\alpha 7$ C-terminal region are conserved from yeast to human. This is important since Ecm29 is conserved and presumably the binding site as well. Figure 1a shows the last resolved $\alpha 7$ residues in a 26S model in red. From this it is clear that the extended tail is in close proximity to the Rpt5 subunit (light blue in Fig. 3.1A) that we have previously shown to bind to Ecm29.

C-terminal tail of $\alpha 7$ subunit is important for Ecm29 binding to the proteasome.

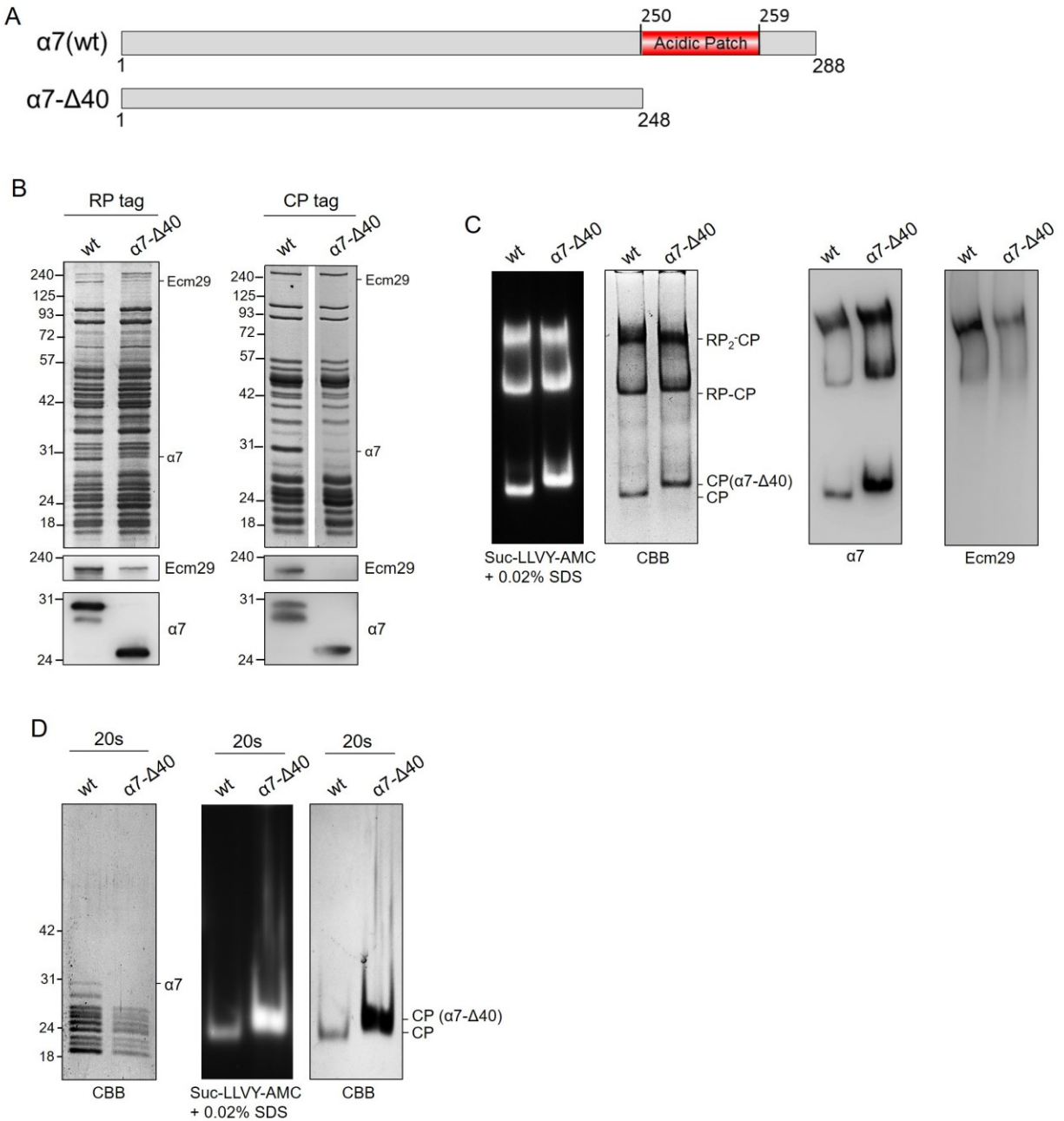
To test if the $\alpha 7$ C-terminal tail is important for the Ecm29-proteasome interaction, we deleted the last 40 amino acid residues from the $\alpha 7$ subunit (Fig. 3. 1A and 3.2a). These are all residues that were not resolved in the crystal structure of the CP²⁸. Strains with this $\alpha 7$ truncation were viable and we refer to strains and proteasomes with this truncation as $\alpha 7$ - $\Delta 40$ from here onwards. To purify proteasomes we introduced this truncation in strains that either contained the protein A-tagged RP subunit Rpn1 or protein A-tagged CP subunit Pre1 ($\beta 4$)¹¹.

Compared with wild type proteasomes, proteasomes purified from these strains show a pattern on Coomassie Brilliant Blue (CBB) stained SDS_PAGE gels. (Fig. 3.2B). Immunoblotting for $\alpha 7$ showed a lower molecular weight for $\alpha 7$ upon truncation that was consistent with the expected reduction in molecular weight from 31.5 kD to 27.3 kD. Purified

proteasomes also showed a strongly reduced level of Ecm29 upon truncation of $\alpha 7$. As is evident from the CBB, proteasome preparations purified using the CP-tag have generally reduced levels of RP and increased amounts of CP as compared to RP-based proteasome purifications. This difference likely explains the lower levels of Ecm29 in CP-tag proteasome purifications. Nevertheless, there is still a clear reduction of Ecm29 levels upon deletion of the $\alpha 7$ tail.

Native gel analyses of proteasome complexes purified from wild type and $\alpha 7$ - $\Delta 40$ strains also showed reduced levels of Ecm29 in the $\alpha 7$ - $\Delta 40$ background. Nevertheless, the remaining small amount of Ecm29 still bound to the same proteasome complexes as has been observed under wild type conditions, namely both singly and doubly capped proteasome (RP-CP and RP₂-CP, Fig. 3.2c). Additionally, we observed a slower migration form of CP in the $\alpha 7$ - $\Delta 40$ samples. A similar slower migration of CP is observed when CP associates with Blm10. However, we did not observe increased levels of Blm10 in $\alpha 7$ - $\Delta 40$ proteasomes compared to wild type proteasomes (Fig. 3.1B). The $\alpha 7$ truncation contains 16 acidic residues and the calculated isoelectric point of the protein changes from pI 5.02 to 7.72, thus instead of other proteins binding to CP, the altered migration might result from a difference in charge between wild type and $\alpha 7$ - $\Delta 40$ CP. To test this we purified CP from wild type as well as from $\alpha 7$ - $\Delta 40$ (Fig 3.2D). The high salt washes required to purify CP also removes any Blm10 that might be bound to the CP as is apparent from the absence of a ~240 kDa bands from CP preparations (Fig. 3.2D). Even in the absence of Blm10, $\alpha 7$ - $\Delta 40$ derived CP showed a retarded migration compared to CP with full-length $\alpha 7$. Thus, the change in migration results from the truncation and is most likely due to the loss of negatively charged amino acid residues. In sum, our results show that the truncation of the $\alpha 7$ tail leads to reduced binding of Ecm29 to singly and doubly capped proteasome.

Figure 3.2 unstructured C-terminal tail of the $\alpha 7$ is involved in the Ecm29 interaction to the proteasome.



(A) Schematic representation of wild type $\alpha 7$ displaying the acidic patch (residues D250 to D259) and the $\alpha 7$ with C-terminal truncation ($\alpha 7$ - $\Delta 40$) that removes all amino acids beyond N248. (b) Proteasomes were purified from wild type and $\alpha 7$ - $\Delta 40$ cells using either an RP tag (*Rpn11*-TEV-ProA; left panel) or CP tag (*Pre1*-TEV-ProA; right panel) and analyzed on SDS-

PAGE as well as by immunoblotting using antibodies against Ecm29 and $\alpha 7$. (B) RP-tag derived proteasome purifications from (B) were resolved on native gel and stained using an in-gel activity assay with LLVY-AMC as substrate in the presence of 0.02% SDS. Gel was coomassie stained or transferred to pvdF membrane to probe for the presence of Ecm29 and $\alpha 7$. (D) CP from wild type and $\alpha 7$ - $\Delta 40$ cells was resolved on SDS-PAGE and stained with CBB (left panel). Same samples were also resolved on native gel, followed by in-gel LLVY-AMC activity assay and CBB staining. Difference in electrophoretic migration of CP from $\alpha 7$ - $\Delta 40$ does not results from an enrichment in Blm10 and is likely due to the difference in charge between $\alpha 7$ and $\alpha 7$ - $\Delta 40$.

Effect of $\alpha 7$ C-terminal tail truncation in vivo.

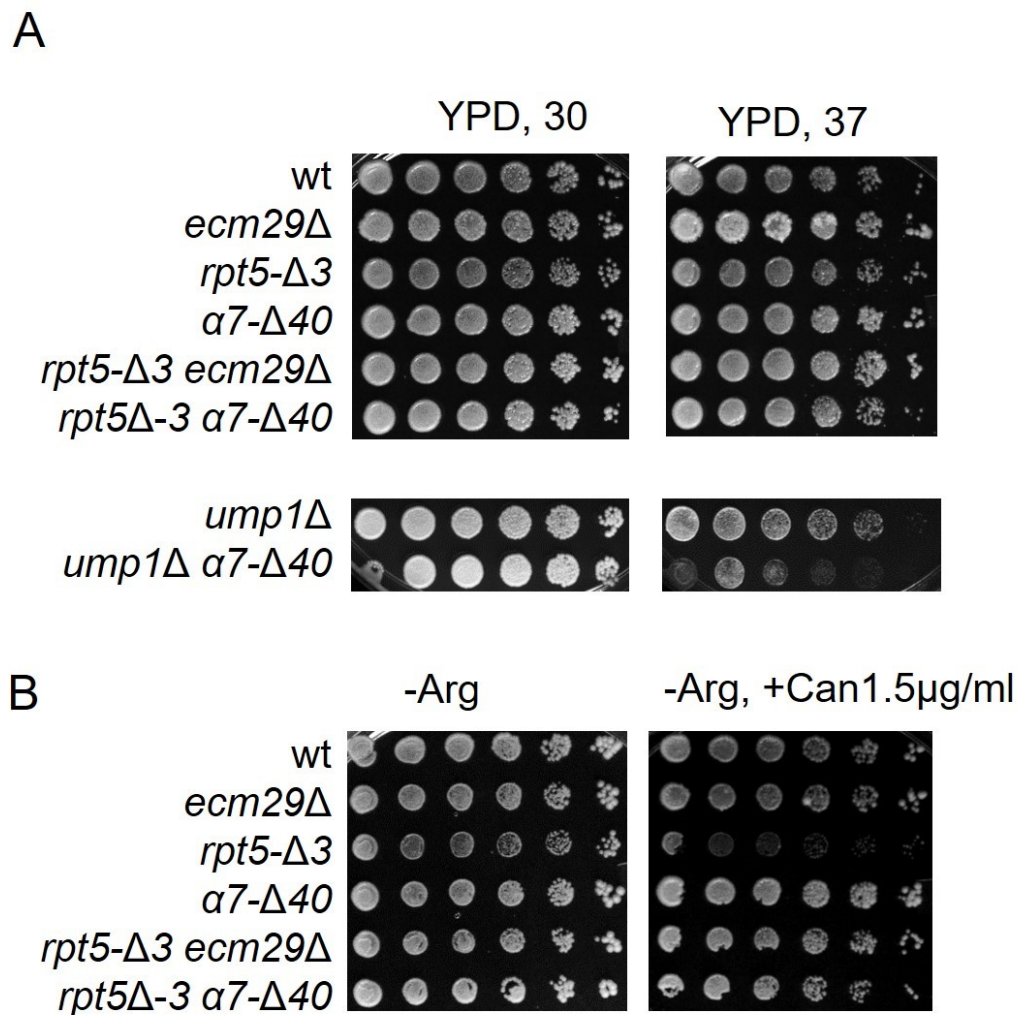
Next, in order to determine the physiological importance of the $\alpha 7$ truncation *in vivo*, we analyzed cells for two phenotypes typical for proteasome mutants: sensitivity to heat stress at 37 °C and canavanine sensitivity. Both of these conditions are thought to introduce protein misfolding stress due to the high temperature or the incorporation of the arginine analog canavanine. Unlike several proteasome mutants or mutants with defects in proteasome assembly, the $\alpha 7$ truncation did not cause increased sensitivity to these conditions (Fig. 3.3A and 3.3B). This suggests there are no major defects in proteasome function upon deletion of the $\alpha 7$ C-terminal tail. Similarly, the deletion of Ecm29 by itself does not cause temperature sensitivity or canavanine sensitivity.

Next, we tested if the truncation can rescue or cause synergistic effects in backgrounds where this has been observed for the deletion of Ecm29. Here, we predict that strains with the $\alpha 7$ C-terminal truncation should, at least in part, mimic phenotypes that resulted from a deletion of *ECM29*, because $\alpha 7$ - $\Delta 40$ results in reduced binding of Ecm29 to proteasome. We have previously characterized the *rpt5*- $\Delta 3$ mutant where last three amino acids of the Rpt5 subunit are absent. In this strain proteasomes are enriched in Ecm29²⁰. The Rpt5 residues that are missing in *rpt5*- $\Delta 3$ strains, are involved in the docking of RP onto CP^{23-26,30}. This suggests that proteasomes from *rpt5*- $\Delta 3$ cells have defects at the RP-CP interface due to improper association. *Rpt5*- $\Delta 3$ strain shows canavanine sensitivity resulting from the cumulative effect of reduced proteasome activity caused by the mutant form of Rpt5 as well as the inhibition by Ecm29¹².

The canavanine sensitivity can be rescued by a deletion of Ecm29. When we introduced the $\alpha 7$ tail truncation in *rpt5*- $\Delta 3$ strains, the canavanine sensitivity was also rescued.

The deletion of Ecm29 in an *ump1* Δ background causes increased sensitivity at 37 °C²¹. Ump1 is a CP assembly chaperone and the deletion of *UMP1* has been results in defects in CP assembly as well as an enrichment of Ecm29 on proteasomes²¹. The $\alpha 7$ C-terminal truncation in *ump1* Δ causes increased sensitivity of these cells for growth at 37 °C, indicating the deletion of the 40 amino acids from the $\alpha 7$ causes a phenotype similar to the deletion of Ecm29 in this background as well. Thus, the $\alpha 7$ truncation phenotypically mimics a deletion of Ecm29, suggesting the $\alpha 7$ tail is important for the recruitment of Ecm29 to mutant proteasomes *in vivo*.

Figure 3.3 $\alpha 7$ C-terminal truncation mimics as Ecm29 Δ .

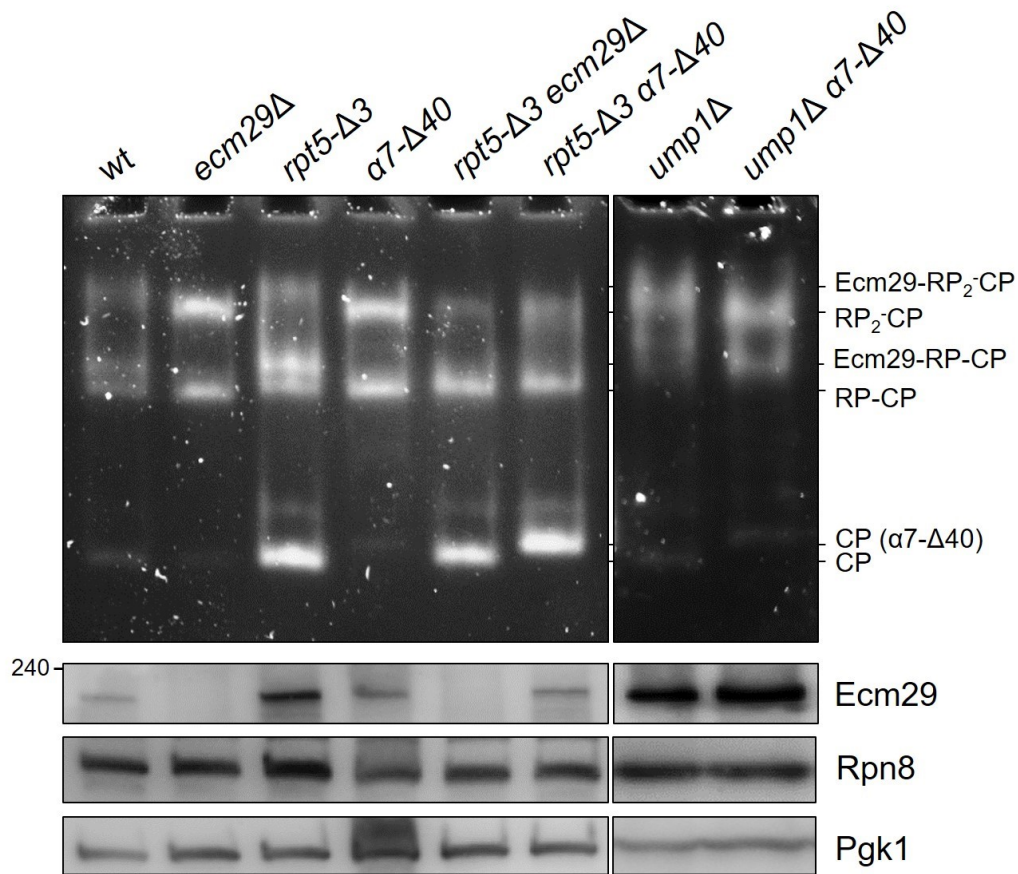


(A+B) Indicated strains were serially diluted (four-fold) and (A) spotted onto YPD medium and grown at the indicated temperatures for 3 days or (B) spotted on SD plates lacking arginine with or without canvanine and grown at 30 °C for 5 to 6 days. The $\alpha 7$ - $\Delta 40$ truncation resemble a deletion of *ECM29* in the different backgrounds.

Next, we biochemically characterized proteasome complexes formed in a mutant strains background. Cell lysates were resolved on the native gel followed by the activity assay using short peptide LLVY-AMC (Fig. 3.4). Singly and double capped proteasomes (RP₂-CP or RP-CP) can associate with Ecm29. This association causes a slower migration on native gel^{11,13}. *Rpt5*- $\Delta 3$ cells are highly enriched in Ecm29 as compared to wild type cells. Consistently, more *rpt5*- $\Delta 3$ proteasomes show a notably slower migrating species on the native gel, which is caused by association of Ecm29 as it is absent from *ecm29* Δ cells (Fig. 3.4 compare lane 3 and 5). Consistent with our phenotype data, truncations of $\alpha 7$ in the *rpt5*- $\Delta 3$ background caused a migration of the proteasomes on native gels similar to that resulting from the deletion of *ECM29*. This indicates a reduced recruitment of Ecm29 to $\alpha 7$ - $\Delta 40$ *rpt5*- $\Delta 3$ proteasomes.

To analyze the level of Ecm29 present in the different strains (Fig. 3.4 lower panel) we ran the same samples on SDS-PAGE and conducted western blot analyses using an antibody that can recognize the endogenous Ecm29 protein. As observed previously, the *rpt5*- $\Delta 3$ strain shows increased levels of Ecm29 in the total cell lysate compared to wild type. Interestingly, the truncation of $\alpha 7$ in this background reduces the levels of Ecm29 back to levels similar to wild type (Fig. 3.4, compare lane 6 with 1). Nevertheless, we did not observed any changes in expression of proteasome subunits. Ecm29 has been reported to be degraded by the proteasome^{21,22}, which might suggest that a loss of interaction with proteasome increases Ecm29 turnover. However, other reports have suggested Ecm29 is stable and increased levels on proteasomes result from higher rates of transcription¹⁵, which would suggest the $\alpha 7$ tail truncation results in a lower level of Ecm29 expression in this mutant. In either case, the effect of the truncation of $\alpha 7$ seems to be background dependent, as in both the *ump1* Δ and the *ump1* Δ $\alpha 7$ - $\Delta 40$, Ecm29 levels are increased as compared to wild type.

Figure 3.4 Effect of $\alpha 7$ C-terminal truncation on Ecm29 expression level and its association to the proteasome.



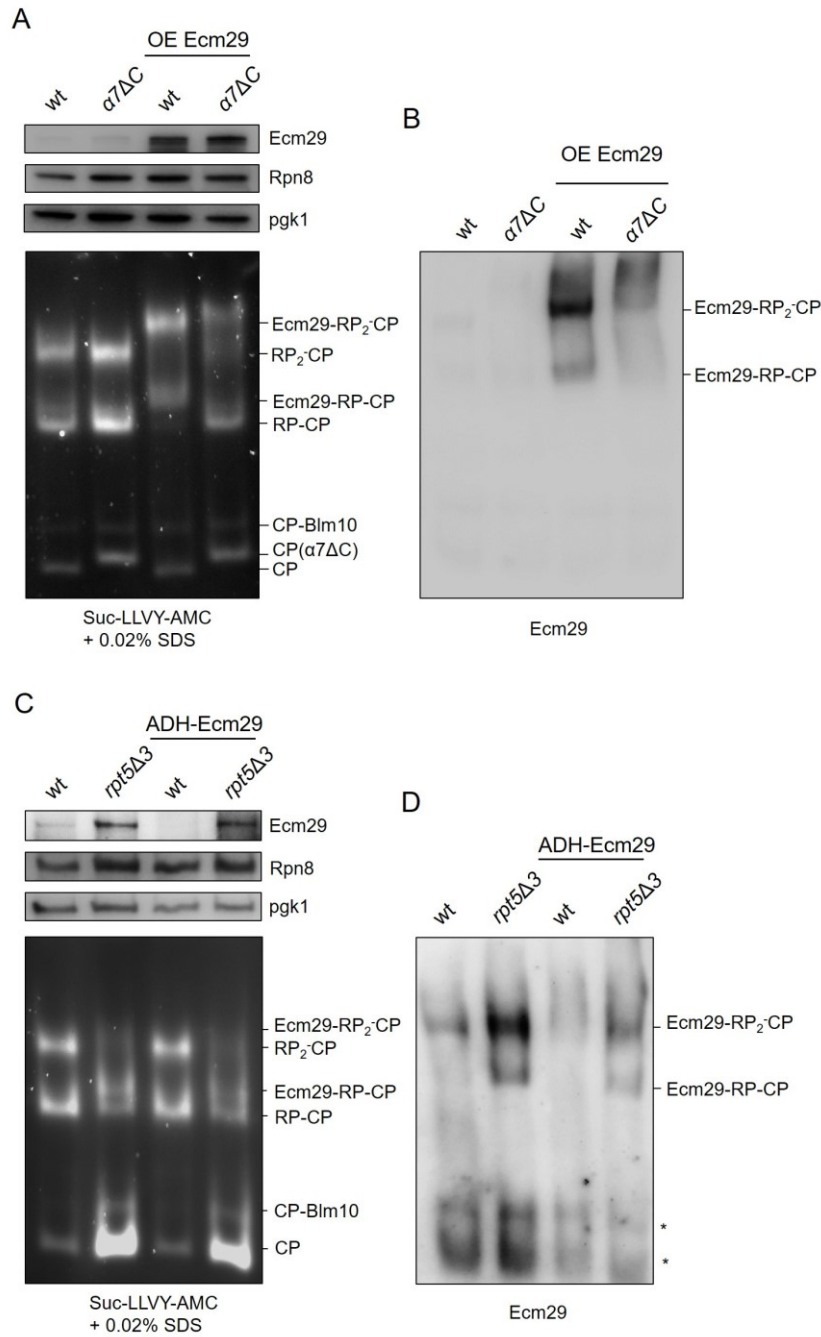
Equal protein amount of total cell lysates from the indicated strains were analyzed on 3.5% nondenaturing gel and stained using the LLVY-AMC activity assay (upper panel). Protein extracts were also resolved on SDS-PAGE, followed by immuno blotting to determine the levels Ecm29 and Rpn8. Immunoblot against Pgk1 was used as a loading control.

To eliminate any complication in our analysis as a result of differences in transcriptional regulation of *ECM29*, we changed the promoter of *ECM29* with the *GDP* promoter. For wild type cells this has been previously shown to increase the levels of Ecm29 in the cell and result in stoichiometric amounts of Ecm29 on proteasomes^{12, 15} (Fig 3.5A and 3.5B). Under these conditions we see high levels of Ecm29 in the cell lysate of both wild type and $\alpha 7$ - $\Delta 40$ cells.

Native gel analyses, however, clearly shows a reduced level of Ecm29 on 26S proteasomes from the $\alpha 7$ - $\Delta 40$ strains, with singly capped proteasome having hardly any Ecm29 associated with the proteasome and strongly reduced amount of doubly capped proteasomes associated with Ecm29. Thus, even under conditions of very strong overexpression of Ecm29 the truncation of $\alpha 7$ causes reduced binding of Ecm29 to proteasomes. Since Ecm29 binds to Rpt5 in addition to $\alpha 7$, the loss of $\alpha 7$ binding probably results in a substantially reduced affinity of Ecm29 for proteasomes, but no complete loss of affinity. The high level of Ecm29 expression resulting from the GDP promoter might thus be able to still drive some Rpt5-mediated binding of Ecm29 to proteasomes, explaining some limited binding of Ecm29 to proteasomes in the $\alpha 7$ - $\Delta 40$ background.

The ability to drive Ecm29 association with the proteasome by increasing the levels of Ecm29 in the cell, suggests that Ecm29 association with proteasomes is driven by the transcriptional regulation of *ECM29* in the cell. However, we have previously shown that Ecm29 shows better binding to a mutant proteasome as compared to a wild type proteasome¹². Thus, an alternatively explanation for the observation of Ecm29 on wild type proteasomes is that a lower affinity of Ecm29 for wild type proteasomes can be obscured by strong overexpression of Ecm29. Ecm29 levels resulting from GDP promoter are for example substantially higher than any increase resulting from upregulation of the endogenous locus through the stabilization of Rpn4. Thus, analyses from GDP promoter driven Ecm29 overexpression results are non-physiological. Therefore, we created strains where Ecm29 expression is not driven by the very strong GDP promoter, but by the much weaker ADH promoter (Fig. 3.5C and 3.5D). Here, we still eliminate the Rpn4 feedback loop by replacing the endogenous promoter, but now have a much lower transcription level of *ECM29*. Consistent with this, there is less Ecm29 in the cells as compared to wildtype cells (Fig. 3.5C). That notwithstanding, the level of Ecm29 in the cell and on the proteasome dramatically increase in *rpt5-D3* cells with the endogenous promoter as well as the ADH promoter. Thus, clearly Rpn4 driven transcriptional upregulation is not required to achieve increased association of Ecm29 with mutant proteasomes.

Figure 3.5 Exchange of Ecm29 promoter to eliminate differential transcription of Ecm29.



(A, B) The endogenous promoter of *Ecm29* was replaced with the *GPD* promoter. This exchange causes a strong overexpression of *Ecm29* that drives binding of *Ecm29* to all most all wild type proteasomes^{12, 15}, as is seen in the immunoblot of total lysates. Native gel analyses of total lysate can visualize presence of *Ecm29* on singly and doubly capped proteasomes because the presence

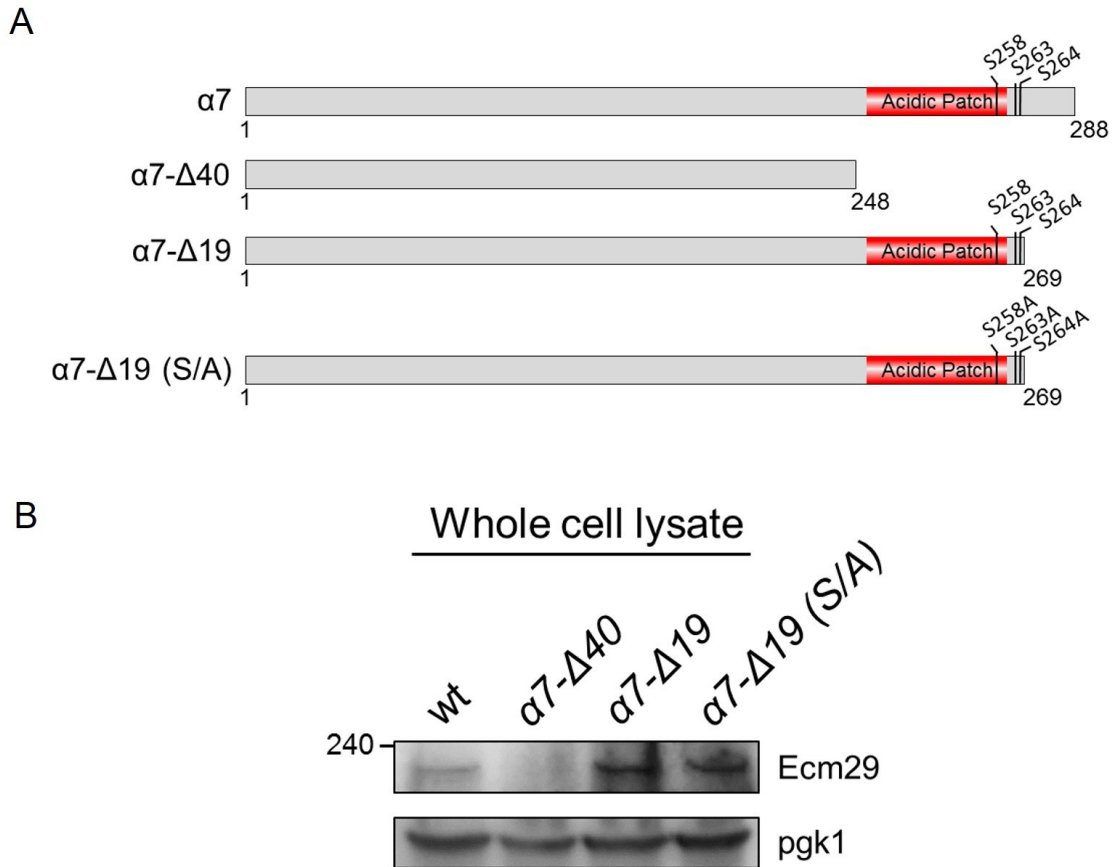
of Ecm29 causes a migrational shift. The presence was also confirmed by immunoblotting the native gel and probing with an anti-Ecm29 antibody. Even under conditions of strong overexpression the $\alpha 7$ - $\Delta 40$ strain shows strongly reduced levels of Ecm29 on singly and doubly capped proteasomes. (C, D) The endogenous promoter of Ecm29 was replaced with the ADH promoter resulting in weak expression of Ecm29 in wild type as well as in *rpt5- $\Delta 3$* strain background. Analyses were identical as for (A, B). With weak promoter the behavior of Ecm29 in wildtype and mutant strains is very similar to cells with the endogenous promoter, suggesting the Rpn4-dependent transcriptional regulation of Ecm29 is not essential for the enrichment of Ecm29 on proteasomes.

$\alpha 7$ phosphorylation is required for Ecm29 interaction to CP.

Seven phosphorylation sites have been identified in yeast $\alpha 7$ ³¹⁻³⁶. Interestingly, five of these sites, S258, S263, S264, T278 and T279, are present in the tail of the $\alpha 7$ that we eliminated. From these, S258, S263, and S264 have been identified multiple times and in studies specifically focused on phosphorylation of the proteasome^{31,33,34,37}. The phosphorylation of $\alpha 7$ has been observed in humans as well, suggesting there is a conserved function for this modification³⁸⁻⁴⁰. CK2 (formerly known as casein kinase 2) has been proposed to be responsible for phosphorylation of the serine residues present at the $\alpha 7$ C-terminal^{31,41}. CK2 generally phosphorylates serine residues in an acidic environment⁴², which is provided by the acid patch present in $\alpha 7$ tail. Furthermore, the phosphorylation by CK2 is often constitutive. This is consistent with the observation that yeast as well as human $\alpha 7$ is present almost exclusively in the phosphorylated form³⁷. To test if $\alpha 7$ is phosphorylated under our conditions, we purified proteasomes and resolved preparations on SDS-PAGE. Gels were stained for CBB and analyzed using the in gel Pro-Q diamond phosphostain. These analyses show a band corresponding to the size of $\alpha 7$ that is strongly phosphorylated. Consistent with our assignment of $\alpha 7$, this band disappears in the phospho-stain analyses when analyzing proteasomes from the $\alpha 7$ - $\Delta 40$ strain. Since no band of lower molecular weight appeared, our data suggest that $\alpha 7$ is mainly phosphorylated in the C-terminal fragment, something that had been suggested before³⁷. To test if T278 and T289 in $\alpha 7$ are essential for the ability of Ecm29 to bind proteasomes, we eliminated these phosphorylation sites by making a truncation that removes only 19 residues instead of 40

from $\alpha 7$, keeping the acidic patch and three serine phosphorylation sites intact, namely S258, S263, and S264. We refer to this mutant as $\alpha 7\text{-}\Delta 19$ (Fig. 3.6A). We tested the cell lysates from the mutated strains if that affects the Ecm29 expression. Elimination of last 19 amino acids from the C-terminal tail of the $\alpha 7$ does not affect the Ecm29 level *in vivo* (Fig. 3.6B).

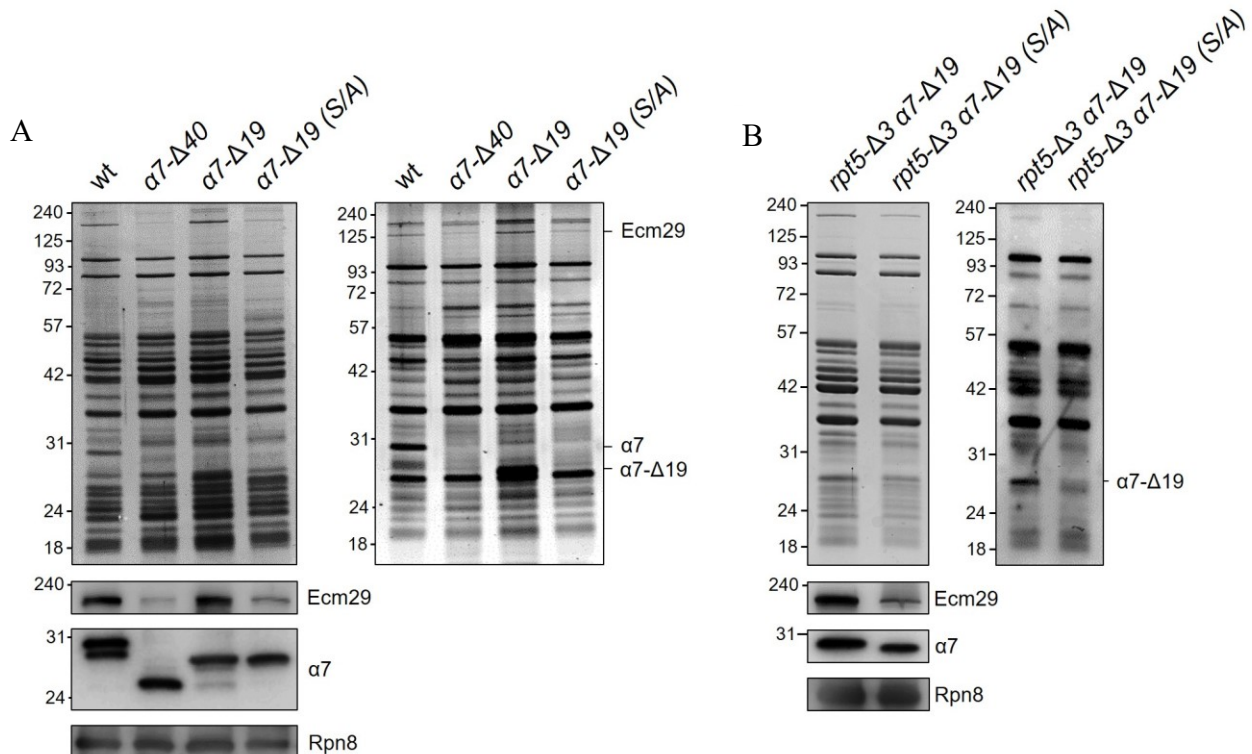
Figure 3.6 Phosphomutations at the C-terminal tail of the $\alpha 7$ and Ecm29 expression level.



(A) Schematic representation of mutations in $\alpha 7$ protein. A short truncation at the C-terminal tail of the $\alpha 7$ were made resulted in $\alpha 7\Delta C\text{-ST}$ (1-269) that contains acidic patch and three serine phosphorylation sites (S258, S263 and S264). Phosphomutant $\alpha 7\Delta C\text{-ST}$ (S/A) were created by replacing three serine residues with alanine. (B) Equal amount of protein extracts from indicated strains were analyzed on immunoblot. Ecm29 level in each extract from indicated strains were observed using Ecm29 antibody and Pgk1 as loading control.

Proteasomes purified from an $\alpha 7$ - $\Delta 19$ strain show a band of the expected size on the phospho-stain gel, indicating that the remaining phosphorylation sites are still phosphorylated (Fig. 3.7A right panel). The levels of Ecm29, as determined by immunoblotting, are similar to the levels of Ecm29 found associated with wild type proteasome (Fig. 3.7A left lower panel). Thus, the Ecm29 binding is mediated by the fragment of the $\alpha 7$ tail that contains the acidic patch and the serine phosphorylation sites. To test the importance for phosphorylation of these serine residues, we introduced serine to alanine mutations into the $\alpha 7$ - $\Delta 19$ background. The strains with all three serine residues mutated to alanine (S258A, S263A, S264A) is referred to as $\alpha 7$ - $\Delta 19$ (S/A). Proteasomes purified from $\alpha 7$ - $\Delta 19$ (S/A) cells showed no detectable phosphorylation of $\alpha 7$ in our phospho-stained gel assay. Interestingly, these proteasomes showed dramatic reduction in the amount of Ecm29, having levels similar to those on $\alpha 7$ - $\Delta 40$ derived proteasomes. Thus, the binding of Ecm29 to requires the phosphorylation at serine residues in the tail of $\alpha 7$.

Figure 3.7 Binding of Ecm29 to proteasomes depends on the phosphorylation of the C-terminal tail of $\alpha 7$.



*(A and B) Proteasome complex were purified from the indicated strains and equal amount of purified proteasome were analyzed on the SDS-PAGE as well as on immunoblot. Ecm29 on the purified proteasomes were identified that shows weak association with the proteasome containing $\alpha 7$ phosphomutants both in wild type as well as in proteasome from *rpt5- $\Delta 3$* (left panel in A and B). Phosphorylation of $\alpha 7$ in indicated strains were also confirmed by using Pro-Q Diamond phosphoprotein gel staining protocol from Thermo Fisher Scientific. Rpn8 level that served as loading control in all purified proteasome samples were detected using Rpn8 antibody.*

It is currently unclear if the binding of Ecm29 to mutant proteasomes relies on fundamentally different proteasomal binding sites or that Ecm29 utilizes the same binding sites for binding to wild type and mutant proteasomes. To test this for the phosphorylated $\alpha 7$ tail, we introduced the $\alpha 7$ - $\Delta 19$ (S/A) mutant in the *rpt5- $\Delta 3$* background. Upon purification of proteasomes we observed that the mutation of the serines in the *rpt5- $\Delta 3$* background still leads to reduced levels of Ecm29 on proteasomes. Thus, the recruitment of Ecm29 to faulty proteasomes relies on the ability of Ecm29 to bind to CP as well as RP (Fig. 3.7B).

Discussion

Many sites of post-translational modification have been identified on the proteasome, including phosphorylation of several core and regulatory particle subunits⁴³. Some functions for proteasome phosphorylation have emerged, like an enhanced degradation of substrates^{44,45}, regulation of proteasome activity in a particular compartments⁴⁶, or regulation of proteasome assembly or stability⁴⁷. While the mechanisms are often unclear, the phosphorylated residues of proteasome subunits have been proposed to (directly) regulate the proteasomal ATPase activity, state of the CP gate, or the proteolytic active sites. For example, it has been suggested that phosphorylation of the $\alpha 7$ tail leads to a conformational change resulting in the closure of the CP gate⁴³. Here, however, we report that the phosphorylated tail of $\alpha 7$ serves as a binding site for the proteasome-associated factor Ecm29. For most proteasomal phosphorylation events it remains unclear how it affects proteasome function and this is one of the first examples where the association of a proteasome interacting proteins depends on a phosphorylated proteasome subunit.

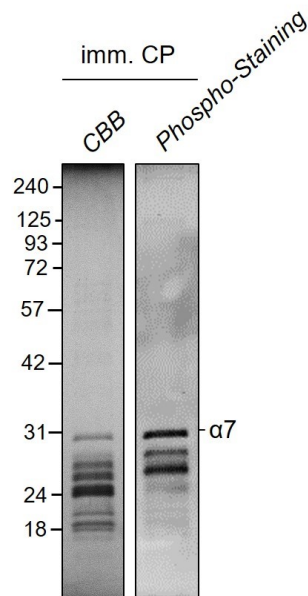
Often phosphorylation is a transient modification that has a local effect for a limited period of time. Consistently, the phosphorylation of a particular site is labile and normally found only a fraction of all proteasomes carry that modification. Both in human and yeast, however, the phosphorylation of the proteasome $\alpha 7$ subunit appears to be constitutive, readily detectable, and present on >95% of the $\alpha 7$ subunits³⁷. Ecm29, on the other hand, is only found on a subpopulation of proteasomes, suggesting that the phosphorylation of $\alpha 7$ is not the distinguishing factor that determines which proteasomes bind Ecm29.

Instead of being a trigger that creates a binding site for Ecm29, $\alpha 7$ appears to provide a pre-requisite for binding. Consistent with this model, the kinase that likely phosphorylates $\alpha 7$, CK2, is a constitutive kinase with many substrates in the cell^{31,41,42}. CK2 phosphorylation has e.g. also been proposed to be a prerequisite for the UBC3 binding to the F-box receptor β -TrCP⁴⁸. CK2 is normally not activated in response to signals leading to a transient phosphorylation, but appears to provide a continuous global signal. Through this, in theory, CK2 could be communicating to many different pathways and processes that e.g. there are high energy levels in the cell. Therefore, to identify functions of $\alpha 7$ phosphorylation it will be crucial to either identify

a phosphatase responsible for the removal of the phospho groups and determine when that is activated, or identify a cellular condition where the phosphorylation is reduced.

An important role for a phosphatases in regulating proteasome function has been reported previously, with UBLCP1 regulating nuclear proteasomes ⁴⁶. The absence or removal of phosphorylation might ensure that no Ecm29 will bind to the proteasome. Thus, the identification of such conditions will inform us when it is important to prevent Ecm29 from binding to proteasomes. We speculated that Ecm29 binding to immature CP might be undesirable as Ecm29 is normally only found on mature assembled proteasomes. However, when we purify immature CP using the Ump1-TAP tag ⁵ we observed that $\alpha 7$ is already phosphorylated in the stage of the assembly process where Ump1 binds to immature CP (Fig. 3.8).

Figure 3.8 $\alpha 7$ in immature CP is already present in phosphorylated form.



Immature CP was purified using TAP affinity tag on Ump1 and analyzed on the SDS-PAGE and stained with CBB as well as with Pro-Q-Diamond phosphostain.

While our data show that the phosphorylation of the $\alpha 7$ tail is important for association of Ecm29 with proteasomes, it is unclear if that is the only function of the phosphorylated tail of $\alpha 7$.

Previous studies have reported that in humans the phosphorylation of $\alpha 7$ is important for regulating the stability of the CP-RP interactions⁴⁰. Interestingly, Ecm29 binds to the RP subunit Rpt5 in addition to the $\alpha 7$ subunit and has been shown to stabilize the CP-RP interaction as well^{12, 13, 20}. This Ecm29-dependent stabilization is particularly striking in the absence of nucleotide, where yeast proteasomes would dissociate otherwise. In the absence of Ecm29 a similar stabilization can be achieved by treating proteasomes with proteasome inhibitors. This indicates an allosteric pathway from the CP active sites to the RP-CP interface exists. The tail and phosphorylation sites of $\alpha 7$ are not responsible for this stabilization in the absence of Ecm29, as $\alpha 7$ - $\Delta 40$ proteasomes still show proteasome inhibitor stabilized CP-RP (Fig. 3.9). Thus, it remains to be determined if $\alpha 7$ can stabilize CP-RP directly as well as through Ecm29.

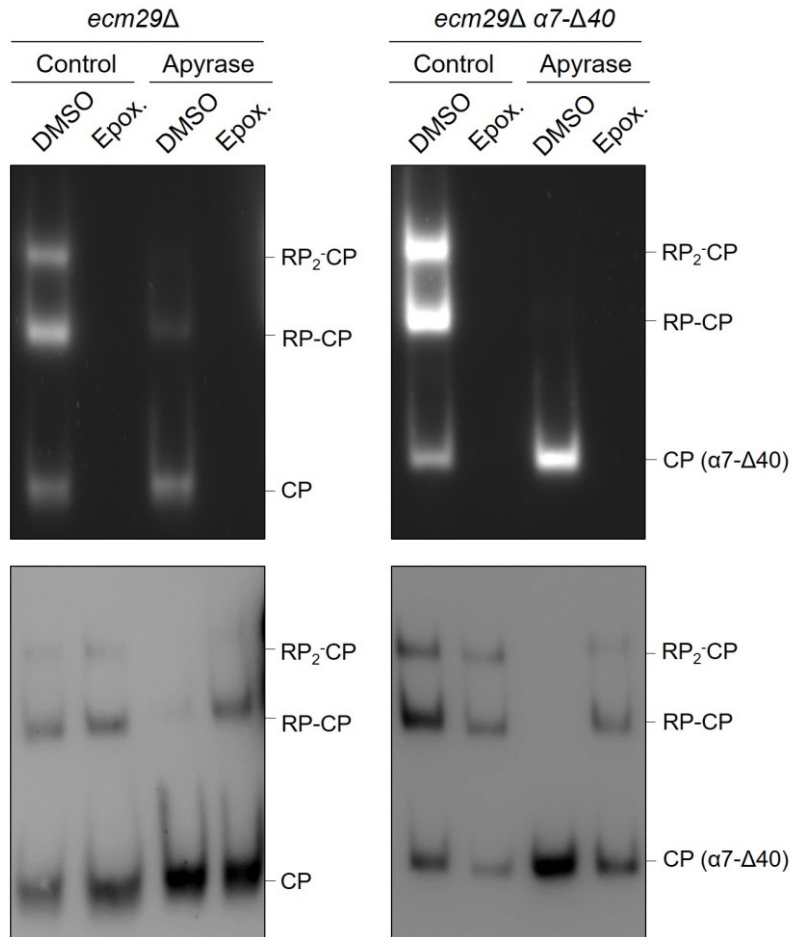
The $\alpha 7$ tail might also serve to bind or recruit other factors besides Ecm29. Several proteins have been reported to bind to $\alpha 7$, like some of the ubiquitin-independent proteasome substrates^{49, 50}. The role of the C-terminal tail here remains to be clarified.

As predicted during the initial identification of Ecm29 as a proteasome associated protein in 2001, Ecm29 binds to both RP and CP^{11, 12}. The identification of these sites provides an important clue towards the mechanism of Ecm29 recruitment to specific proteasomes. Nevertheless, we do not fully understand why Ecm29 is present in substoichiometric amounts on wild type proteasomes, but is highly enriched on a variety of proteasome mutants. Here, Ecm29 does not appear to compensate for defects by stabilizing proteasomes, but instead to specifically bind and inhibit them^{12, 15, 20}. Phenotypically, the effect of deleting Ecm29 is rather pleiotropic, suggesting it has multiple functions in the cell or becomes a dominant negative factor under certain conditions. Eitherway, the mechanisms responsible for enrichment of Ecm29 on mutant proteasomes are still poorly understood.

Three models have been put forward; First, Rpn4-dependent enrichment¹⁵. In this model, reduced proteasome activity as results of a mutation in the proteasome subunits leads to the accumulation of the unstable transcription factor Rpn4⁵¹. Rpn4 recognizes the PACE element found in promoter of many proteasome subunit as well as Ecm29⁵². As a result both proteasome subunits and Ecm29 are upregulated, however, Ecm29 upregulation is stronger thereby causing a relative increase in Ecm29 as compared to proteasomes¹⁵. Since we observed Ecm29 enrichment

on mutant proteasomes in strains where the endogenous promoter was replaced by the ADH promoter (Fig. 3.5C), it is clear that this mechanism is not required for proteasomal enrichment of Ecm29. That said, it might be a contributing factor.

Figure 3.9 RP-CP stabilization is not affected with the $\alpha 7$ C-terminal truncation.



Proteasome purified from indicated strains were inhibited by Epoxomicin and then subjected to apyrase treatment. Dissociation of proteasome is monitored on nondenaturing gel by in-gel activity assay using LLVY-AMC followed by immunoblotting with CP antibody $\alpha 7$.

The second model proposes a high affinity of Ecm29 for mutant proteasomes¹². This model is consistent with our observation that strong overexpression of Ecm29 can compensate for a weaker affinity and drive proteasomal binding of Ecm29 to normal proteasomes. However, weaker promoters, like the ADH promoter, prevent this and thus result in an almost exclusive

accumulation of Ecm29 on mutant proteasomes. Although we lack the molecular insight into a mechanism that would allow for such a difference in affinity, it might involve the alignment of CP relative to RP.

The interaction between CP and RP has some flexibility as the tails of Rpt5 subunits has been detected to interact with CP at different positions²³. Furthermore, many mutants that accumulate Ecm29 are linked to RP-CP interactions, either direct or indirectly^{12, 20, 21, 30}. Now, we have shown that Ecm29 binds to specific subunits on both RP and CP. Thus, any rotational flex in the CP-RP binding interface will likely change the relative position of these two binding sides, thereby potentially creating optimal and suboptimal binding position depending on the distance or angle between the two binding sites. Such a difference can be the basis of a difference in affinity.

Alternatively, a higher affinity of Ecm29 to proteasomes could be induced by local changes in the structure, e.g. if a mutation of the Rpt5 subunit changes the shape directly or through affecting the nucleotide occupancy of Rpt5. Then, if Ecm29 has a higher affinity for that changed surface, it causes a higher affinity. For the later, the higher affinity of Ecm29 resulting from RP mutations would not depend on the ability of Ecm29 to bind CP. Our data, however, show the enrichment of Ecm29 on RP-mutant proteasomes still depends on the ability of Ecm29 to bind to the phosphorylated $\alpha 7$ tail. Therefore, we propose that an ability of Ecm29 to detect differences in RP-CP alignment is the basis for the better binding to mutant proteasomes.

The difference in affinity cannot by itself explain all our observations. In particular the striking difference in cellular Ecm29 levels in ADH promoter driven Ecm29 in mutant versus wild type cell (Fig. 3.5C). Since, Ecm29 is controlled from the same promoter, differences in cellular level of Ecm29 most likely result from differences in degradation of Ecm29. Consistent with the third model, Ecm29 enrichment based on differences in degradation rate. This model proposes that Ecm29 is degraded by the proteasome. Hence, any defects in proteasome function result in stabilization of Ecm29 and a subsequent enrichment of Ecm29 on proteasomes. Indeed, Ecm29 has been shown to be degraded^{21, 22}, although others have reported it to be stable¹⁵. While this model is simple and elegant, it is complicated by our observations that Ecm29 inhibits proteasomes, suggesting it would prevent its own degradation. It could be that depending on

which proteasomes Ecm29 binds to (wild type or mutant), internal disordered regions are more or less accessible for engagement by the proteasome. Availability of such regions can dramatically change protein half-life⁵³.

In sum, our data show that phosphorylation of the tail of $\alpha 7$ is a prerequisite for the binding of Ecm29 to proteasomes. While this suggest that this interaction is regulated by phosphorylation, it remains to be identified, which conditions lead to the dephosphorylation of $\alpha 7$ and thus the regulation of Ecm29 binding through phosphorylation.

Contributions

P.S.W., X.C., A.O. and J.R. performed the experiments and constructed the yeast strains. Studies were conceived by P.S.W. and J.R. Manuscript was written by P.S.W., and J.R. with input from all authors.

Acknowledgements

We thank Alina De La Mota-Peynardo and members of the Roelofs lab for discussions and feedback on the manuscript.

Funding

This research was supported in part by grants from National Institute of General Medical Sciences of the National Institutes of Health to J.R. [1R15GM112142 - 01A1 and an Institutional Development Award (IDeA) P20 GM103418] and by the Johnson Cancer Research Center.

References – Chapter3

1. Finley D, Ulrich HD, Sommer T, Kaiser P. The ubiquitin-proteasome system of *Saccharomyces cerevisiae*. *Genetics* 2012; 192:319-60.
2. Bedford L, Paine S, Sheppard PW, Mayer RJ, Roelofs J. Assembly, structure, and function of the 26S proteasome. *Trends Cell Biol* 2010; 20:391-401.
3. Tomko RJ, Jr., Hochstrasser M. Molecular architecture and assembly of the eukaryotic proteasome. *Annu Rev Biochem* 2013; 82:415-45.
4. Kock M, Nunes MM, Hemann M, Kube S, Dohmen RJ, Herzog F, Ramos PC, Wendler P. Proteasome assembly from 15S precursors involves major conformational changes and recycling of the Pba1-Pba2 chaperone. *Nat Commun* 2015; 6:6123.
5. Wani PS, Rowland MA, Ondracek A, Deeds EJ, Roelofs J. Maturation of the proteasome core particle induces an affinity switch that controls regulatory particle association. *Nat Commun* 2015; 6:6384.
6. Roelofs J, Park S, Haas W, Tian G, McAllister FE, Huo Y, Lee B-H, Zhang F, Shi Y, Gygi SP, et al. Chaperone-mediated pathway of proteasome regulatory particle assembly. *Nature* 2009; 459:861-5.
7. Barrault MB, Richet N, Godard C, Murciano B, Le Tallec B, Rousseau E, Legrand P, Charbonnier JB, Le Du MH, Guerois R, et al. Dual functions of the Hsm3 protein in chaperoning and scaffolding regulatory particle subunits during the proteasome assembly. *Proc Natl Acad Sci U S A* 2012; 109:E1001-10.
8. Ehlinger A, Park S, Fahmy A, Lary JW, Cole JL, Finley D, Walters KJ. Conformational dynamics of the rpt6 ATPase in proteasome assembly and rpn14 binding. *Structure* 2013; 21:753-65.
9. Park S, Li X, Kim HM, Singh CR, Tian G, Hoyt MA, Lovell S, Battaile KP, Zolkiewski M, Coffino P, et al. Reconfiguration of the proteasome during chaperone-mediated assembly. *Nature* 2013; 497:512-6.
10. Schmidt M, Hanna J, Elsasser S, Finley D. Proteasome-associated proteins: regulation of a proteolytic machine. *Biol Chem* 2005; 386:725-37.
11. Leggett DS, Hanna J, Borodovsky A, Crosas B, Schmidt M, Baker RT, Walz T, Ploegh H, Finley D. Multiple associated proteins regulate proteasome structure and function. *Mol Cell* 2002; 10:495-507.
12. De La Mota-Peynado A, Lee SY, Pierce BM, Wani P, Singh CR, Roelofs J. The Proteasome-associated Protein Ecm29 Inhibits Proteasomal ATPase Activity and in Vivo Protein Degradation by the Proteasome. *J Biol Chem* 2013; 288:29467-81.

13. Kleijnen MF, Roelofs J, Park S, Hathaway NA, Glickman M, King RW, Finley D. Stability of the proteasome can be regulated allosterically through engagement of its proteolytic active sites. *Nat Struct Mol Biol* 2007; 14:1180-8.
14. Kajava AV, Gorbea C, Ortega J, Rechsteiner M, Steven AC. New HEAT-like repeat motifs in proteins regulating proteasome structure and function. *J Struct Biol* 2004; 146:425-30.
15. Park S, Kim W, Tian G, Gygi SP, Finley D. Structural defects in the regulatory particle-core particle interface of the proteasome induce a novel proteasome stress response. *J Biol Chem* 2011; 286:36652-66.
16. Wang X, Yen J, Kaiser P, Huang L. Regulation of the 26S proteasome complex during oxidative stress. *Sci Signal* 2010; 3:ra88.
17. Gorbea C, Goellner GM, Teter K, Holmes RK, Rechsteiner M. Characterization of mammalian Ecm29, a 26 S proteasome-associated protein that localizes to the nucleus and membrane vesicles. *J Biol Chem* 2004; 279:54849-61.
18. Gorbea C, Pratt G, Ustrell V, Bell R, Sahasrabudhe S, Hughes RE, Rechsteiner M. A protein interaction network for Ecm29 links the 26 S proteasome to molecular motors and endosomal components. *J Biol Chem* 2010; 285:31616-33.
19. Gorbea C, Rechsteiner M, Vallejo JG, Bowles NE. Depletion of the 26S proteasome adaptor Ecm29 increases Toll-like receptor 3 signaling. *Sci Signal* 2013; 6:ra86.
20. Lee SY, De la Mota-Peynado A, Roelofs J. Loss of Rpt5 protein interactions with the core particle and Nas2 protein causes the formation of faulty proteasomes that are inhibited by Ecm29 protein. *J Biol Chem* 2011; 286:36641-51.
21. Lehmann A, Niewianda A, Jechow K, Janek K, Enenkel C. Ecm29 Fulfills Quality Control Functions in Proteasome Assembly. *Molecular Cell* 2010; 38:879-88.
22. Panasenko OO, Collart MA. Not4 E3 ligase contributes to proteasome assembly and functional integrity in part through Ecm29. *Molecular and Cellular Biology* 2011; 31:1610-23.
23. Tian G, Park S, Lee MJ, Huck B, McAllister F, Hill CP, Gygi SP, Finley D. An asymmetric interface between the regulatory and core particles of the proteasome. *Nat Struct Mol Biol* 2011; 18:1259-67.
24. Lander GC, Estrin E, Matyskiela ME, Bashore C, Nogales E, Martin A. Complete subunit architecture of the proteasome regulatory particle. *Nature* 2012; 482:186-91.
25. Lasker K, Forster F, Bohn S, Walzthoeni T, Villa E, Unverdorben P, Beck F, Aebersold R, Sali A, Baumeister W. Molecular architecture of the 26S proteasome holocomplex determined by an integrative approach. *Proc Natl Acad Sci U S A* 2012; 109:1380-7.

26. Beck F, Unverdorben P, Bohn S, Schweitzer A, Pfeifer G, Sakata E, Nickell S, Plitzko JM, Villa E, Baumeister W, et al. Near-atomic resolution structural model of the yeast 26S proteasome. *Proc Natl Acad Sci U S A* 2012; 109:14870-5.
27. Groll M, Bajorek M, Kohler A, Moroder L, Rubin DM, Huber R, Glickman MH, Finley D. A gated channel into the proteasome core particle. *Nat Struct Biol* 2000; 7:1062-7.
28. Groll M, Ditzel L, Lowe J, Stock D, Bochtler M, Bartunik HD, Huber R. Structure of 20S proteasome from yeast at 2.4 Å resolution. *Nature* 1997; 386:463-71.
29. Harshbarger W, Miller C, Diedrich C, Sacchettini J. Crystal structure of the human 20S proteasome in complex with carfilzomib. *Structure* 2015; 23:418-24.
30. Park S, Roelofs J, Kim W, Robert J, Schmidt M, Gygi SP, Finley D. Hexameric assembly of the proteasomal ATPases is templated through their C termini. *Nature* 2009; 459:866-70.
31. Iwafune Y, Kawasaki H, Hirano H. Identification of three phosphorylation sites in the alpha7 subunit of the yeast 20S proteasome in vivo using mass spectrometry. *Arch Biochem Biophys* 2004; 431:9-15.
32. Helbig AO, Rosati S, Pijnappel PW, van Breukelen B, Timmers MH, Mohammed S, Slijper M, Heck AJ. Perturbation of the yeast N-acetyltransferase NatB induces elevation of protein phosphorylation levels. *BMC Genomics* 2010; 11:685.
33. Soufi B, Kelstrup CD, Stoehr G, Frohlich F, Walther TC, Olsen JV. Global analysis of the yeast osmotic stress response by quantitative proteomics. *Mol Biosyst* 2009; 5:1337-46.
34. Gnad F, de Godoy LM, Cox J, Neuhauser N, Ren S, Olsen JV, Mann M. High-accuracy identification and bioinformatic analysis of in vivo protein phosphorylation sites in yeast. *Proteomics* 2009; 9:4642-52.
35. Albuquerque CP, Smolka MB, Payne SH, Bafna V, Eng J, Zhou H. A multidimensional chromatography technology for in-depth phosphoproteome analysis. *Mol Cell Proteomics* 2008; 7:1389-96.
36. Swaney DL, Beltrao P, Starita L, Guo A, Rush J, Fields S, Krogan NJ, Villen J. Global analysis of phosphorylation and ubiquitylation cross-talk in protein degradation. *Nat Methods* 2013; 10:676-82.
37. Gersch M, Hackl MW, Dubiella C, Dobrinevski A, Groll M, Sieber SA. A mass spectrometry platform for a streamlined investigation of proteasome integrity, posttranslational modifications, and inhibitor binding. *Chem Biol* 2015; 22:404-11.
38. Wang X, Chen CF, Baker PR, Chen PL, Kaiser P, Huang L. Mass spectrometric characterization of the affinity-purified human 26S proteasome complex. *Biochemistry* 2007; 46:3553-65.

39. Claverol S, Burlet-Schiltz O, Girbal-Neuhauser E, Gairin JE, Monsarrat B. Mapping and structural dissection of human 20 S proteasome using proteomic approaches. *Mol Cell Proteomics* 2002; 1:567-78.
40. Bose S, Stratford FL, Broadfoot KI, Mason GG, Rivett AJ. Phosphorylation of 20S proteasome alpha subunit C8 (alpha7) stabilizes the 26S proteasome and plays a role in the regulation of proteasome complexes by gamma-interferon. *Biochem J* 2004; 378:177-84.
41. Castano JG, Mahillo E, Arizti P, Arribas J. Phosphorylation of C8 and C9 subunits of the multicatalytic proteinase by casein kinase II and identification of the C8 phosphorylation sites by direct mutagenesis. *Biochemistry* 1996; 35:3782-9.
42. Meggio F, Pinna LA. One-thousand-and-one substrates of protein kinase CK2? *FASEB J* 2003; 17:349-68.
43. Sha Z, Peth A, Goldberg AL. Keeping proteasomes under control--a role for phosphorylation in the nucleus. *Proc Natl Acad Sci U S A* 2011; 108:18573-4.
44. Djakovic SN, Schwarz LA, Barylko B, DeMartino GN, Patrick GN. Regulation of the proteasome by neuronal activity and calcium/calmodulin-dependent protein kinase II. *J Biol Chem* 2009; 284:26655-65.
45. Zhang F, Hu Y, Huang P, Toleman CA, Paterson AJ, Kudlow JE. Proteasome function is regulated by cyclic AMP-dependent protein kinase through phosphorylation of Rpt6. *J Biol Chem* 2007; 282:22460-71.
46. Guo X, Engel JL, Xiao J, Tagliabracci VS, Wang X, Huang L, Dixon JE. UBLCP1 is a 26S proteasome phosphatase that regulates nuclear proteasome activity. *Proc Natl Acad Sci U S A* 2011; 108:18649-54.
47. Satoh K, Sasajima H, Nyomura KI, Yokosawa H, Sawada H. Assembly of the 26S proteasome is regulated by phosphorylation of the p45/Rpt6 ATPase subunit. *Biochemistry* 2001; 40:314-9.
48. Semplici F, Meggio F, Pinna LA, Oliviero S. CK2-dependent phosphorylation of the E2 ubiquitin conjugating enzyme UBC3B induces its interaction with beta-TrCP and enhances beta-catenin degradation. *Oncogene* 2002; 21:3978-87.
49. Sanchez-Lanzas R, Castano JG. Proteins directly interacting with mammalian 20S proteasomal subunits and ubiquitin-independent proteasomal degradation. *Biomolecules* 2014; 4:1140-54.
50. Geng S, White SN, Paine ML, Snead ML. Protein Interaction between Ameloblastin and Proteasome Subunit alpha Type 3 Can Facilitate Redistribution of Ameloblastin Domains within Forming Enamel. *J Biol Chem* 2015; 290:20661-73.
51. Xie Y, Varshavsky A. RPN4 is a ligand, substrate, and transcriptional regulator of the 26S proteasome: a negative feedback circuit. *Proc Natl Acad Sci U S A* 2001; 98:3056-61.

52. Mannhaupt G, Schnell R, Karpov V, Vetter I, Feldmann H. Rpn4p acts as a transcription factor by binding to PACE, a nonamer box found upstream of 26S proteasomal and other genes in yeast. *FEBS Lett* 1999; 450:27-34.
53. Fishbain S, Inobe T, Israeli E, Chavali S, Yu H, Kago G, Babu MM, Matouschek A. Sequence composition of disordered regions fine-tunes protein half-life. *Nat Struct Mol Biol* 2015; 22:214-21.
54. Goldstein AL, McCusker JH. Three new dominant drug resistance cassettes for gene disruption in *Saccharomyces cerevisiae*. *Yeast* 1999; 15:1541-53.
55. Longtine MS, McKenzie A, 3rd, Demarini DJ, Shah NG, Wach A, Brachat A, Philippsen P, Pringle JR. Additional modules for versatile and economical PCR-based gene deletion and modification in *Saccharomyces cerevisiae*. *Yeast* 1998; 14:953-61.
56. Elsasser S, Schmidt M, Finley D. Characterization of the Proteasome Using Native Gel Electrophoresis. *Methods in Enzymology* 2005; 398:353-63.
57. Finley D, Ozkaynak E, Varshavsky A. The yeast polyubiquitin gene is essential for resistance to high temperatures, starvation, and other stresses. *Cell* 1987; 48:1035-46.
58. Leggett DS, Glickman MH, Finley D. Purification of proteasomes, proteasome subcomplexes, and proteasome-associated proteins from budding yeast. *Methods Mol Biol* 2005; 301:57-70.

Chapter 4 - Discussion and future prospective

Protein homeostasis in the cell is maintained by balancing protein synthesis and protein degradation. Protein synthesis is necessary to make new proteins in order to drive variety of biochemical reactions in the cell. Once synthesized as a nascent polypeptide chain, protein goes through numerous steps of not only structural modifications to form three dimensional active conformation but also through a quality control process assisted by chaperones. The quality control factors (e.g. Heat shock proteins: Hsp70, Hsp40 and Hsp104) here through its interaction with the polypeptide, assisting protein folding into the shape that can carry out necessary biological functions. However protein misfolding can occur and misfolded proteins go through multiple refolding attempts. Proteins that fail to be properly folded or proteins that forms aggregates are eliminated through the protein degradation process¹. Besides misfolded proteins, properly folded proteins can also needed to be degraded. Here, the removal of such proteins is an important part of the regulation of biological processes. Hence, protein degradation is important not only for the clearance of the unwanted proteins, but also for the timely removal of functional proteins.

The ubiquitin-proteasome system is responsible for clearing of many proteins. The proteins are first tagged with ubiquitin and then degraded by the proteasome. The Proteasome is made up of 33 unique polypeptides that need to assemble precisely to form this complex molecular machine. At least ten assembly chaperones are required to make the proteasome assembly process efficient and accurate. Similar to the protein quality control required for protein folding, proteasome assembly also goes through quality control. Here, one of the function of the proteasome pre-assembly quality control is to assure accurate and efficient proteasome formation with the help of assembly chaperones by avoiding premature assembly intermediate formations. If the defective proteasome is formed, quality control process detects the defective proteasomes possibly for their clearance². The research work presented in this dissertation describes one of such mechanism of pre-assembly quality control that occur during core particle (CP) assembly as well as uncover mechanistic steps involved in the post-assembly quality control of the proteasome by quality control factor Ecm29. We found that the phosphorylation of CP subunit $\alpha 7$ is a prerequisite for Ecm29 binding to proteasome.

Pre-assembly quality control during CP assembly

CP is the most abundant form of the proteasome subcomplex present in the cell compared to other subcomplexes. The regulated activation of the CP for substrate degradation is a key mechanistic feature of the proteasome. Because CP can interact with many CP interacting factors (CPIFs) either at one or both ends of the CP there is an additional layer of proteasome regulation. In yeast four such factors are known, namely RP, Pba1-Pba2 (PAC1-PAC2 in human), Blm10 (PA200) and Fub1 (PI31). Interestingly all four CPIFs are attached to the CP through their direct interaction with α -ring. Here, a C-terminal three amino acids HY-b-X motif found in all these factors is important as it docks into pocket formed between α subunits^{3,4}. However, their interaction to the CP has varied effect on regulation of CP activity. Moreover, these interactions occur at different assembly stages of CP. For example, Pba1-Pba2 associates with immature CP, Blm10 associates with immature as well as mature CP, RP is mostly found associated with mature CP, and Fub1 is also associated with mature CP⁵. Since all the CPIFs share the same seven subunits α -ring as CP interacting surface, it is crucial to elucidate how the timely interactions of these CPIFs with CP is regulated and controlled. This is also important in a sense that various stress conditions affect the dynamics of the type of proteasome complexes formed, moreover this dynamic is also specific to the cell types⁶.

The work presented in this thesis sheds light on one of the mechanisms that regulates the interactions between CP and two CPIFs. Here, we reported the regulation of interactions between Pba1-Pba2 and RP with immature CP (CP assembly intermediate) and mature CP (20S). In order to analyze these interactions we purified CP assembly intermediate. Presence of CP assembly chaperone Ump1 is a hallmark of the immature CP where β 7 subunit has not yet been incorporated and proteolytic β subunits are still inactive. We were able to purify sufficient amount of immature CP for the analysis by adding TAP-tag on the Ump1. This was likely facilitated by a slower maturation of CP due to the bulky TAP tag on Ump1. Consistent with this, immature CP purified using the Ump1-TAP tag lacked the β 6 besides the β 7 subunit that is normally absent from immature CP. This slower CP assembly process enabled us to capture immature CP in a large amount. We observed Pba1-Pba2 almost exclusively on immature CP, when purified proteasome complexes from yeast. Previous reports hypothesized a role for Pba1-

Pba2 in α -ring assembly as well as the prevention of α -ring dimerization⁷. We further investigate the role of Pba1 and Pba2 heterodimer with regards to its proposed role in blocking RP during CP maturation. We observed the interaction of RP subunits with the immature CP in the absence of Pba1 and Pba2. Moreover amount of RP associated with immature CP was modestly increased upon additional knockout of Blm10 showing Pba1-Pba2 prevents RP to prematurely associate with CP intermediates.

Blm10 and its affinity with immature and mature CP.

During analysis of the immature and mature CP in the absence as well as in the presence of Pba1-Pba2 complex we observed that Blm10 has similar binding affinity with the immature and mature CP. Interestingly Blm10's C-terminal HY-b-X motif uses same pocket ($\alpha 5$ - $\alpha 6$) on α -ring as Pba1 on immature CP α -ring and Rpt5 on mature CP⁸. Therefore it is not fully understood how the regulation of such competitive binding is achieved in the cell. Blm10 has been suggested to help during CP assembly⁹ and also shown to help in localization of proteasome to the nucleus. Blm10 can also locate the Blm10-CP in proteasome storage granules under certain physiological stress conditions¹⁰. Moreover it promotes the degradation of specific substrates. Thus, suggesting that Blm10-CP association is physiological state specific and has some specificity towards substrates¹¹. However the mechanism of selection of Blm10 over RP for CP interaction remains obscure.

Crystal structure of immature CP.

Affinity switch described in this thesis was recently complimented by the cryoEM studies of 15S and 20S complex¹². We showed that the higher affinity of Pba1-Pba2 to the immature CP than mature CP contributed through the C-terminal tail of the Pba2. The cryoEM structure also displayed the significant differences in docking of Pba2 onto immature CP vs mature CP. Additionally, the slight conformational changes in the α -ring has been noted during CP maturation. However, this study lacks the resolution particularly with respect to detailed interactions of Pba2 with the α -ring pocket residues. Hence, high resolution crystal structure of immature CP with Pba1-Pba2 is needed. The previously described crystal structure is from reconstituted Pba1-Pba2 on mature CP. Since the mature CP *in vivo* does not associate with Pba1-Pba2, this diminishes the physiological importance of the existing crystal structure model with mature CP. Crystal structure of immature CP with Pba1-Pba2 will further elucidate the

detailed changes responsible for the affinity switch that occurs upon CP maturation . This will improve our knowledge in terms of both CP α -ring configuration and its effect on the Pba2 interaction with the $\alpha 6$ - $\alpha 7$ pocket residues. It will provide insights for Blm10-mature/immature CP interactions. Since Blm10-mature CP crystal structure is available¹³, direct comparison of α -ring from both structures might be helpful.

Fate of immature CP-RP complex

The mathematical modeling presented in chapter 3 suggests that the formation of these immature CP-RP complexes can act as a deadlock to the proteasome assembly process and will hinder the efficiency of proteasome formation. The fate of these immature CP-RP complexes is yet to be clarified. Interestingly, we have observed the presence of Ecm29 on these complexes. Ecm29 has been known to perform a quality control function by binding to the defective proteasomes through its interaction with RP as well as CP together. It will be interesting to study if Ecm29 has any role in regulation of these complexes and possibly help in their clearance from the cell through any autophagic processes.

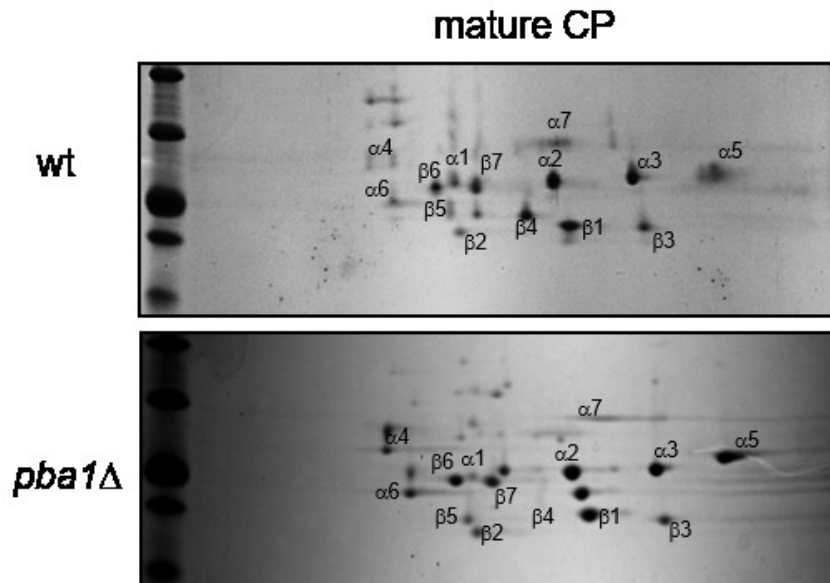
CP formed in the absence of Pba1-Pba2 complex.

Our 2D gel analysis indicated that in the absence of Pba1, CP formation is delayed due to slow incorporation of $\alpha 5$ and $\alpha 6$. However Pba1 knockout does not show any severe phenotypic growth effect in yeast¹⁴. Nevertheless, in mammals PAC1 knockout mice shows early embryonic lethality indicating its role in the development. The conditional knockout mice also showed severe phenotype including deformation of brain structure and substantially reduced proteasome activity in the brain¹⁵. Here, PAC1 knockout does not cause complete loss of the 20S CP. Overall, this suggests that CP formation ultimately takes place and Pba1-Pba2 independent pathway might be present. The question remains to be answered that is there any difference in CP formed in the presence and in the absence of Pba1?

We suspect that apart from delaying the CP formation, Pba1-Pba2 may have additional biological function in CP maturation and CP formed in Pba1 independent manner can be different. We have noticed enrichment of Blm10 on the CP when proteasome is purified from the Pba1 Δ background. With the notion that Blm10 used the same pocket as Pba1 to interact with CP, two models can be proposed. First, *blm10* Δ can function as redundant protein in the absence

of Pba1 and as previously proposed can help in CP maturation⁹. However its role in maturation is still a matter of debate since CP can form in *pba1Δ blm10Δ* cells and yeast does not show any phenotype. Second, CP formed from *pba1Δ* may have different conformational α -ring surface that favor Blm10 binding than RP and hence the enrichment.

Figure 4.1 CP subunits comparison between CP from wt and from Pba1 Δ



CP from wt and pba1 Δ strains were purified and analyzed by IEF followed by SDS PAGE. Indicated CP subunits in wt are identified using mass spec. The proteins spots in case of Pba1 Δ CP were assigned based on wt gels. Additional spots found on Pba1 Δ CP gel need to be identified.

We purified CP from wt yeast as well as from Pba1 knockout and analyzed it on 2D gel (preliminary data). Some additional protein spots in Pba1 Δ CP were observed those absent in wt CP (Figure 4.1). These extra spots can either be modifications of CP subunits or proteins that remains associated with the CP during Pba1-Pba2 independent assembly. Further confirmation and analysis of these proteins through mass spectrometry will reveal if the CP formed is different or the same.

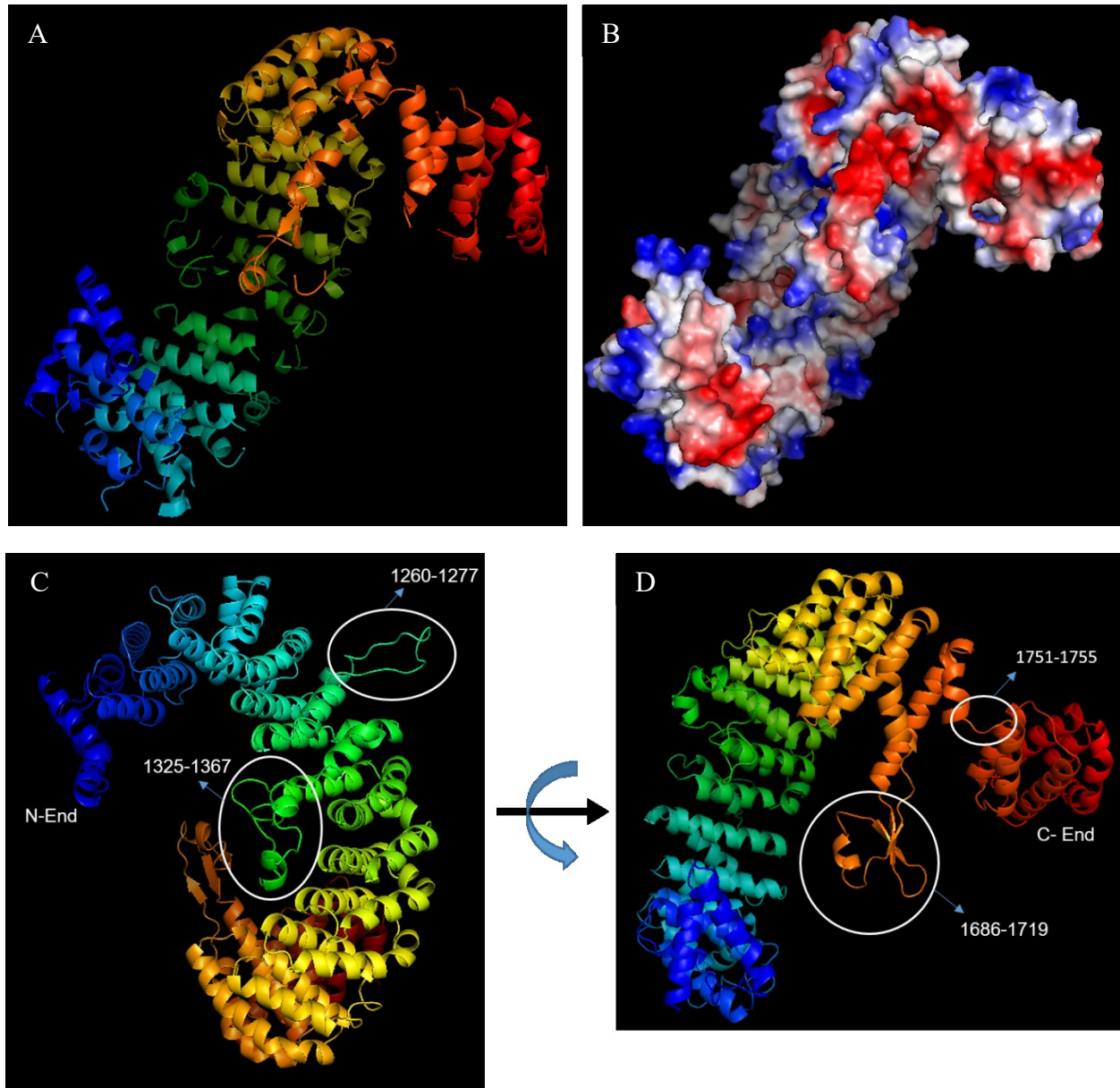
Post-assembly Quality control

The work in this thesis improves our knowledge on the Ecm29 interactions with the proteasome. We previously identified RP subunit Rpt5 that interacts with the Ecm29 and the current work reported here shows that the CP subunit $\alpha 7$ phosphorylation is required for the Ecm29 binding. However this does not fully answer how Ecm29 recognizes the proteasome. The constitutively active CK2 in mammals has been reported to phosphorylate $\alpha 7$, suggesting that $\alpha 7$ might be always phosphorylated^{16,17}. Considering Ecm29 as a quality control factor that recognizes defective proteasome, additional biochemical analyses are required to understand the mechanism behind the recruitment of Ecm29 to proteasome. Identifying residues on Ecm29 that interacts with proteasome might be helpful if there are any interaction differences when Ecm29 is associated with the normal proteasome vs mutant proteasome.

Possible interaction sites on Ecm29

Ecm29 is a large protein with molecular weight around 210Kda and difficult to purify. As a result, limited structural information is present. The only available EM images are of low resolution and provide little information concerning the detailed interactions¹⁸. Alternative strategies can be used to tackle these challenges. We used the structure prediction program Phyre² and generated the putative structure of the Ecm29 based on yeast Ecm29 amino acids sequence (Figure 4.2). The predicted structure shows a curved nature of the protein consistent with the EM structure. This structure prediction of Ecm29 can be used to predict potential interaction surface. For example, the electrostatic surface potential from this structure shows cluster of charged residues that can be favorable to interact with CP and RP (Fig. 4.2B). Alternatively, several mutated or truncated protein versions can be created and possible binding domain can be analyzed. Additionally, Phosphorylation sites (Ser1396 and Ser1695) on the Ecm29 has been identified¹⁹ those have casein kinase 1 motifs. Involvement of phosphorylation dependent interaction can be tested by creating phosphomutants.

Figure 4.2 Predicted structure from amino acid sequence of yeast Ecm29 using Phyre² program.



(A) Online Phyre² program was used to predict the structure of Ecm29. The predicted structure shows elongated and curved molecule consistent with the most HEAT repeat motif containing structures. (B) The electrostatic surface potential of the Ecm29. Blue color indicates positive charge and red color indicates negative charge surface whereas white color indicates neutral charge surface. The polar residues hot spots at the Ecm29 surface can be a potential interaction sites to the proteasome. (C and D) unstructured linker regions on Ecm29 (circled) can provide flexibility to the Ecm29 to interact with variety of misaligned proteasome complexes.

Specificity of Ecm29 for mutant proteasomes

Our results with the over-expression of Ecm29 show that Ecm29 can be associated with the wild type proteasome when present in excess. However, we previously observed that Ecm29 preferably interacts with mutant proteasome (Rpt5- Δ 3) over wild type proteasome if Ecm29 is under the control of the endogenous promoter²⁰. This raises the question how Ecm29 recognizes mutant proteasome over wild type proteasome? One prediction would be that mutation in the proteasome might result in the changes in the alignment of the RP and CP structures. This can be due to either improper docking of the RP subunit tails into the pockets between α subunits or changes in proteasome subunits conformation due to mutation. This changed alignment might favor the Ecm29 binding to mutant proteasome over normal proteasome. Misaligned conformation might lock the RP ATPase subunits in specific nucleotide state that use different word Ecm29 interaction to the proteasome. This model is consistent with our observations that Ecm29 is more abundant on the proteasome purified in the presence of AMP when compared in the presence of ATP. Alternatively, additional factors might be involved in the recognition of defective proteasome. One such factor is Not4, an E3 ligase whose absence has shown to disturb the Ecm29 interaction with the proteasome²¹. However, the Not4 dependent interaction did not show any specificity for the mutant proteasome. Further experiments are needed to explore specificity for mutant proteasome recognition process through Ecm29.

Post-translation modification of the proteasome subunits and regulation of proteasome activity in disease conditions.

To our knowledge the CP α 7-subunit phosphorylation dependent interaction of Ecm29 is the first example for a role of proteasome subunit posttranslational modification in regulating the interaction with associated proteins. Many posttranslational modifications have been reported for proteasome subunits such as oxidative modifications, ubiquitination, N-acetylation, N-myristoylation, phosphorylation, and glycosylation²². While some modifications have been proposed to regulate proteasome activity, proteasome translocation to the specific compartments, or RP-CP stability^{1,23}. Most of these data are derived from the large proteomic analyses and lack biochemical and cell biological studies that could reveal the physiological function of these modification. Furthermore, some of the function proposed to be a direct consequence of the PTM

actually could result from changes in the presence of proteasome-associate proteins, which are known to regulate these functions.

Many proteins have been identified which are not classified under group of proteins related to the ubiquitin proteasome pathway (proteasome associate proteins), but their direct interaction with the proteasome has been studied biochemically. For example a tumor suppressor retinoblastoma protein pRb has been shown to directly interact with $\alpha 7$ subunit. A misfolded PrP protein has been suggested to regulate the CP activity by direct interaction with CP from the outer side of the CP cylinder. Parkinson associated protein Dj1 also physically interact with the 20S proteasomes²⁴⁻²⁸. More in detail studies are required to know if interactions of all these proteins to the CP are dependent on the posttranslational modification of the proteasome subunits which can add an extra layer of regulation of proteasome activity during various disease conditions.

Figure 4.3 Model of quality control mechanism during pre-assembly and post-assembly of the proteasome.

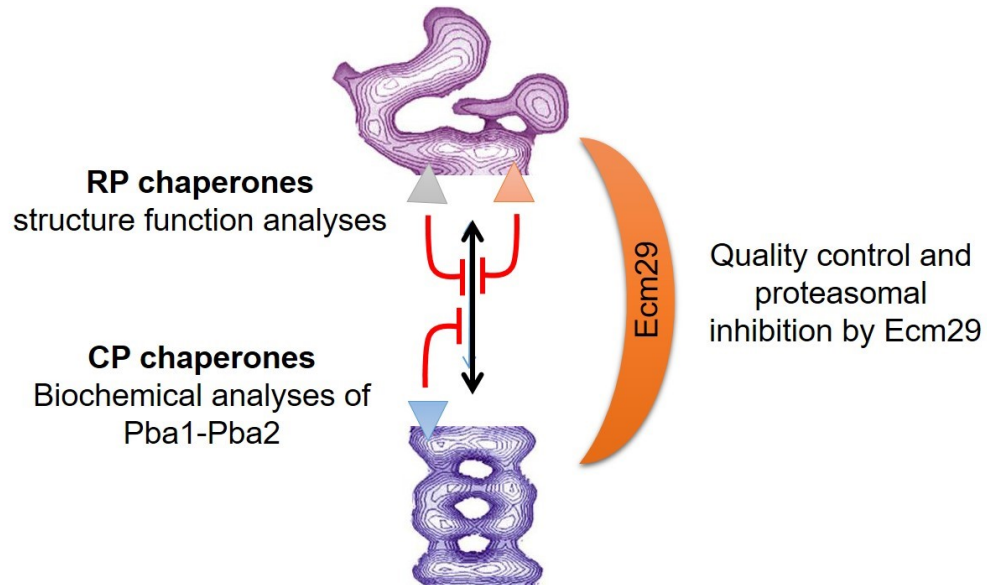


Figure 4.3 summarizes our finding about overall quality control in the proteasome. Chaperones functions as a pre-assembly quality control to avoid the formation of nonproductive deadlock assembly intermediate complexes and assures the efficient and accurate proteasome formation. If the assembled proteasome is defective then Ecm29 recognizes the mutant/defective proteasome and inhibit it to avoid the aberrant protein degradation.

References – Discussion and future prospective

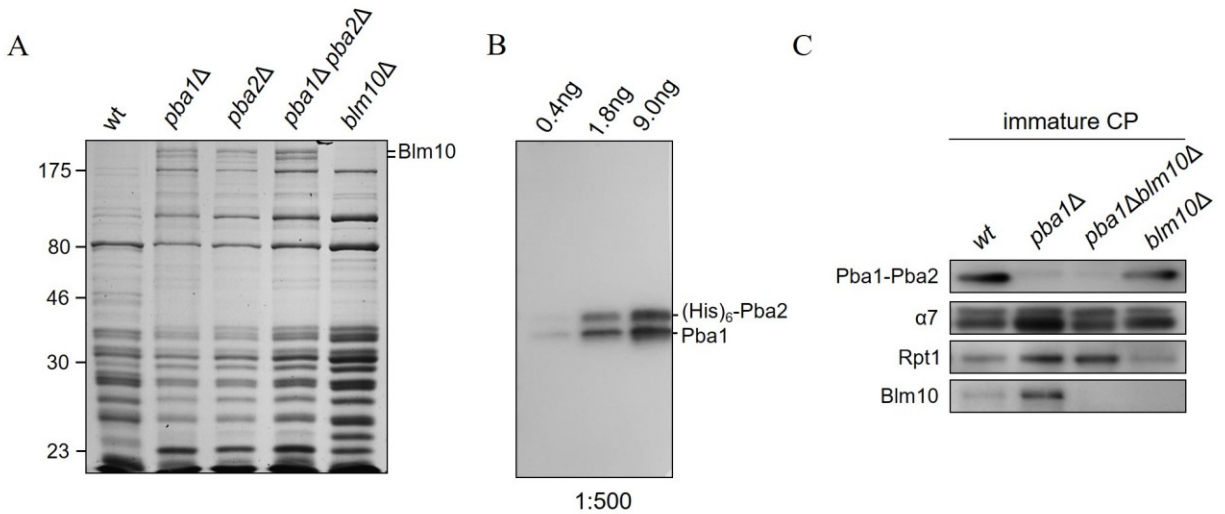
1. Wang, X., Pattison, J.S., Su, H. (2013) Posttranslational modification and quality control. *Circ Res.* **112**, 367-381.
2. Peters, L.Z., Karmon, O., David-Kadoch, G., Hazan, R., Yu, T., Glickman, M.H., Ben-Aroya, S. (2015) The protein quality control machinery regulates its misassembled proteasome subunits. *PLoS Genet.* **11**, e1005178.
3. Kusmierczyk, A.R., Kunjappu, M.J., Kim, R.Y., Hochstrasser, M. (2011) A conserved 20S proteasome assembly factor requires a C-terminal HbYX motif for proteasomal precursor binding. *Nat Struct Mol Biol.* **18**, 622-629.
4. Li, X., Thompson, D., Kumar, B., DeMartino, G.N. (2014) Molecular and cellular roles of PI31 (PSMF1) in regulation of proteasome function. *J Biol Chem.*
5. Zaiss, D.M., Standera, S., Holzhutter, H., Kloetzel, P., Sijts, A.J. (1999) The proteasome inhibitor PI31 competes with PA28 for binding to 20S proteasomes. *FEBS Lett.* **457**, 333-338.
6. Fabre, B., Lambour, T., Garrigues, L., Manuelle Ducoux-Petit, François Amalric, Monsarrat, B., Odile Burette-Schiltz, Marie-Pierre Bousquet-Dubouch. (2014) Label-free quantitative proteomics reveals the dynamics of proteasome complexes composition and stoichiometry in a wide range of human cell lines. *Journal of Proteome Research.* **13**, 30273037.
7. Hirano, Y., Klavs, B.H., Yashiroda, H., Shun-ichiro Iemura, Nagane, R., Hioki, Y., Natsume, T., Tanaka, K., Murata, S. (2005) A heterodimeric complex that promotes the assembly of mammalian 20S proteasomes. *Nature.* **437**, 1381-1385.
8. Lehmann, A., Jechow, K., Enenkel, C. (2008) Blm10 binds to pre-activated proteasome core particles with open gate conformation. *EMBO Rep.* **9**, 1237-1243.
9. Fehlker, M., Wendler, P., Lehmann, A., Enenkel, C. (2003) Blm3 is part of nascent proteasomes and is involved in a late stage of nuclear proteasome assembly. *EMBO Rep.* **4**, 959-963.
10. Weberuss, M.H. (2013) Blm10 facilitates nuclear import of proteasome core particles. *EMBO J.* **32**, 2697-2707.
11. Lopez, A.D., Tar, K., Krugel, U., Dange, T., Ros, I.G., Schmidt, M. (2011) Proteasomal degradation of Sfp1 contributes to the repression of ribosome biogenesis during starvation and is mediated by the proteasome activator Blm10. *Mol Biol Cell.* **22**, 528-540.
12. Kock, M., Nunes, M.M., Hemann, M., Kube, S., Dohmen, R.J., Herzog, F., Ramos, P.C., Wendler, P. (2015) Proteasome assembly from 15S precursors involves major conformational changes and recycling of the Pba1-Pba2 chaperone. *Nat Commun.* **6**, 6123.

13. Sadre-Bazzaz, K., Whitby, F.G., Robinson, H., Formosa, T., Hill, C.P. (2010) Structure of a Blm10 complex reveals common mechanisms for proteasome binding and gate opening. *Mol Cell*. **37**, 728-735.
14. Stadtmueller, B.M., Erik Kish-Trier, Ferrell, K., Petersen, C.N., Robinson, H., Myszka, D.G., Eckert, D.M., Formosa, T., Hill, C.P. (2012) Structure of a proteasome Pba1-Pba2 complex IMPLICATIONS FOR PROTEASOME ASSEMBLY, ACTIVATION, AND BIOLOGICAL FUNCTION. *J Biol Chem*. **287**, 37371-37382.
15. Sasaki, K., Hamazaki, J., Koike, M., Hirano, Y., Komatsu, M., Uchiyama, Y., Tanaka, K., Murata, S. (2010) PAC1 gene knockout reveals an essential role of chaperone-mediated 20S proteasome biogenesis and latent 20S proteasomes in cellular homeostasis. *Mol Cell Biol*. **30**, 3864-3874.
16. Bose, S., Stratford, F.L., Broadfoot, K.I., Mason, G.G., Rivett, A.J. (2004) Phosphorylation of 20S proteasome alpha subunit C8 (alpha7) stabilizes the 26S proteasome and plays a role in the regulation of proteasome complexes by gamma-interferon. *Biochem J*. **378**, 177-184.
17. Iwafune, Y., Kawasaki, H., Hirano, H. (2004) Identification of three phosphorylation sites in the alpha7 subunit of the yeast 20S proteasome in vivo using mass spectrometry. *Arch Biochem Biophys*. **431**, 9-15.
18. Leggett, D.S. (2002) Multiple associated proteins regulate proteasome structure and function. *Mol Cell*. **10**, 495-507.
19. Helbig, A.O., Rosati, S., Pijnappel, P.W., van Breukelen, B., Timmers, M.H., Mohammed, S., Slijper, M., Heck, A.J. (2010) Perturbation of the yeast N-acetyltransferase NatB induces elevation of protein phosphorylation levels. *BMC Genomics*. **11**, 685-2164-11-685.
20. Mota, D.L. (2013) The proteasome-associated protein Ecm29 inhibits proteasomal ATPase activity and in vivo protein degradation by the proteasome. *J Biol Chem*. **288**, 29467-29481.
21. Olesya, O.P., Martine, A.C. (2011) Not4 E3 ligase contributes to proteasome assembly and functional integrity in part through Ecm29. *Mol Cell Biol*. **31**, 1610-1623.
22. Kikuchi, J., Iwafune, Y., Akiyama, T., Okayama, A., Nakamura, H., Arakawa, N., Kimura, Y., Hirano, H. (2010) Co- and post-translational modifications of the 26S proteasome in yeast. *Proteomics*. **10**, 2769-2779.
23. Sha, Z., Peth, A., Goldberg, A.L. (2011) Keeping proteasomes under control--a role for phosphorylation in the nucleus. *Proc Natl Acad Sci U S A*. **108**, 18573-18574.
24. Sdek, P., Ying, H., Chang, D.L., Qiu, W., Zheng, H., Touitou, R., Allday, M.J., Xiao, Z.X. (2005) MDM2 promotes proteasome-dependent ubiquitin-independent degradation of retinoblastoma protein. *Mol Cell*. **20**, 699-708.
25. Ying, H., Xiao, Z.X. (2006) Targeting retinoblastoma protein for degradation by proteasomes. *Cell Cycle*. **5**, 506-508.

26. Andre, R., Tabrizi, S.J. (2012) Misfolded PrP and a novel mechanism of proteasome inhibition. *Prion*. **6**, 32-36.
27. Deriziotis, P., Andre, R., Smith, D.M., Goold, R., Kinghorn, K.J., Kristiansen, M., Nathan, J.A., Rosenzweig, R., Krutauz, D., Glickman, M.H., Collinge, J., Goldberg, A.L., Tabrizi, S.J. (2011) Misfolded PrP impairs the UPS by interaction with the 20S proteasome and inhibition of substrate entry. *EMBO J*. **30**, 3065-3077.
28. Moscovitz, O., Ben-Nissan, G., Fainer, I., Pollack, D., Mizrachi, L., Sharon, M. (2015) The parkinson's-associated protein DJ-1 regulates the 20S proteasome. *Nat Commun*. **6**, 6609.

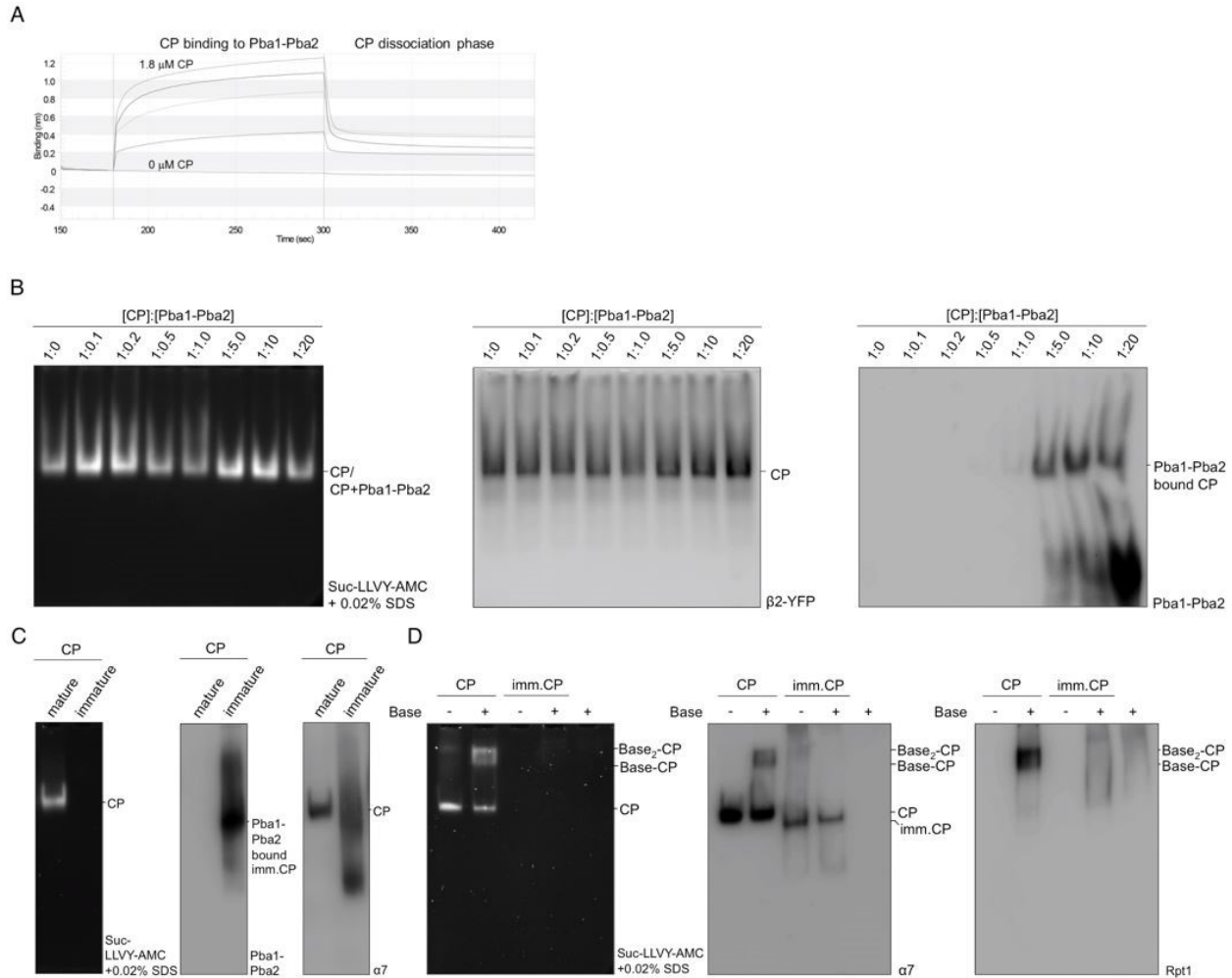
Appendix A - Supplementary Information for Chapter 2

Figure A.1 Supporting data related to Figure 2.1 Pba1-Pba2 prevents RP association with immature CP



(A) Proteasome from strains deleted for PBA1 or PBA2 shows increased levels of Blm10. Proteasomes were purified from indicated strains using an affinity-tag on the $\beta 4$ subunit. Samples were resolved on SDS-PAGE and stained with CBB. In this preparation some Blm10 was cleaved at the N-terminus, causing the presence of a second faster migrating species of Blm10. **(B) Pba1-Pba2 antibody recognizes Pba1 and Pba2.** GST-tagged Pba1 and His-tagged Pba2 were co-expressed in *E.coli* and purified using glutathione resin. Protein dimer was eluted using Precision protease, which cleaved between GST and Pba1. The purified protein was used to raise antibody against Pba1-Pba2. Immunoblot using the serum (#1940) from immunized rabbit showed the antibody recognizes both Pba1 and Pba2. **(C) Deletion of Blm10 does not cause an accumulate RP on immature CP.** Immature CP from indicated strains was purified and resolved on SDS-PAGE followed by immunoblotting for indicated proteins. The enrichment in RP (Rpt1 blot) on immature CP observed for *pba1Δ* strains was not observed upon deletion of BLM10.

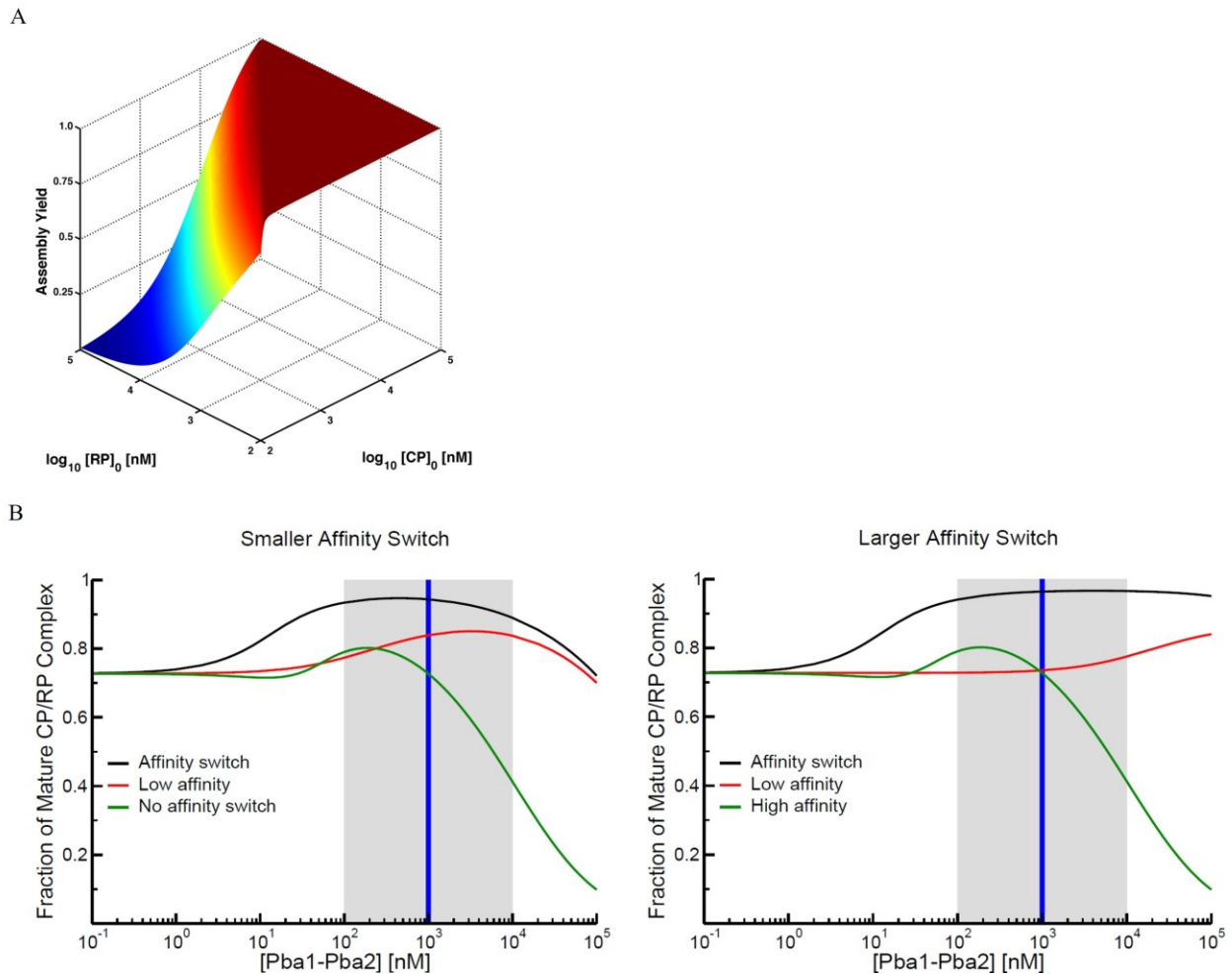
Figure A.2 Supporting data related to Figure 2.2 CP undergoes affinity switch upon maturation.



(A). Binding kinetics for the interaction between CP and the Pba1-Pba2 dimer. *E.coli* expressed and purified His-tagged Pba1-Pba2 dimer (see Fig. A.1.B) was loaded onto a Ni²⁺-NTA sensor tip for the BLITZ (ForteBio). The Blitz uses bio-layer interferometry to measure the association constant (k_a) and dissociation constant (k_d), which can be used to obtain the affinity constant $K_D (= k_d/k_a)$. The tip was transferred to an exchange buffer (150-175 seconds) to remove unbound protein. Next, tip is transferred to solution without or with increasing concentrations of CP (starting at 0.22 nM and doubling up to 1.8 μ M). Analysis of the complete data set with baseline corrections yielded a K_D of 1.2 μ M ($K_a = 8.6 \pm 0.8 * 10^4 M^{-1}s^{-1}$ and $K_d 0.10 \pm 0.04 s^{-1}$). This K_D is similar to data obtained by SPR¹. **(B) Titrations of Pba1-Pba2 to**

determine saturated binding on CP. CP from β 2-YFP tagged strains was purified using an affinity-tag present on the β 4 subunit. Next, purified CP was incubated with increasing amounts of His-tagged Pba1-Pba2 dimer for 30 minutes at 30 °C. Samples were resolved on native gel and stained in gel for suc-LLVY-AMC (left panel) or analyzed for YFP signal using a Typhoon 9410 imager (Middle panel). Gels were also transferred to membranes and immunoblotted for the presence of Pba1-Pba2 (right panel). At 5 fold molar excess maximum CP binding was observed. **(D + E) Base fails to replace Pba1-Pba2 from immature CP.** **(D)** Native gel analysis of mature and immature CP purified as prior. Samples were stained with suc-LLVY-AMC, showing proteolytic activity for mature CP, but not immature CP (left panel). Native gel was also transferred to pvdF membranes for immunoblotting. Middle panel shows immunoblot for Pba1-Pba2, indicating this dimer is absent from mature CP, but abundant on the immature CP. Right panel shows the α 7 subunit of the proteasome. The mature CP sample has one major band, being mature CP with proteolytic activity (left panel), while immature CP shows two major species containing α 7, one migrating close to mature CP, which lacks proteolytic activity but has Pba1-Pba2. The second faster migrating band is presumably an early assembly intermediate that still lacks the Pba1-Pba2 chaperones. **(E)** Samples from (d) were used in a reconstitution assay with the base (an RP subcomplex) in 10 fold molar excess. Reconstitution assays were resolved by native gel electrophoresis followed by in gel suc-LLVY-AMC activity assay or immunoblotting (α 7 is a CP subunit and Rpt1 and base subunit subunit). Data show that the base reconstitutes efficiently on mature CP (lane 2), however, no reconstitution onto immature CP was observed (compare lane 2 with 4 and 5 in right panel).

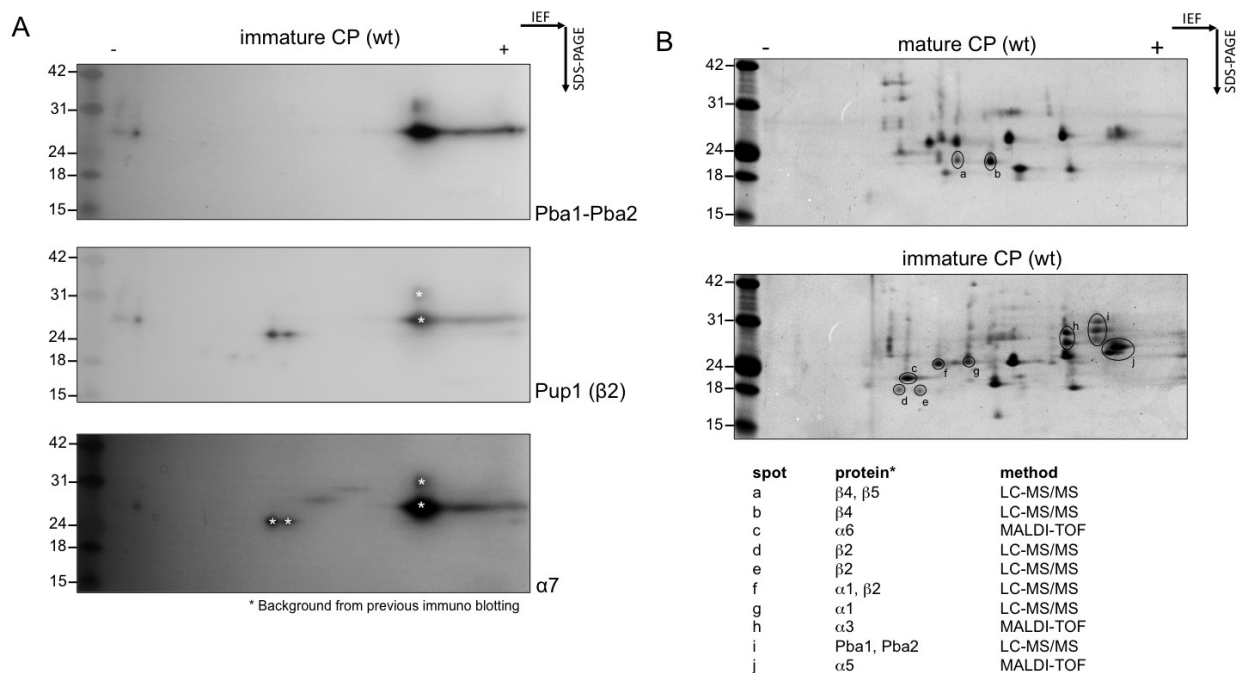
Figure A.3 Supporting data related to Figure 3 Pba1-Pba2 prevents assembly deadlock.



(A) *Assembly yield is robust to variations in RP and CP concentration in the model. These results are from the mathematical model described in the main text and described in greater detail in the [supplemental methods online](#). Aside from variations in total RP and CP concentration ($[RP]_0$ and $[CP]_0$, respectively), all the parameters are identical to those used for the "Affinity Switch" model in the main text. The concentration of the chaperone Pba1-Pba2 was held constant at $1 \mu\text{M}$. Since the CP and RP are at different concentrations in this case, the assembly yield is defined as the concentration of the RP-CP complex divided by the total concentration of RP or CP, depending on which is smaller. We find that near 100% yield is obtained for a wide variety of concentrations of both RP and CP, indicating that the results in Figure 2.3 of the chapter 2 do not depend on a specific set of RP and CP concentrations. **(B)***

Changes in the magnitude of the affinity switch do not qualitatively effect our predictions. *Left panel; this is an analogue of Figure 2.3A in the main text, but with an affinity switch that is smaller (100 times instead of 1,000 times). In this model, the K_D of Pba1-Pba2 for the immature CP is unchanged at 1 nM, but it binds more tightly to the mature CP ($K_D = 100$ nM). Right panel; this is an analogue of Figure 2.3A in the main text, but with an affinity switch that is larger (10,000 times instead of 1,000 times). The K_D of the interaction with the immature CP is again unchanged at 1 nM, but the K_D of the mature interaction is weaker at 10 μ M. Note that in both cases, there is a broad range of Pba1-Pba2 concentration that provides near-100% assembly yields. Modifying the affinity switch by making the K_D to the immature form stronger (or weaker) give similar results (data not shown).*

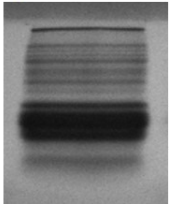
Figure A.4 Supporting data related to Figure 4 Pba1-Pba2 are required for efficient incorporation of α 5 and α 6.



(A) Immunoblot analysis of purified immature CP from strains containing an UMP1-TAP. 2D-gel electrophoresis of immature CP from a wildtype strain (see Fig. 2.4C main Chapter 2) was subjected to sequential immunoblotting. Panels show sequential probing of the membrane

for Pba1-Pba2 (top panel), β 2 (middle panel) and finally α 7 (lower panel). Spots indicated with an asterisk are signals derived from prior immunoblot, newly obtained signals are consistent with the expected PI and MW of proteins probed for. **(B)** Mass Spectrometry analysis of spots on 2D gel. Indicated spots were excised and submitted for analysis by MALDI-TOF, spots for which no result was obtained were subsequent analyzed by LC-MS/MS. MALDI-TOF analyses each time identified only one protein with significant score ($p < 0.05$). For LC-MS/MS only the identified proteins that contributed more than $>20\%$ to the total sample spectral count are reported to eliminate low abundant background contamination.

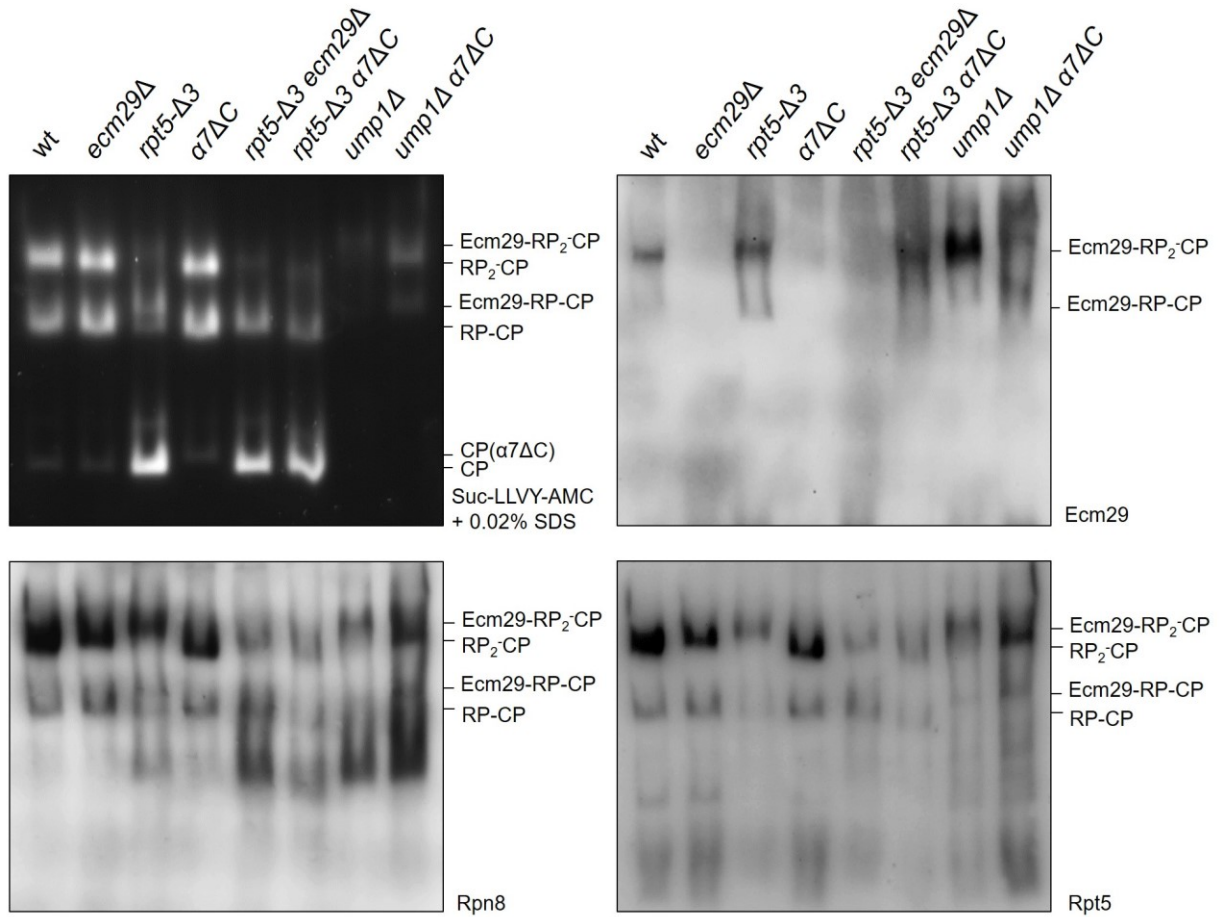
Table 4.1 Mass spectrometry analysis of immature CP purified from Ump1-TAP tagged strain.

Ump1-TAP purification	Proteasome subunit	Systematic Gene Name	Standard name	# unique sequences	# total spectra
	α 1	YGL011C	Scl1	16	28
	α 2	YML092C	Pre8	8	11
	α 3	YGR135W	Pre9	12	24
	α 4	YOL038W	Pre6	10	15
	α 5	YGR253C	Pup2	11	29
	α 6	YMR314W	Pre5	9	19
	α 7	YOR362C	Pre10	9	11
	β 1	YJL001W	Pre3	5	5
	β 2	YOR157C	Pup1	8	29
	β 3	YER094C	Pup3	6	18
	β 4	YER012W	Pre1	4	6
	β 5	YPR103W	Pre2	8	10
	β 6	YBL041W	Pre7	n.d.	n.d.
	β 7	YFR050C	Pre4	n.d.	n.d.
	Ump1	YBR173C	Ump1	7	8
	Pba1	YLR199C	Pba1	13	29
	Pba2	YKL206C	Add66	7	13

Sequences that cover the propeptides	
β 2	M. AGLSFDNYQR . N R. NNFLAENSHTQPK . A
β 5	R. LAPSLTVPPIASPQQFLR . A K. ELQYDNEQNLESDFVTGASQFQR . L

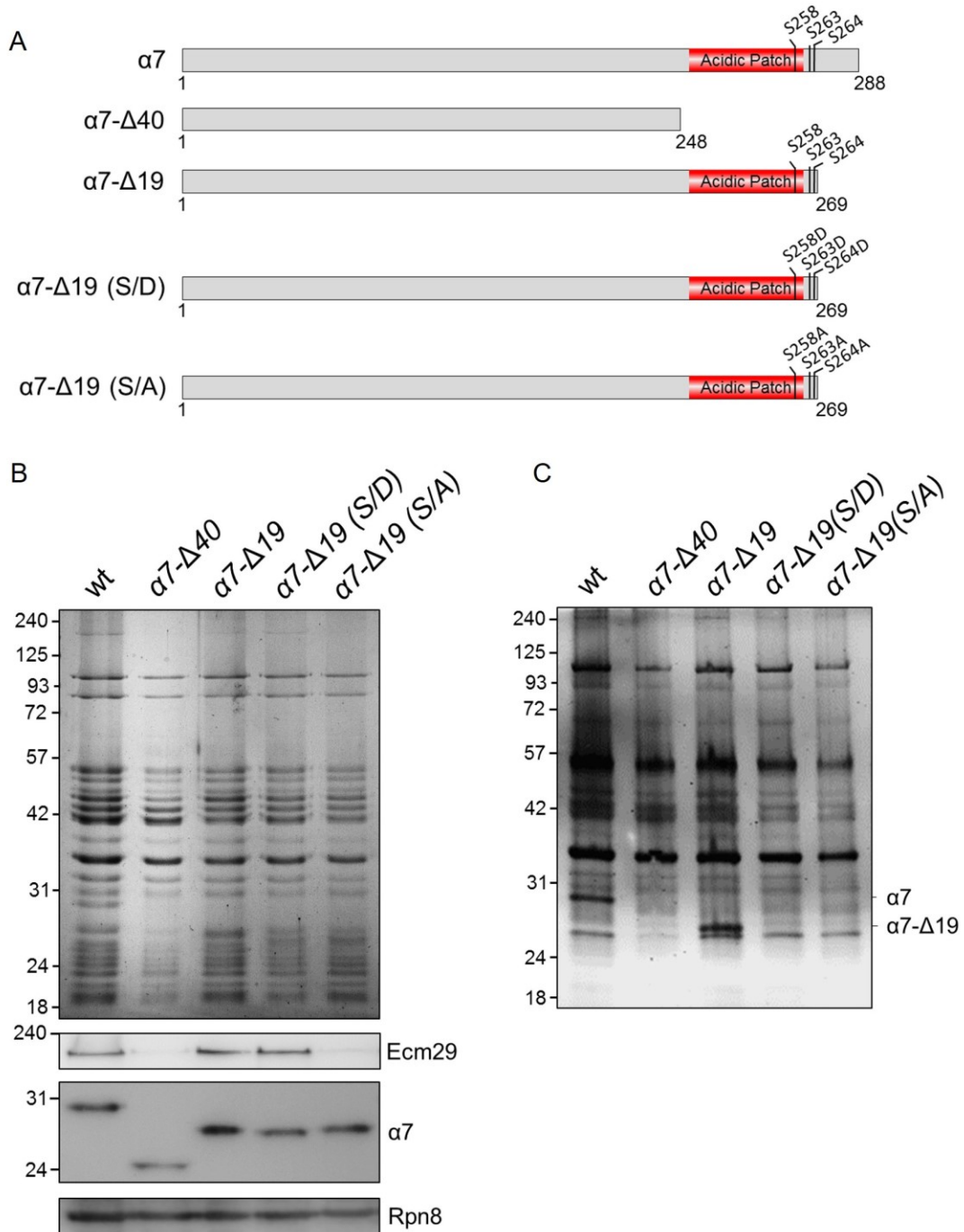
Appendix B - Supplementary information for chapter 3

Figure B.1 Supporting data related to figure 3.4 Effect of $\alpha 7$ C-terminal truncation on Ecm29 expression level and its association to the proteasome.



Equal amount of proteins from cell lysates of indicated strains were analyzed on the non-denaturing gel. Type of proteasome complex formed is observed by in-gel activity assay by monitoring LLVY-AMC substrate degradation. The gel is then subjected to the western blotting and immunoblotted with indicated antibodies.

Figure B.2 Supporting data related to figure 3.7 Phosphorylation at the C-terminal tail of the $\alpha 7$ is necessary for the Ecm29 interaction to the proteasome.



(A) In addition to the $\alpha 7$ - $\Delta 19$ (S/A), phosphomimic mutant was also created by replacing serine with aspartate $\alpha 7$ - $\Delta 19$ (S/D). (B) Proteasome from the indicated strains were purified and equal amount of protein was analyzed on SDS-PAGE (upper panel). Amount of Ecm29 present on

proteasome complex and truncations of $\alpha 7$ in strains were confirmed by immunoblotting with respective antibodies. Ecm29 association with the proteasome was not affected in case of $\alpha 7$ - $\Delta 19$ (S/D) (C) Phosphomutants are confirmed by staining SDS-PAGE with Pro-Q-Diamond phosphostain. $\alpha 7$ - $\Delta 19$ that gets phosphorylated shows as faster migrating $\alpha 7$ band compared to wt. $\alpha 7$ - $\Delta 19$ (S/A) and $\alpha 7$ - $\Delta 19$ (S/D)mutants does not get phosphorylated hence no bands were observed after phosphostaining.